CONDUCTING POLYMER COMPOSITE FILMS FOR THE ELECTROCATALYTIC REDUCTION OF OXYGEN

by

Evelyn K. W. Lai

B.Sc., Simon Fraser University, British Columbia, Canada, 1994

THESIS SUBMITTED IN PARTIAL FULFILLMENT OF

THE REQUIREMENT FOR THE DEGREE OF

MASTER OF SCIENCE

in the Department

of

Chemistry

SIMON FRASER UNIVERSITY

December 1997

APPROVAL

Name: Evelyn K. W. Lai

Degree: Master of Science

Title of Thesis: Conducting Polymer Composite Films for the Electrocatalytic Reduction of Oxygen

Examining Committee:

Chairperson: Dr. F.W.B. Einstein (or delegate)

Dr. S. Holdcroft, Associate Professor
Senior Supervisor

Dr. G. R. Agnes, Assistant Professor

Dr. P. W. Percival, Professor

Dr. L. K. Peterson, Associate Professor
Internal Examiner

Date Approved: December 12, 1997

ABSTRACT

Deposition of metal particles into polymer modified electrodes has been found to be useful in the field of electrocatalysis. Among the electrocatalytic reactions, oxygen reduction reaction is one of the most extensively studied due to its importance in both the natural and industrial processes. Polyaniline, an electronically conducting polymer, was investigated as a conductive matrix for the deposition of platinum for application in the electrocatalytic reduction of oxygen. A motivation behind this research was to increase the active surface area of a given quantity of electrocatalyst and another was to understand the role of the conducting polymer matrix in electrocatalysis.

Polyaniline was synthesized chemically and doped by reaction with (±) 10-camphorsulfonic acid (PANI-CSA). PANI-CSA was soluble in chloroform/*m*-cresol. It was found to be conductive between the potential limits 0.0V to +0.7V vs. SCE (+0.242V vs. NHE). These limits overlap favorably with the potential region over which the oxygen reduction reaction occurs.

Pt deposited electrochemically at PANI-CSA coated electrodes was found to be localized on the surface of the polymer (i.e., at the polymer/electrolyte interface). The electrocatalytic current was found to be higher than that found for the same quantity of Pt deposited on a bare carbon electrode in the absence of the polymer film, and indicates that the active surface area of the Pt was increased.

The permeability of PANI-CSA towards oxygen was determined by rotating disk voltammetry to be relatively low (1.18×10^{-12} mol cm^{-1} s^{-1}). In order to increase the accessibility of O_2 to the electrocatalyst, a perfluorinated sulfonic acid polymer,

Nafion, was incorporated into the conducting polymer. Nafion is an ionically conducting polymer which has high O_2 solubility. PANI-Nafion composites containing 10% wt% PANI possessed a permeability towards oxygen of 1.74 x 10^{-12} mol cm^{-1} s^{-1}, i.e., a 47% increase over pure PANI-CSA.

Pt electrochemically deposited at electrodes modified with PANI-Nafion composite films disperse into the polymer film to a greater extent compared to pure conducting polyaniline films. However, the electrocatalytic activity was lower for reasons that are not yet clear. A chemical method of incorporating Pt was investigated. A Pt precursor, K_2PtCl_6, was chemically reduced to Pt in a solution of Nafion which contained various alcohols. The Nafion solution containing the Pt suspension was mixed with PANI to form a PANI-Nafion-Pt composite. The Pt particles were found to be dispersed homogeneously in the matrix and the electrocatalytic activity towards oxygen reduction reaction was very promising. The chemical incorporation of Pt into polyaniline composite films is a promising method of obtaining three-dimensionally dispersed electrocatalyst systems for the oxygen reduction reaction.

TO MY FATHER, MOTHER AND BROTHER

ACKNOWLEDGEMENTS

I would like to thank my senior supervisor, Dr. Steven Holdcroft, for his guidance, support and patience throughout my studies.

I would like to express my gratitute to Dr. Paul D. Beattie for all his help and input into my project.

Thanks also go to Frank. P. Orfino (Department of Chemistry) and Dr. Brett Heinrich (Department of Physics) for their help in Auger Electron Spectroscopy and Dr. Albert Curzon (Department of Physics) for his help in the Scanning Electron Microscopy and Transmission Electron Microscopy work.

Thanks also go to members of our groups for their support, discussion and friendship.

Thanks also go to Dr. Stephen A. Campbell and Dr. Jurgen Stumper for proof-reading my thesis and their helpful discussion.

Lastly, I would like to express my special thanks to my parents, my brother and Perry for their support and encouragement throughout my studies.

TABLE OF CONTENTS

LIST OF TABLES

LIST OF FIGURES

Chapter 1

Introduction

1.1. Electronically Conducting Polymers

In the field of polymer technology, one of the most valued characteristics of synthetic polymers is the ability to act as excellent electrical insulators. More recently, there has been great interest in the possibility of producing electrically conducting polymers to combine, in one material, the electrical properties of a semiconductor and metals with the advantages of the ease and low cost of their preparation and fabrication. Flexibility, density and chemical inertness are other important advantages.

There are four different kinds of electrically conductive polymers: (1) ion-polymer solid electrolyte systems which involve dissolution and solvation of salts in a polymer matrix. The polymer solvates the ions and facilitates ion separation. The ions are sufficiently mobile to move along the polymer when an electric field is applied; (2) conversion of electrically insulating polymer to conducting material by pyrolysis to graphite; (3) incorporation of graphitic powder or metal particles into an insulating polymer matrix. The conductivity in these composite materials are attributed to the presence of conducting domains embedded in the polymer matrix. The conductivity depends on the contact between the conducting particles and therefore high loadings of conducting materials are usually needed; (4) The fourth class of electrically conducting polymers are those in which electrical conductivity arises from the presence of conjugated π-bonds. It is known that conjugated organic molecules can exhibit semiconductor properties [1]. Due to the fact that the conductivity arises from the

inherent properties of the polymer, these polymers are also known as intrinsically conducting polymers. This thesis focuses on the studies of intrinsically conducting polymers in the area of electrocatalysis.

1.1.1. Intrinsically Conducting Polymers

The polymer that attracted most attention in the early development of intrinsically conducting polymer is polyacetylene, $(CH)_x$, which has alternating single and double carbon-carbon bonds. It was first synthesized in the late 1950s, but for 20 years researchers were interested only in spectroscopic and theoretical studies, i.e. as the ultimate member of the polyene family. However, in 1977 MacDiarmid *et al.* discovered that treatment of polyacetylene with Lewis acids or bases increased its conductivity by up to 13 orders of magnitude [2]. Since then there has been a rapid growth of research into conjugated polymer structures. Figure 1.1 shows the structures of a few common conducting polymers.

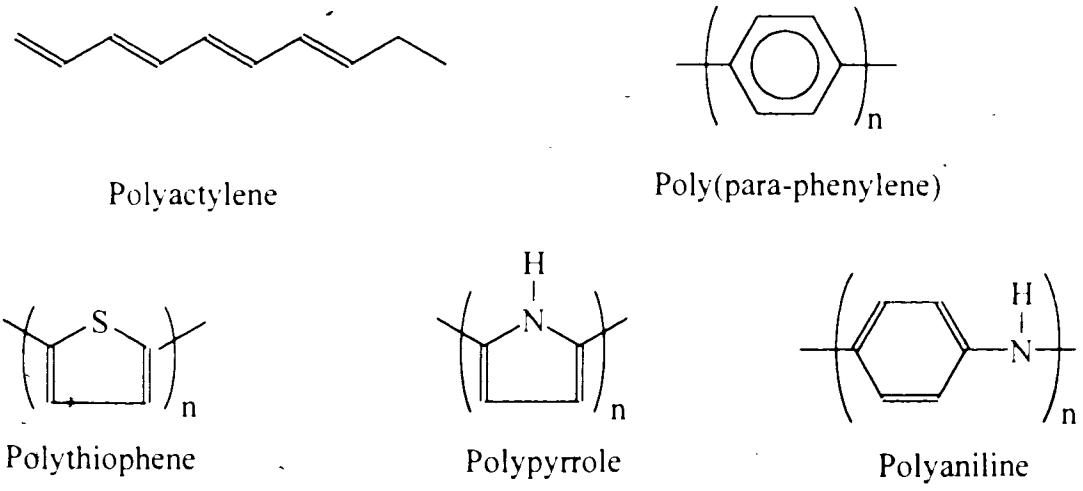

Figure 1.1 Chemical structures of common conducting polymers

In addition to the long chain of conjugated double bonds in polyacetylene, aryl rings also contribute to a delocalized skeletal structure, e.g., poly(para-phenylene). Another group of conducting polymers are the poly(heterocycles) such as polypyrrole and polythiophenes. Polyaniline has also attracted a lot of research interest due to its environmental stability, simple doping processes and its ease of processability.

1.1.2. Polyaniline

Figure 1.2 shows the general chemical structure of polyaniline (PANI). It contains y reduced and (1-y) oxidized repeating units.

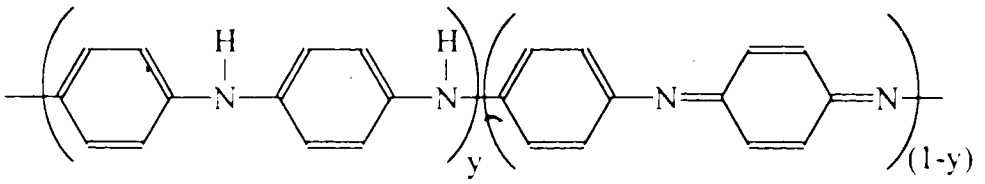

Figure 1.2 General chemical structure of polyaniline

The value of y can be varied from zero, to give the completely oxidized polymer known as pernigraniline, to one, which gives the completely reduced form known as leucoemeraldine. When y = 0.5, i.e. the number of reduced units is equal to the number of the oxidized units, it is known as emeraldine form (Figure 1.3). The imine nitrogen atom in any of the species below can be protonated completely or partially to yield the corresponding salts.

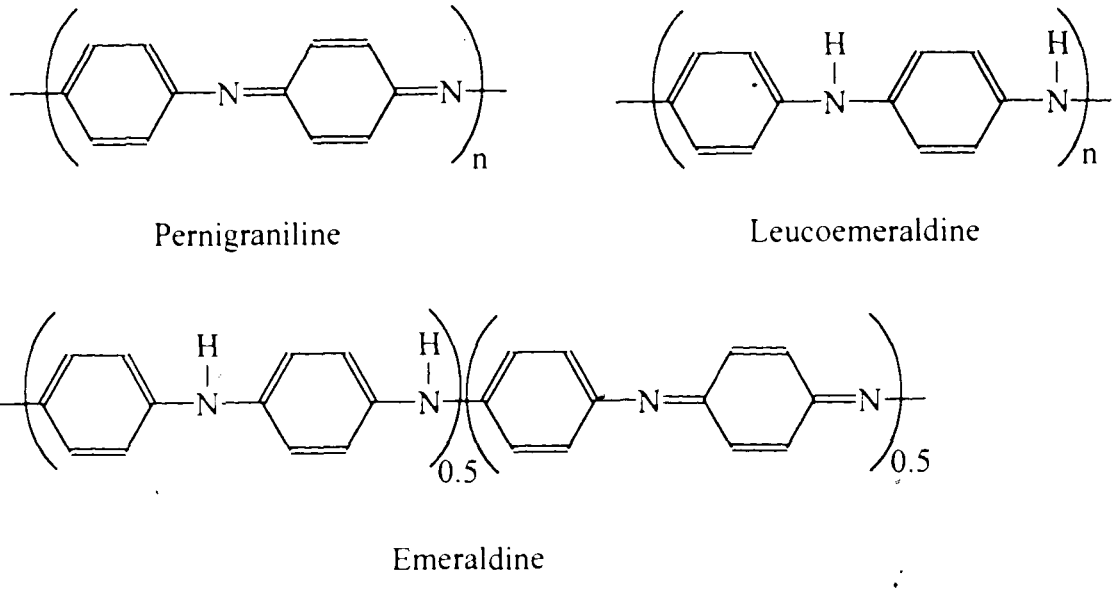

Figure 1.3 Polyaniline at different oxidation states.

1.2. Conduction Mechanism of Conducting Polymers

The electrical properties of a material are determined by its electronic structure. The electronic structure of materials is usually described by band theory. In the solid state, the atomic orbitals of each atom overlap with the neighboring orbitals to form molecular orbitals similar to those in small molecules. The large number of orbitals involved in the solid state are spaced together in a given range of energies, these give rise to continuous energy bands. The bonding energy band is known as the valence band and the antibonding energy band is known as the conduction band (Figure 1.4). They are separated by the band gap.

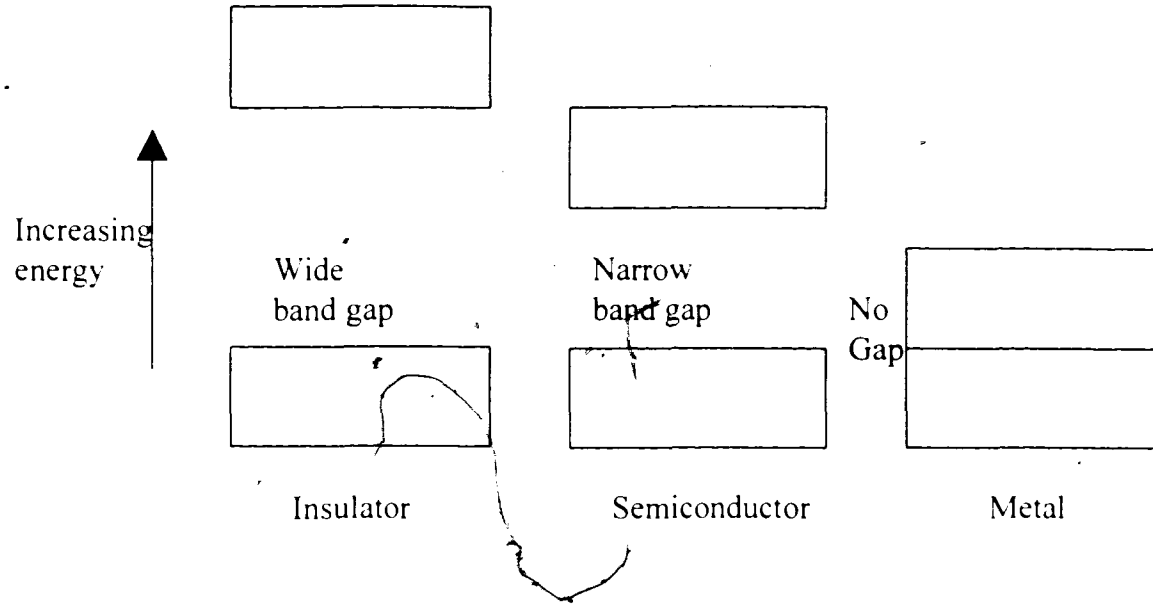

Figure 1.4 Schematic Diagram of the conduction band and valence band in solid materials.

The electrical conduction of conductive polymers cannot be explained well by simple band theory and other concepts including soliton, polaron, and bipolaron theory have been applied to conducting polymers [3-5]. When an electron is removed from the top of the valence band of a conjugated polymer, a radical cation (or hole) is created that does not delocalize completely, as would be expected from classical band theory. It delocalizes only partially, extending over several monomeric units and causing them to structurally deform. The energy level associated with this radical cation represents a destabilized bonding orbital and thus has a higher energy than the energy in the valence band, i.e. its energy is in the band gap. In solid-state physics, a radical cation that is partially delocalized over a polymer segment is called a polaron (Figure 1.5). If another electron is removed, it can be taken from another segment of the polymer chain, thus creating another independent polaron, or it could come from the first polaron creating a "dication" , which is known as a bipolaron. Both polarons and bipolarons are mobile and can travel along the polymer chain by the rearrangement of double and single bonds in the conjugated system upon application of an electric field.

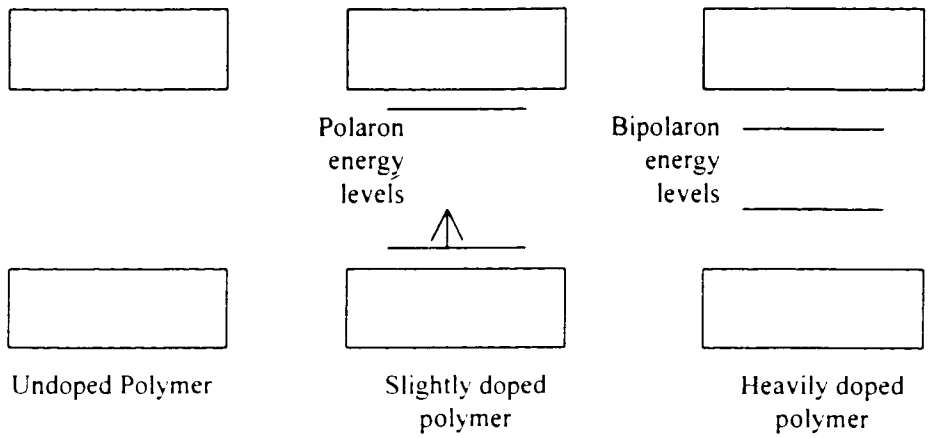

Figure 1.5 Schematic diagram of the polaronic and bipolaronic states of conductive polymers.

Figure 1.6 shows the neutral, polaronic and bipolaronic states of two common conducting polymers.

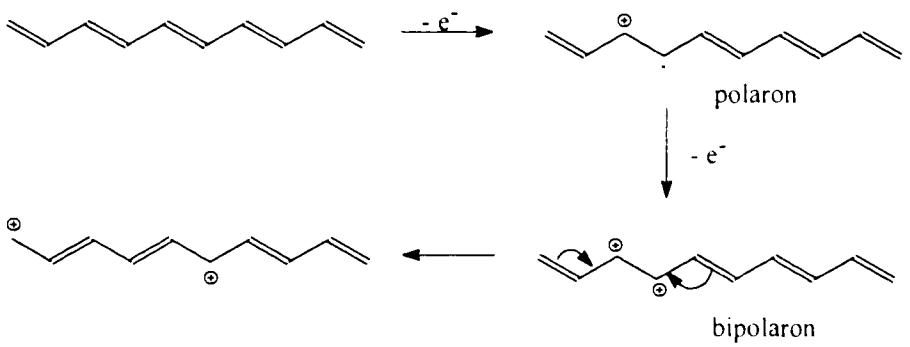

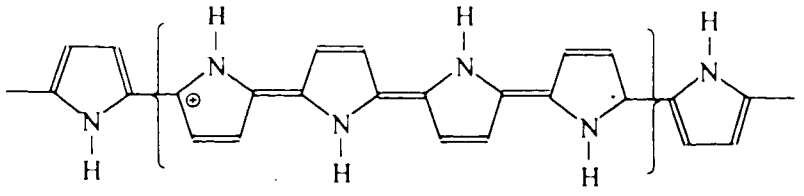

Polaron

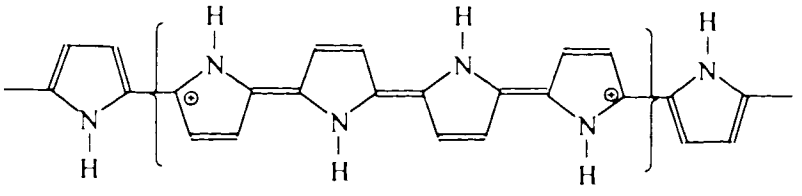

Bipolaron

Figure 1.6 Polaronic and bipolaronic states of polyacetylene and polypyrrole.

1.2.1. Oxidative Doping of Polyaniline

The oxidative doping of polyaniline involves the removal of electrons from the polymer chain (analogous to p-type doping). The totally reduced state of polyaniline, leucoemeraldine, can be oxidatively doped to the conductive emeraldine state either by chemical or electrochemical means. The progressive oxidative doping of leucoemeraldine base to emeraldine and finally to pernigraniline by electrochemical means can be clearly observed using cyclic voltammetry and this will be further discussed in Chapter 3.

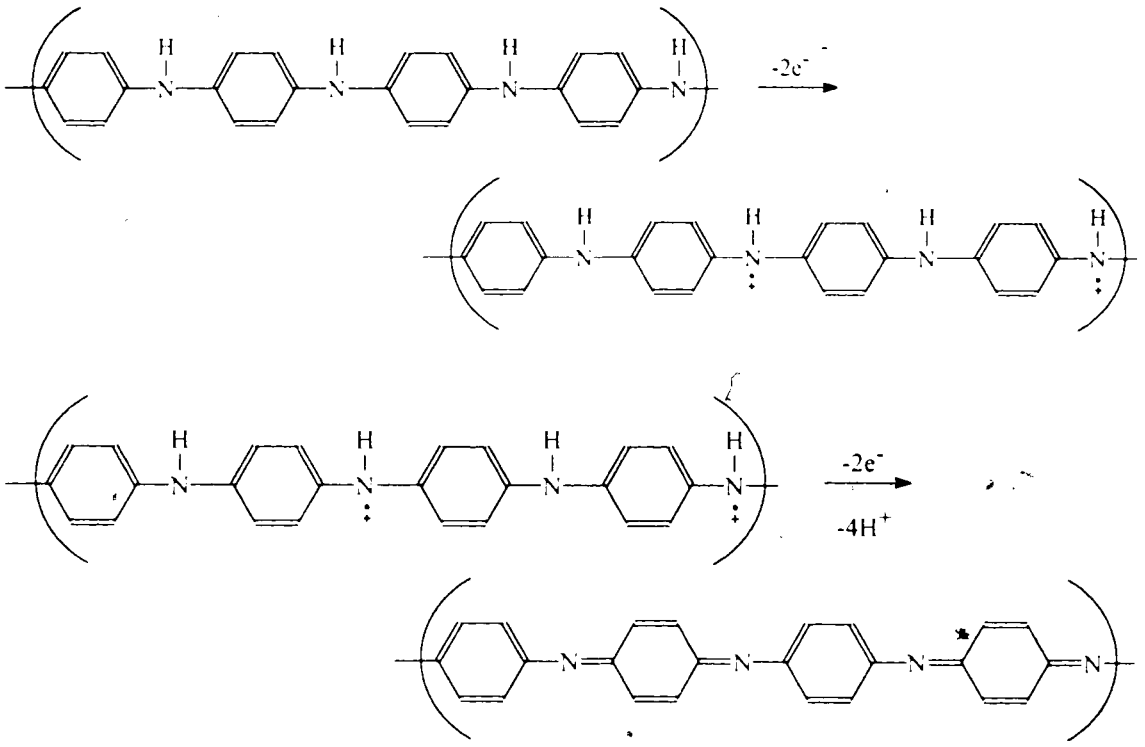

1.2.2. Protonic Doping of Polyaniline

Until very recently, conducting polymers were doped to the conducting state by partial oxidation or reduction of their π system of the polymer, i.e. the number of electrons associated with the polymer was either decreased or increased during the doping process. Polyaniline was the first well established example of doping a conjugated polymer to its conducting regime without any change in the number of electrons

associated with the polymer [6]. This was accomplished by treating the emeraldine base with aqueous protonic acids. For example, emeraldine base can be doped by HCl to yield the conducting emeraldine hydrochloride.

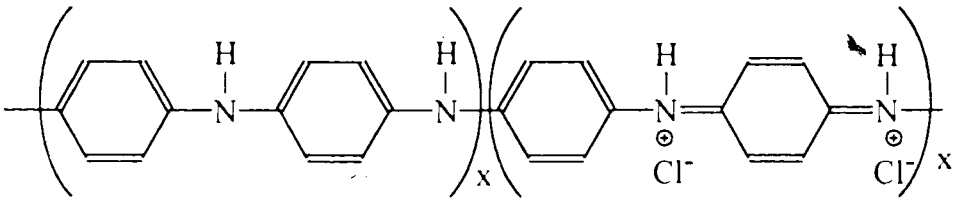

This dication can form a resonance structure, consisting of two separated polarons.

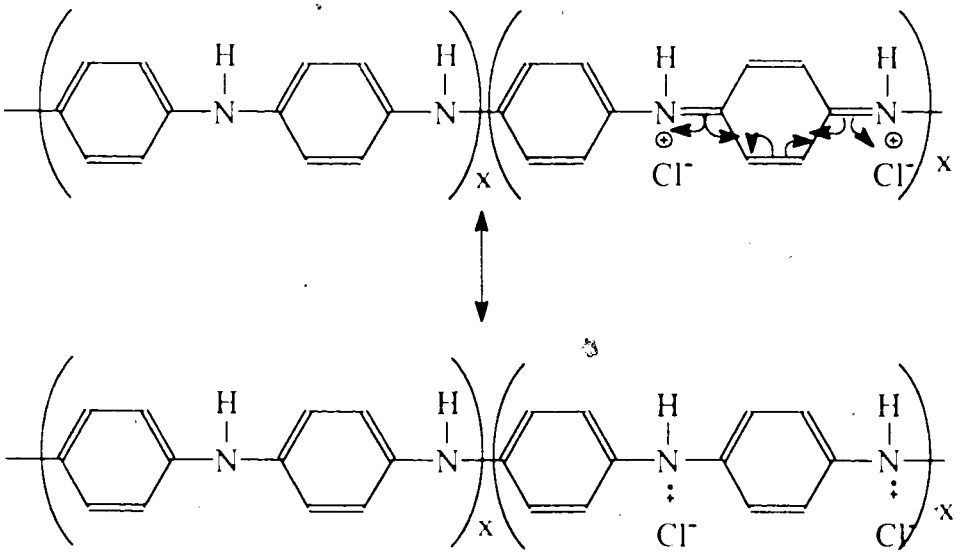

The protonic doping process is reversible, i.e. protonated emeraldine hydrochloride can be deprotonated by rinsing with H_2O to yield the emeraldine base.

1.3. Application of Conducting Polymers for Electrocatalysis

The extensive research work so far performed on conductive polymers has led to a wide variety of potential applications for this new class of material. Their application range from semiconductor devices and integrated circuits, to electrodes, light weight

battery components, sensors, electrochromic displays, and static-free packaging materials [7-11]. In this thesis, studies on the application of conducting polymers in the area of electrocatalysis will be presented.

Electrocatalysis can be defined as the heterogeneous catalysis of electrochemical reactions by an electrode material [12]. Most electrocatalytic reactions are dependent on an adsorption process, therefore the electrocatalytic activity depends strongly on the nature and the structure of the catalytic electrode. In order to increase the overall catalytic activity, which is proportional to the active surface area of the electrode surface, the catalyst material is sometimes dispersed in a convenient electron conducting substrate. In principle, electronically conducting polymers can serve as a conductive matrix provided that the polymer meets the following criteria:

(1) it is sufficiently stable under the experimental conditions

(2) it is sufficiently conductive to avoid an Ohmic drop in the film

(3) it is sufficiently porous to allow electroactive species to reach the catalytic sites.

Lack of stability precludes the use of many conducting polymers as conductive matrices for electrocatalytic purposes. Conducting polymers with good stability are polythiophene, polypyrrole, and polyaniline.

The concept of dispersing the electrocatalyst in a conductive matrix can be depicted in Figure 1.7. Various types of catalyst such as metallic particles, metallic oxides, metal complexes, and transition metal macrocycles, have been incorporated into host matrices depending on the electrochemical reaction to be catalyzed. This concept of dispersing the catalysts becomes especially interesting and important when noble metals

are considered because a high active surface area could be obtained with a much lower amount of metal used. This also means a reduction in the cost of the catalyst required.

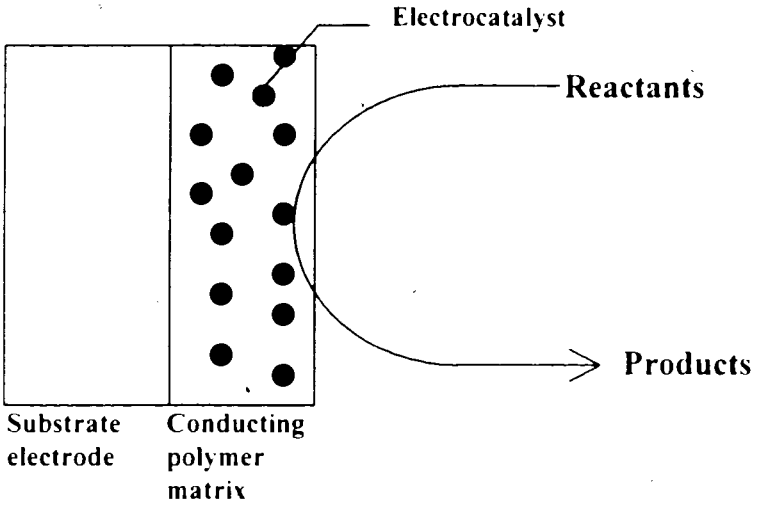

Figure 1.7 Schematic diagram of dispersed electrocatalyst in a conducting polymer matrix.

Electrochemical reactions catalyzed by incorporating noble metals in conducting polymers include hydrogen oxidation, hydrogen evolution, oxygen reduction, and oxidation of small organic molecules. For example, Tourillon and Garnier incorporated Ag-Pt particles into poly-3-methylthiophene for the electrocatalytic reduction of protons. Enhanced catalytic activity was observed compared to a platinized Ag-coated gold electrode at Pt loading as low as 10 $\mu g/cm^2$ [13]. Chen *et al.* developed nanodispersed Pt in polypyrrole-modified electrodes and the catalytic activity towards electrooxidation of hydrogen was comparable to bulk Pt electrodes [14]. The activity increased as the film thickness was increased and showed no diffusion limitation of H_2 through the film.

The electrooxidation of methanol has also gained significant research attention because methanol is considered as one of the most promising fuels for fuel cells [15]. Platinum and its binary or ternary alloys are found to have superior activity towards

methanol oxidation. Kost *et al.* dispersed Pt into polyaniline films for the oxidation of methanol [16]. They observed that poisoning of the Pt was supressed. The Pt/Polyaniline/Glassy Carbon composite electrode was stable for up to 20 hours during the methanol oxidation reaction.

Oxygen reduction is one of the most extensively studied electrochemical reactions due to its significance in both natural and industrial processes. Oxygen reduction is the cathodic reaction in both H_2/O_2 and Direct Methanol fuel cells. However, the slow kinetics of this reaction is an impediment in their development. Improvements in the efficiency of the oxygen reduction reaction would lead to an improvement in the overall efficiency of fuel cells. Vork and Barendrecht studied the reduction of oxygen at polypyrrole-modified electrodes incorporated with Pt particles [17]. They observed a difference in catalytic effect between Pt confined at the surface of the polypyrrole electrode and homogeneously dispersed in the film. They also observed a difference in the mechanistic route for the oxygen reduction reaction in the two situations described. When Pt was confined on the polymer surface, O_2 was reduced to H_2O via a 4-electron reduction step whereas when Pt was dispersed in the bulk, the slow diffusion of O_2 into the film led to a lower activity and a 2-electron reduction step was followed to give H_2O_2. Holdcroft and Funt also deposited Pt into polypyrrole and studied the oxygen reduction reaction, they also found that the electrocatalytic activity is limited by the slow diffusion of O_2 into the polypyrrole film [18]. However, Chen *et al* did not observe a rate saturation behavior in their catalytic system which consisted of nanodispersed Pt particles in a polypyrrole matrix [14]. Vork and Barendrecht also addressed the issue of stability of the polypyrrole-modified electrode system [17]. They found that polypyrrole was sensitive to

H_2O_2 and that subsequent destruction of the conducting polymer backbone led to a decrease in the electrocatalytic activity of the electrode. The polymer also became insulating at negative potentials leading to a decrease in electrocatalytic activity in that potential region. Although polypyrrole is the most commonly used conducting polymer matrix for the electrocatalytic reduction of oxygen, the degradation of polypyrrole in the presence of H_2O_2 and the low permeability of polypyrrole towards O_2 are two major drawbacks. It should also be noted that in all the previous work performed on polymer modified electrodes, the conducting polymers were deposited by electrochemical means. In this thesis, the use of chemically synthesized polyaniline, as a conductive matrix for the oxygen reduction reaction is investigated. Potential advantages of polyaniline over polypyrrole are:

(1) It is stable in air (i.e. it does not react with O_2)

(2) Polyaniline is protonically doped which will favor the facile transport of protons (protons are required in the reduction of oxygen)

(3) The region of conductivity for polyaniline is compatible with the potentials associated with the oxygen reduction reaction

(4) Polyaniline can be synthesized chemically and it is processable

(5) Polyaniline is permeable to O_2 [19].

1.3.1. The Oxygen Reduction Reaction

The oxygen reduction reaction is a multielectron reaction that may include a large number of intermediates and rate-determining steps involving various pathways.

Although it is not the intent of this work to study the mechanistic route of oxygen reduction reaction, it is useful to describe the nature of these mechanisms.

The reduction of oxygen in acidic medium may proceed by two overall pathways:

(1) The direct 4-electron pathway

$$O_2 + 4H^+ + 4e^- \longrightarrow 2H_2O \qquad E^\circ = 1.229\ V$$

(2) The peroxide pathway

$$O_2 + 2H^+ + 2e^- \longrightarrow H_2O_2 \qquad E^\circ = 0.67\ V$$

followed by either the reduction of peroxide

$$H_2O_2 + 2H^+ + 2e^- \longrightarrow 2H_2O \qquad E^\circ = 1.77\ V$$

or the decomposition of peroxide

$$2H_2O_2 \longrightarrow 2H_2O + O_2$$

Depending on the electrode material, oxygen reduction may proceed by either pathway (1) or (2) or by a parallel pathway. Oxygen reduction on noble metals (Pt, Pd, Ag) predominantly occurs via pathway (1) [20].

The performance of electrochemical systems which employ oxygen electrode reactions e.g. fuel cells, is limited by the slow kinetics of the reduction of oxygen. The kinetics or rate of an electrochemical reaction can be related to its exchange current density according to the following equation [21]:

$$i_o = nFk_o C_O^{(1-\alpha)} C_R^{\alpha} \qquad \text{[Eqn.1.1]}$$

where i_o is the exchange current density (A/cm^2), n is the number of electrons transferred, F is the Faraday constant, k_o is the heterogeneous rate constant, C_O and C_R are the concentration of the oxidized and reduced species respectively, and α is the transfer

coefficient. The exchange current density also depends on the electrode material, the electrolyte, and physicochemical factors such as solubility and diffusivity of oxygen. The exchange current density for the oxygen reduction reaction on noble metals is in the range of 10^{-9} and 10^{-10} A/cm^2 [22]. This is small compared to simple electrochemical reductions (e.g. the exchange current density of the oxidation/reduction of $Fe(CN)_6^{3-}/Fe(CN)_6^{4-}$ is 10^{-3}A/cm^2) [23].

The kinetics of the oxygen reduction reaction depends strongly on the electronic properties, i.e., work function, % d character and d-band vacancies of the electrocatalyst. Geometric parameters, i.e., crystal structure, interatomic distance, grain size, structural irregularities are also important. In heterogeneous catalysis, the catalytic parameters are usually governed by the strength of the adsorption of intermediates to the catalyst. Figure 1.8 shows the relationship between oxygen reduction kinetics and the calculated M-O bond strength.

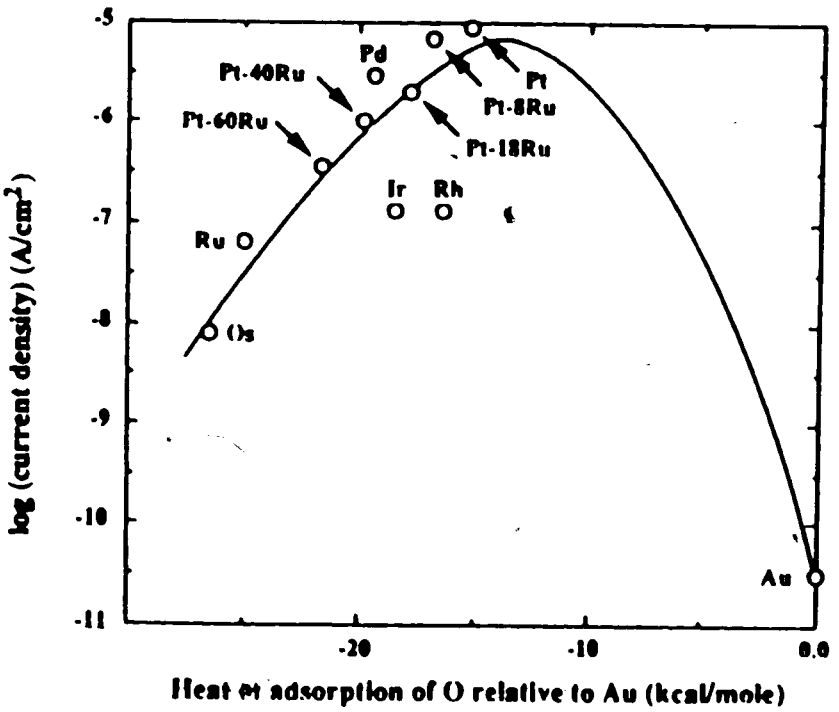

Figure 1.8 Plot of current density against calculated M-O bond strength, relative to Au. For oxygen reduction (overpotential of 0.46V) in 85% H_3PO_4 at 25°C [24]

It can be seen that if the M-O bond is too strong, the adsorbed species will be less reactive, although coverage may be high. On the other hand, if the coverage is too low, the adsorbed species are reactive but few in number. Pt is therefore the optimum catalyst for oxygen reduction reaction.

Solubility and diffusivity of oxygen are two physicochemical properties that affect the rate of the oxygen reduction reaction in the mass transport limited regime. The magnitude of these two parameters plays a significant role in the limiting current density for oxygen reduction as shown in the following equation [25]:

$$\frac{i_l}{nF} = \frac{DC}{\delta} \qquad \text{[Eqn.1.2]}$$

where i_l is the limiting current density, n is the number of electrons transferred, F is the Faraday's constant, D is the oxygen diffusion coefficient, C is the solubility of oxygen in the bulk electrolyte and δ is the thickness of the mass transfer boundary layer (or the hypothetical stagnant diffusion layer). The limiting current increases with increases in both the solubility and diffusivity of oxygen.

1.3.2. Electrochemical Techniques

In this study, two electrochemical techniques are used for both qualitative and quantitative analysis. The theory of these two electroanalytical techniques will be discussed briefly.

A. Cyclic Voltammogram

Cyclic voltammetry is a versatile and widely used electroanalytical technique available for both the determination of mechanisms and redox potentials of a redox

system. The potential of the electrode in quiescent solution is scanned linearly between two potential limits with time. Then the potential scan is reversed to complete a cycle. The current response during the potential scan is recorded. Figure 1.9 shows a typical cyclic voltammogram of a reversible system in quiescent solution.

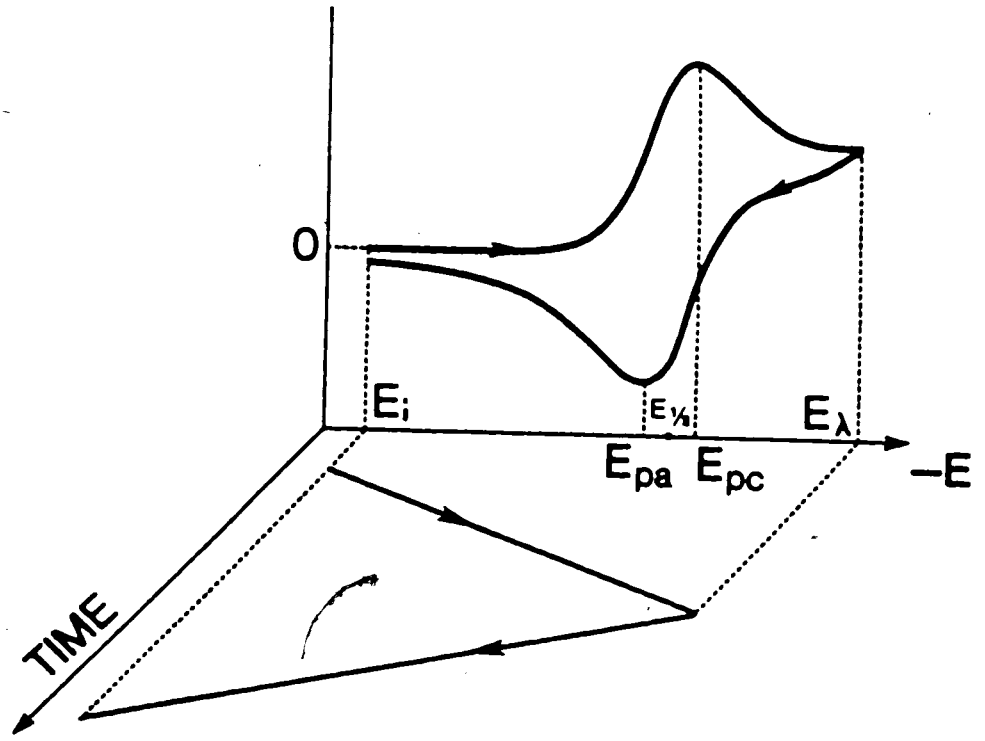

Figure 1.9 A typical cyclic voltammogram for a reversible redox system.

For a reversible electrochemical reaction in solution:

$$O + n\,e^- \rightleftharpoons R$$

The current and potential is related by the Butler-Volmer equation:

$$i = i_o\left\{exp\left[\frac{-\alpha nF\eta}{RT}\right] - exp\left[\frac{(1-\alpha)nF\eta}{RT}\right]\right\} \qquad \text{[Eqn. 1.3]}$$

where i_o is the exchange current density, α is the transfer coefficient, n is the number of electron involved, F is the Faraday constant, η is the overpotential (the

difference between the applied potential and the equilibrium potential), R is the gas constant and T is the temperature. The current has an exponential relationship with the applied voltage and the onset of the cyclic voltammogram illustrates this relationship. As the species at the electrode surface is depleted, the rate of diffusion of the reactant species is not fast enough to compensate for the species being depleted at the surface and the current becomes limited by the mass transport of the reactant to the electrode surface. The current becomes independent of overpotential and it decays with time. When the scan is reversed, the species at the electrode surface becomes the reactant species and a reverse peak is observed in the voltammogram. This technique is often the first experiment performed in an electrochemical study. It enables the electrode potential to be rapidly scanned in search of redox couples and this technique is used in this study as a qualitative tool for studying the conducting polymer matrix, in addition to the oxygen reduction reaction.

B. Rotating Disk Voltammetry

Unlike cyclic voltammetry which relies on the linear diffusion of species to the electrode surface, rotating disk voltammetry provides much more quantitative information because electrolysis occurs under forced convection.

In a rotating disk experiment, the electrode is rotated at an angular velocity of ω, and the thin layer of electrolyte near the surface of the electrode acquires rotational momentum and spins out radially from the centre of the disk. The electrolyte at the surface is replenished by the upward flow as shown in Figure 1.10.

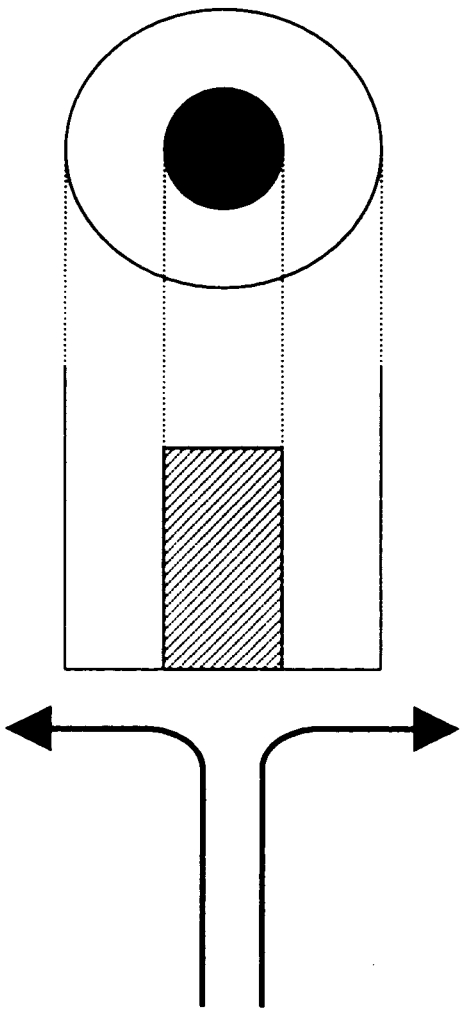

Figure 1.10 A rotating disk electrode.

The potential of the electrode is scanned linearly with time and the current response is recorded. The current is given by the following equation:

$$\frac{1}{i} = \frac{1}{i_k} + \frac{1}{i_L} \qquad \text{[Eqn. 1.4]}$$

where i is the observed limiting current, i_L is known as the Levich current given by:

$$i_l = 0.62nFAC_o D^{2/3} \upsilon_k^{-1/6} \omega^{1/2} \qquad \text{[Eqn.1.5]}$$

where C_o and D are the concentration and diffusion coefficient of the reactant in the electrolyte, ν_k is the kinematic viscosity and w is the angular velocity of the electrode, and i_k is the kinetic contribution to the current given by:

$$i_k = nFAC_o k^o exp[\frac{-\alpha nF(E - E^{o'})}{RT}] \qquad \text{[Eqn.1.6]}$$

where k^o is the heterogeneous rate constant and $E^{o'}$ is the formal potential.

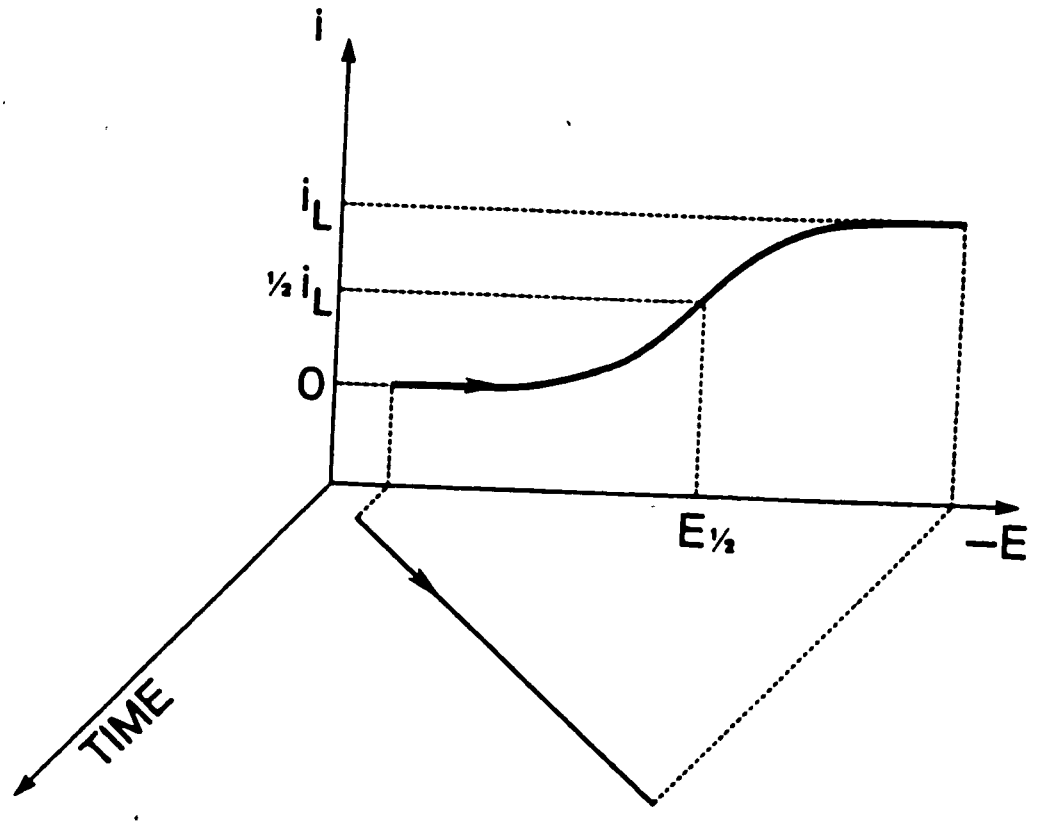

Figure 1.11 A typical rotating disk voltammogram.

Figure 1.11 shows a typical rotating disk voltammogram. From Eqn. 1.4, it can be seen that at high overpotentials, i_k is sufficiently large that the term $1/i_k$ becomes negligible and the limiting current is dominated by the mass transfer Levich current, i.e. $i = i_L$. A

plot of i_L vs. $\omega^{1/2}$ yields information about the diffusion parameter of the species in the electrolyte solution.

In a polymer modified electrode, the current-potential relationship is complicated by the diffusion of reactive species through the polymer film. The limiting current is given by:

$$\frac{1}{i} = \frac{1}{i_k} + \frac{1}{i_f} + \frac{1}{i_L} \qquad \text{[Eqn. 1.7]}$$

where i_f is the diffusion current through the polymer film given by:

$$i_f = \frac{nFD_f C_f}{d} \qquad \text{[Eqn. 1.8]}$$

D_f, C_f are the diffusion coefficient and solubility of the reactant species in the polymer film respectively, and d is the thickness of the polymer film.

At high overpotentials, the term $1/i_k$ is negligible. A plot of $1/i$ vs. $1/\omega^{1/2}$ yields an intercept equal to $1/i_f$. Therefore, the permeability of the reactant in the polymer matrix, which is the product of D_f and C_f, can be determined by this technique.

1.4. Goals of This Project

Chemically synthesized, processable polyaniline provides a potentially practical means for its large scale production compared to electrochemical growth of polymer. The proton conductivity in polyaniline should enhance the efficiency of the oxygen reduction reaction. However, the stability of the polymer matrix and the accessibility of oxygen to the catalyst site have to be determined.

The goals of this project are:

(1) to demonstrate a microheterogeneous electrocatalytic system for oxygen reduction reaction using Pt particles dispersed in a polyaniline-modified electrode,

(2) to chemically synthesize processable polyaniline,

(3) to demonstrate that the efficiency of catalyst for the electrocatalytic reaction can be improved by dispersing it in a conductive matrix,

(4) to study the mass transport properties of the oxygen through polyaniline film as it relates to the oxygen reduction reaction.

Chapter 2

Experimental

2.1. Chemicals

Aniline (BDH) was purified by vacuum distillation before polymerization. Lithium chloride (Sigma Chemicals), hydrochloric acid (Anachemia), sulfuric acid (Anachemia), ammonium solution (Anachemia), ammonium peroxydisulfate (Anachemia), (±)-10-camphorsulfonic acid (Sigma Chemicals), *m*-cresol (Anachemia), N-methylpyrrolidinone (Sigma Chemicals), chloroform (Caledon), potassium hexachloroplatinate (Johnson Matthey Chemicals Ltd.) and Nafion (5%, EW 1100) solution (DuPont) were used as received. In all the electrochemical studies, the electrolytes were prepared using Millipore water.

2.2. Synthesis of Polyaniline

2.2.1. Preparation of Polyaniline Salt

LiCl (10.607 g) was dissolved in 125 mL of HCl (1.0 M) to yield a 2.0 M solution of LiCl/HCl. Aniline (5.0 mL, 0.055 mol) was added to 75 mL of the 2.0 M LiCl/HCl solution. The mixture was cooled, with stirring, to ~0°C using an ice bath. Ammonium peroxydisulfate, $(NH_4)_2S_2O_8$ (2.876 g, 0.0126 mol) was added to the remaining 50 mL of LiCl/HCl solution. This solution was also cooled with stirring to ~0°C. The polymerization process was initiated by the slow addition of the $(NH_4)_2S_2O_8$ solution to the aniline solution. The addition process took approximately 30 minutes. The temperature of the reaction mixture was kept below 4°C throughout the whole

polymerization process. The colour of the reaction mixture was observed to change from light blue to blue-green and finally to dark green. The polymerization was terminated after 3.5 hours by filtering the blue/green precipitate through a Buchner funnel. The precipitate was washed with 1.0 M HCl until the filtrate obtained was colourless. The precipitate was dried by placing the polymer under vacuum for 44 hours in a dessicator.

2.2.2. Preparation of Polyaniline Base

The polyaniline salt (PANI-Cl) was deprotonated to yield the emeraldine base by stirring the polyaniline salt in 500 mL of NH_4OH (0.1 M) for 30 hours. The precipitate was filtered and dried under vacuum at room temperature for 60 hours. The polyaniline base was black in colour and exhibited a slight metallic reflection.

2.2.3. Doping of Polyaniline by (±)-10-camphorsulfonic Acid

Processable polyaniline was prepared by mixing emeraldine base with (±)-10-camphorsulfonic acid (CSA), in a 2:1 ratio, using an agate mortar and pestle in a dry bag filled with N_2. The resultant mixture was dissolved in chloroform to yield a 2% (w/w) solution. The polymer solution obtained was blue-green in colour and contained some suspended particulate matter. The solution was sonicated for 36 hours after which some undissolved fine particulates were still observed.

The mixture was soluble in *m*-cresol and yielded a dark green solution. A 5 mg/mL polymer solution in *m*-cresol was prepared as a stock solution. Due to the high viscosity of *m*-cresol solution, chloroform was added to facilitate the film casting process. The final stock polymer solution was a 2.5 mg/mL polyaniline (PANI-CSA) in 1:1

chloroform/*m*-cresol solvent mixture.

2.3. Synthesis of Polyaniline/Nafion Composite

A series of polyaniline-Nafion composites with different PANI:Nafion weight ratio were prepared in such a way that the final concentration of the composites (regardless of the polyaniline:Nafion ratio) was the same. It was assumed that the density of these composites was the same. The thickness of the films cast from the different solutions were therefore assumed to be the same if the same volume of composite solution were used. The amount of PANI and Nafion used in the preparation is shown in Table 2.1. The concentration of the polyaniline base in N-methyl-2-pyrrolidinone (NMP) stock solution was 2 mg/mL. The concentration of the Nafion solution was 5% (w/w). The density of the Nafion solution was determined by weighing 0.1 mL portions of Nafion solution and was determined to be 0.99±0.01 g/mL. Excess NMP was added to the solution to make up all the solution concentrations to be 6.67 mg of polymer composite/mL of solvent mixture.

PANI (wt %)-Nafion Composites	**5%**	**10%**	**15%**	**20%**	**25%**
Mass of PANI Base (mg)	0.5	1.0	1.5	2.0	2.5
Vol. of PANI Base solution(mL)	0.25	0.50	0.75	1.00	1.25
Mass of Nafion (mg)	9.5	9.0	8.5	8.0	7.5
Mass of Nafion solution (mg)	190	180	170	160	150
Vol. of Nafion solution (mL)	0.192	0.182	0.172	0.162	0.152
Vol. of excess NMP (mL)	1.058	0.818	0.578	0.338	0.098
Total mass of composite (mg)	10	10	10	10	10
Total vol. (mL)	1.5	1.5	1.5	1.5	1.5
Concentration (mg/mL)	6.67	6.67	6.67	6.67	6.67

Table 2.1 Preparation of PANI-Nafion composites

Nafion solution was slowly added to the polyaniline base solution with constant stirring. The colour of he polyaniline base solution turned from deep blue to dark green. The solutions were stirred for 48 hours to allow complete doping.

Due to the high boiling point of NMP, the solvent evaporation process for the PANI-Nafion composites was very slow. A new batch of PANI(10%wt%)-Nafion composite solution without the excess NMP was prepared for electrochemical studies.

Nafion solution, 0.36 mL, was added to 0.4mL of PANI-base in NMP (5 mg/mL) dropwise with continuous stirring. The solution was stirred for 2 hours and then sonicated for 1 hour.

2.4. Characterization of Polyaniline

2.4.1. Spectroscopic Studies

The FT-IR spectrum of the emeraldine base in the form of a KBr pellet was obtained in the transmission mode with a Bomem Hartmann & Braun, MB-Series FT-IR Spectrometer. UV-Vis spectra were obtained using a Cary 3E UV-Visible Spectrometer. Film were cast from an NMP solution of the base form and a chloroform/*m*-cresol solution for the camphorsulfonic acid doped form of polyaniline.

2.4.2. Conductivity of Polyaniline

The conductivity of the camphorsulfonic acid doped polyaniline films were measured by the 4-point probe technique. Films were cast from a 1:1 chloroform / *m*-cresol solution of PANI-CSA onto a glass slide and dried under vacuum. The thickness of the films was determined using a Mitutoyo micrometer.

The dependence of the conductivity on the applied electrochemical potential was determined using a 2-band electrode constructed according to Ref.[26]. Briefly, a piece of Mylar film of thickness 80 μm was placed between two sheets of Pt foil (0.3 cm x 0.3 cm x 0.01 cm) and electrical contacts were made at the back of each of the Pt sheets. The assembly was embedded in epoxy inside a glass tube (0.6 cm internal diameter) as shown in Figure 2.1. The sandwich assembly exposed at the end of the tube was polished with emery paper and diamond paste.

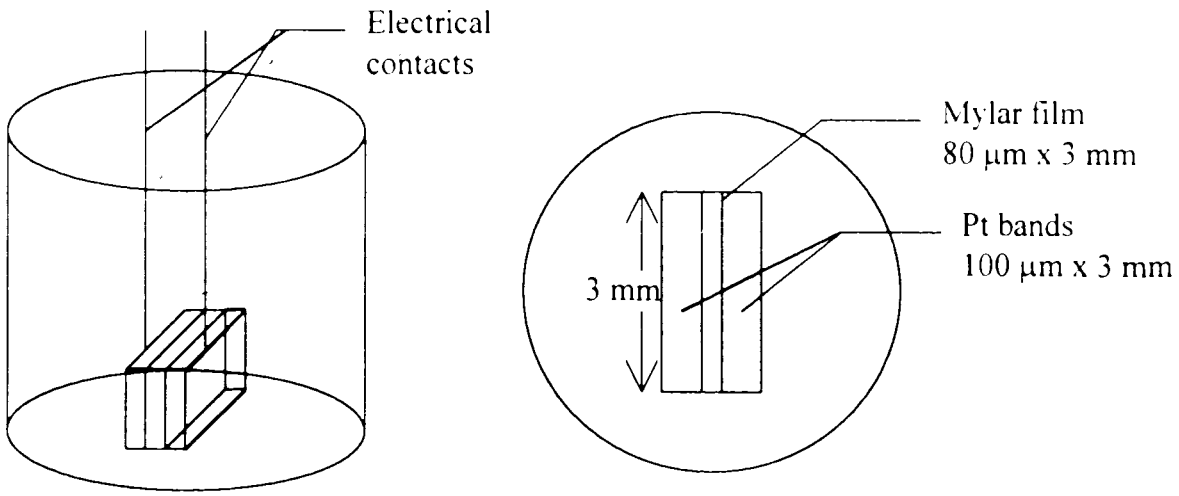

Figure 2.1 Side view and top view of the 2-band electrode for conductivity measurement.

A thin film (~13μm) of PANI-CSA was deposited onto the 2-band electrode from the chloroform/*m*-cresol solution. The quantity of polymer was sufficient to bridge both electrodes. The apparatus set up was illustrated in Figure 2.2.

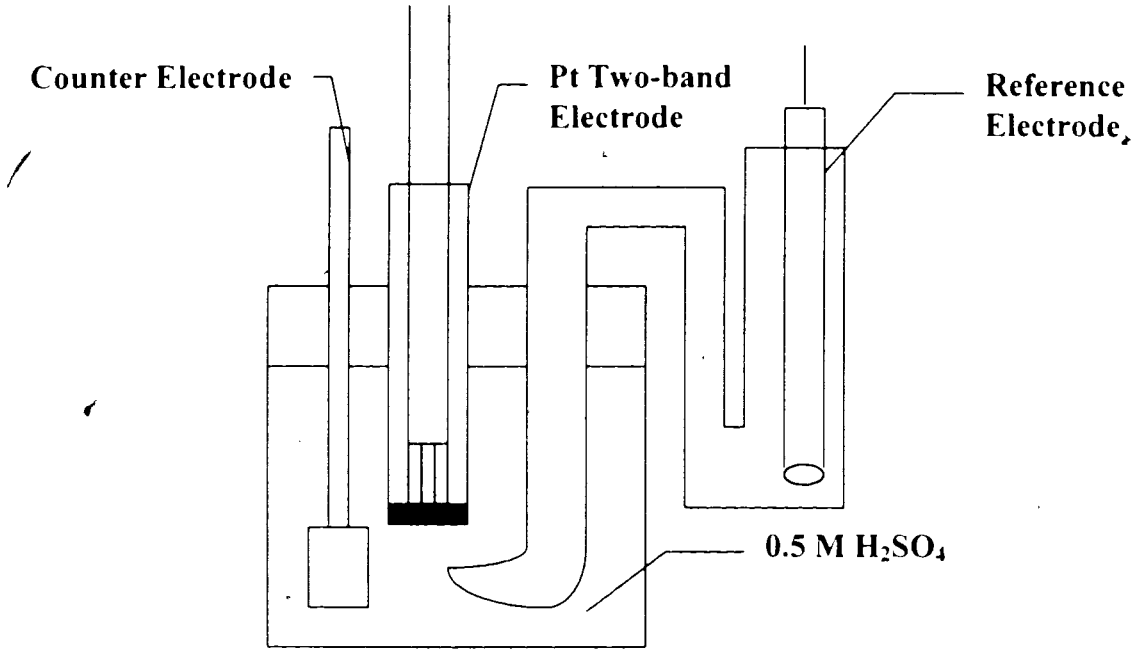

Figure 2.2 Electrochemical cell for in-situ conductivity measurement.

The two band electrodes were connected to a bipotentiostat. The two working electrodes were brought to a desired potential. After attainment of equilibrium of the polymer film, a 20 mV d.c. voltage was applied to one of the electrodes. The potential difference across a resistor R connected in series to one of the electrode was recorded. The potential difference is directly proportional to the current passing through the resistor, and hence is a direct indication of the conductivity of the polymer. The potential of the 2-band electrodes and thus the polymer was varied from +1.0V to 0.0V vs. SCE with 0.1V increment. Measurements were performed from the oxidized conducting form to the neutral insulating form of the polymers as suggested in Ref.[26] because it was previously found that this procedure allows quicker attainment of equilibrium.

2.4.3. Cyclic Voltammetry

Cyclic voltammograms were obtained using a Pine Instrument Model RDE4 Bipotentiostat in conjunction with an Allen X-Y recorder. A three compartment cell, as illustrated in Figure 2.3 was used for all electrochemical studies. A Pt flag (area ~1cm^2) was used as a counter electrode and a saturated calomel electrode (SCE) was used as a reference electrode (+0.242 V vs.NHE). The counter electrode was separated from the working compartment by a porous glass frit to prevent the mixing of products from the cathodic and anodic reactions. The reference compartment was separated from the working compartment through a Luggin capillary which minimizes the potential drop between the reference electrode and the working electrode.

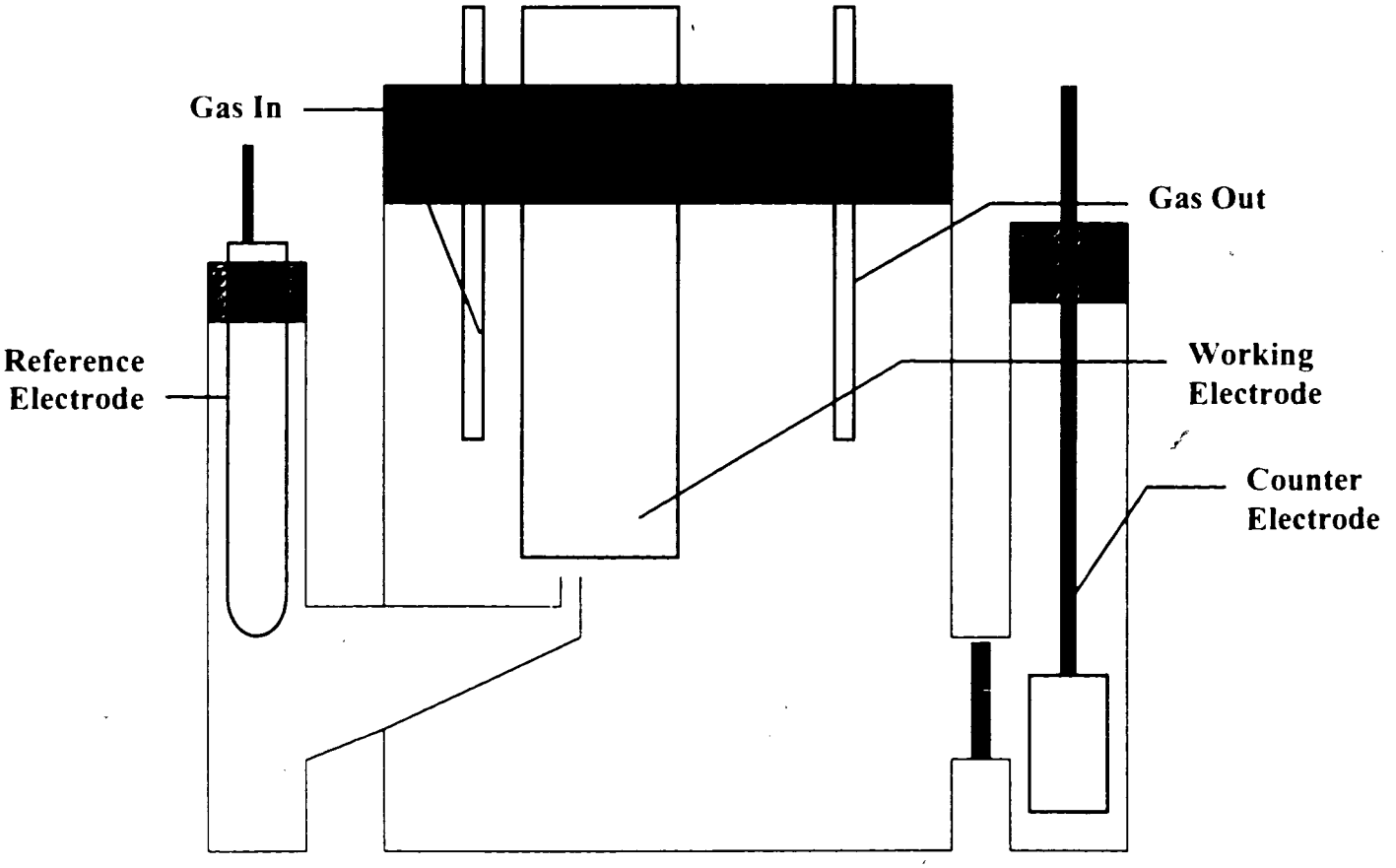

Figure 2.3 Three-compartment electrochemical cell.

The cyclic voltammogram of the polyaniline salt was obtained by grinding the solid polymer into fine powder and impregnating it into a piece of filter paper by hand pressure. The filter paper was agitated to remove the excess polymer powder. This was then placed in contact with a Pt mesh and rolled to form the working electrode.

Cyclic voltammograms of the camphorsulfonic acid doped polyaniline (PANI-CSA) were obtained on a glassy carbon (GC) disk electrode (area = 0.4418cm^2). The electrodes were polished successively with 5 μm, 3 μm, and 1 μm diamond paste to a mirror-like surface before film casting. A thin film (~10μm) of PANI-CSA was obtained by casting the chloroform/*m*-cresol solution of the polymer onto the glassy carbon surface. Films were dried at room temperature under ambient air.

Voltammograms were obtained by cycling the potential between +1.0V and -0.2V vs. SCE using a scan rate of 100mV/s in aqueous 0.5 M H_2SO_4.

2.5. Methods for Incorporation of Pt

2.5.1. Incorporation of Pt into PANI-CSA Modified Electrode

Pt was incorporated into the polyaniline film by electrochemical reduction of K_2PtCl_6. A glassy carbon disk electrode (area = 0.4418 cm^2) was used as the substrate electrode. A thin film of PANI-CSA (0.4 μm) was solution cast onto the glassy carbon electrode from a chloroform/*m*-cresol PANI-CSA solution. The PANI-CSA modified electrode was then cycled between +0.5V and -0.3V vs. SCE in 0.5 M H_2SO_4 for 30 cycles. The cathodic charge (the amount of charge registered during the cathodic scan), Q_{PANI}, was recorded by an ESC Digital Coulometer. The PANI-CSA modified electrode was then soaked in a 1 mM K_2PtCl_6/0.5 M H_2SO_4 solution for 30 minutes and the

electrode was again cycled between +0.5V and -0.3V vs. SCE for 30 cycles. The cathodic charge, Q_{total} was recorded by the coulometer. The charge, Q_{Pt}, associated with the reduction of K_2PtCl_6 to Pt(0) was calculated from the difference of the cathodic charge for the polymer in 0.5 M H_2SO_4, Q_{PANI}, and the cathodic charge for the polymer in 1 mM K_2PtCl_6, Q_{total}. The mass of Pt deposited was determined by assuming a 4-electron reduction of K_2PtCl_6 to Pt(0) (Section 4.1).

2.5.2. Incorporation of Pt onto Glassy Carbon Electrode

Pt was also deposited on a bare glassy carbon disk electrode (area = 0.4418cm^2) by electrochemical reduction of K_2PtCl_6. The potential was cycled between +0.5V and -0.3V vs. SCE at 100 mV/s in a 1 mM K_2PtCl_6/0.5 M H_2SO_4 solution.

2.5.3. Incorporation of Pt into PANI-Nafion Composite Films

A. Electrochemical Reduction of K_2PtCl_6

Pt was also incorporated into the PANI(10% wt%)-Nafion film by the same method as described in Section 2.5.1.

B. Incorporation of Pt Black into PANI-Nafion Composite Films

Platinum Black (Johnson Matthey Chemicals Ltd.) (1.1 mg), was added to 1.0 mL of Nafion solution (5%) and sonicated for 2 hours. The Pt black formed a grey suspension in the Nafion solution. This Pt black suspension was then added slowly to PANI base in NMP (5 mg/mL) yielding a PANI(10% wt%)-Nafion-Pt black composite. The composite solution was sonicated for 2 hours.

C. Chemical Reduction of K_2PtCl_6 in Nafion Solution

K_2PtCl_6 was dissolved in Nafion solution (5%) yielding a clear yellow solution. This solution was heated to ~90 °C under reflux for 2 hours. The yellow colour was observed to fade while a grey Pt suspension was observed to form. The Nafion-Pt solution was slowly added to PANI base in NMP (5 mg/mL) with constant stirring and it was sonicated for 2 hours.

2.6. Characterization of Pt Incorporated Polymer-Modified Electrodes

2.6.1. Auger Electron Spectroscopy

Auger Electron Spectroscopy (AES) was performed with the help of F. Orfino, Department of Chemistry and Dr. Heinrich, Department of Physics, using a Perkin-Elmer 595 Scanning Auger Microprobe. This technique was used to study the distribution of Pt in the polymer matrix. The sample was analysed using a 3 keV electron beam and a beam current of 0.1 - 0.2 μA. Elements were identified from their characteristic peak positions: Pt (64 eV), S (153 eV), C (273 eV), N (387 eV), O (516 eV) and F (664 eV) [27]. Depth profile analysis was performed by sputtering the polymer film with a 3 keV Ar^+ ion beam. The rate of sputtering varied from sample to sample depending on its composition. The PANI-CSA or PANI-Nafion composite films were deposited onto a graphite block

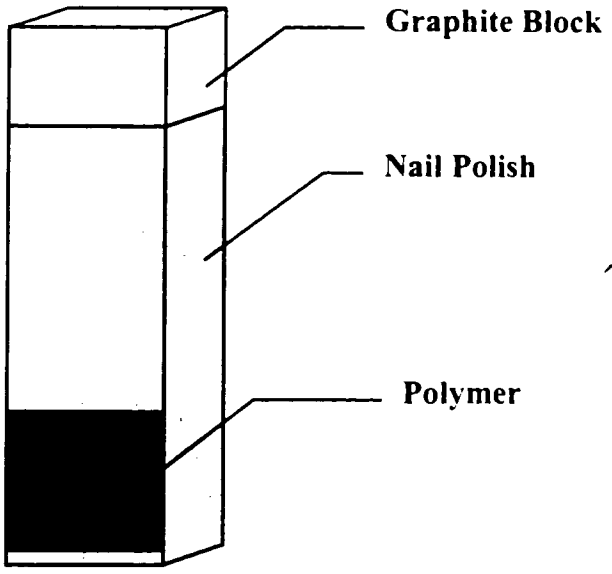

Figure 2.4. Sample prepared for Auger Electron Spectroscopy.

(5 cm x 1 cm x 0.5 cm) by solution casting, covering only an area of (1 cm x 1 cm). The rest of the graphite block surface was covered by nail polish to prevent Pt depositing onto the graphite surface in the subsequent electrochemical Pt deposition step. The graphite block was immersed into an aqueous 1mM K_2PtCl_6 solution and Pt was deposited by cycling the potential between +0.5V and -0.3V vs. SCE. After deposition of Pt, the graphite electrode was rinsed with H_2O and the nail polish was removed. The graphite block was cut into a size of 1 cm x 1 cm x 0.3cm block in order that it may fit into the Auger spectrometer.

2.6.2. Scanning Electron Microscopy & Transmission Electron Microscopy

Scanning Electron Microscopy (SEM) and Transmission Electron Microscopy (TEM) were performed by Prof. A. Curzon of the Department of Physics using a ISI DS-130 Scanning Electron Microscope equipped with a EG&G EDDS II Ortec Energy Dispersive X-ray Analyser and a Hitachi H-8000 Transmission Electron Microscope equipped with a LINK QX2000 Thin Window Energy Dispersive X-ray Analyser.

For SEM pictures, the samples of the polymer composite were prepared by

casting the appropriate solutions onto an indium-tin oxide (ITO) coated glass slides. For TEM pictures, the samples were prepared by casting the corresponding polymer onto ITO glass slide. After solvent evaporation, the ITO glass slide was immersed in water in a petri-dish and the polymer film peeled off from the slide to form a free standing thin film. A copper mesh was used as the substrate and the thin films were lifted up by one side of the mesh and encased in it by folding the other half on top of the polymer films. Elemental analysis of Pt was performed using an X-ray analyser (in conjunction with the SEM and TEM.

2.7. Permeability of O_2 Through Polymer-Modified Electrode

In order to study the permeability of O_2 through the polymer film, a Pt rotating disk electrode (area = 0.159cm^2) was used as the substrate electrode. The polymer films were deposited by solution casting to cover the whole surface of the Pt disk electrode. Rotating disk voltammetry was performed for PANI-CSA films with thickness of: 0.5 μm, 1.0 μm, 1.5 μm, 1.9 μm and 2.4 μm. PANI (10%wt)-Nafion films of thickness : 1.1 μm, 1.8 μm, 2.2 μm, 2.7 μm and 3.3 μm were also studied by using the same Pt disk electrode.

All rotating disk experiments were performed using a Pine Instrument RDE4 Bipotentiostat and a Pine Instrument Analytical Rotator. O_2 saturated 0.5 M H_2SO_4 solution was used as the electrolyte and the rotation speed was varied between 100 rpm and 900 rpm.

Chapter 3

Polyaniline

3.1. Synthesis of Polyaniline

Polyanilines can be prepared either by chemical or electrochemical oxidation of aniline under acidic conditions.

A. Electrochemical Oxidation

Electrochemical polymerization is usually carried out at a Pt electrode by dissolving aniline in an aqueous protonic acid using one of the following three methods:

(i) galvanostatic - constant current

(ii) potentiostatic - constant potential

(iii) potentiodynamic - sweeping the potential between 2 potential limits

Diaz and Logan demonstrated that high quality films of polyaniline can be obtained by continuously cycling the potential between -0.2V and +0.8V (vs.SCE) [28]. The polyaniline film obtained was reported to be homogeneous and adhered strongly to the Pt electrode. Figure 3.1 shows typical cyclic voltammograms recorded during the growth of polyaniline adopted from [29]. The potential was cycled between -0.19 V and +1.2 V vs. Ag/AgCl at a scan rate of 50 mV/s. The sharp increase in current at ~ +0.9 V corresponds to the oxidation of aniline. New peaks corresponding to the electrochemical response of PANI formed during the oxidation process appear after the first cycle. A steady growth process can be observed upon repeated cycling. Much effort has been devoted to the development of relationships between the synthesis conditions and the properties of PANI obtained by electrochemical polymerization [30-35]. Although these will not be discussed in this thesis, it is important to stress that these relationships are

complex and depend on many factors associated with the conditions, e.g. the acidity of the electrolyte solution and the molar ratio of the oxidant to the monomer.

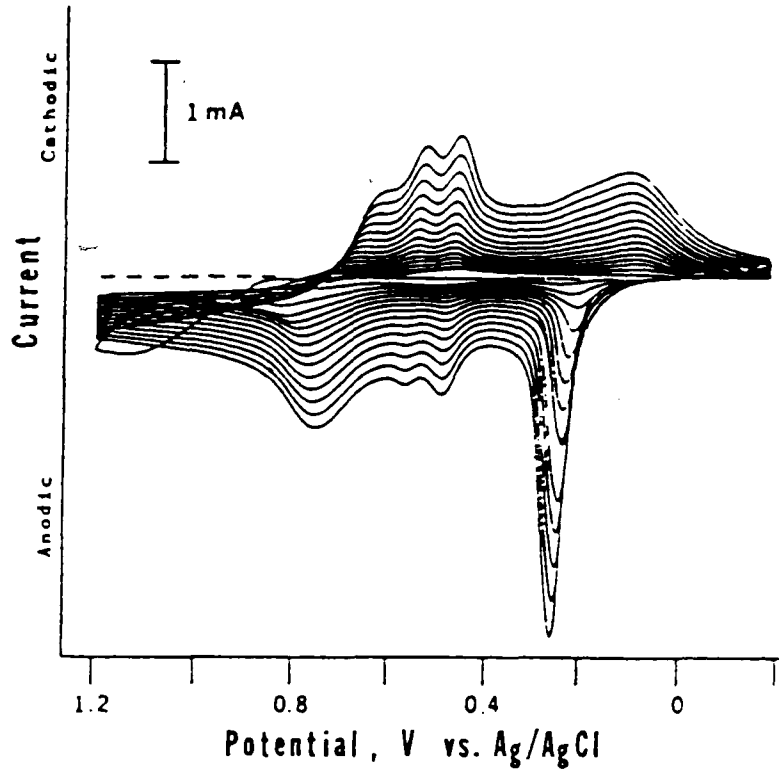

Figure 3.1 Cyclic voltammogram of electrochemical polymerization of aniline, in 1.0M H_2SO_4 at 50mV/s adopted from Ref. [29]

B. Chemical Oxidation

In order to obtain polymer films with reproducible properties, the chemical synthesis of PANI was investigated. This route is of particular importance since this is the feasible way for the large scale synthesis of polyaniline. The most commonly used chemical polymerization process involves the use of either hydrochloric acid or sulphuric acid in the presence of ammonium peroxydisulfate, $(NH_4)_2S_2O_8$, as an oxidant. The oxidative polymerization is a two-electron reaction and hence, requires one mole of peroxydisulfate per mole of monomer. However, a smaller quantity of oxidant is usually used to avoid the oxidative degradation of the resultant polymer. During polymerization, the anilinium cation radical is assumed to be an intermediate [36]:

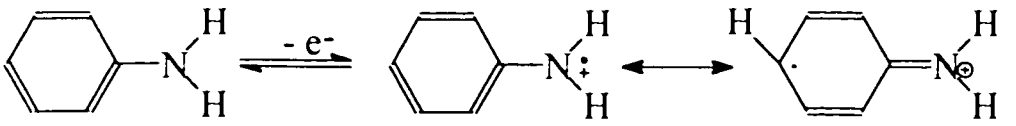

The peroxydisulfate is at the same time being reduced to sulfate :

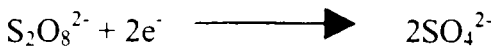

The aniline cation radical combines with another cation radical to form a dimer:

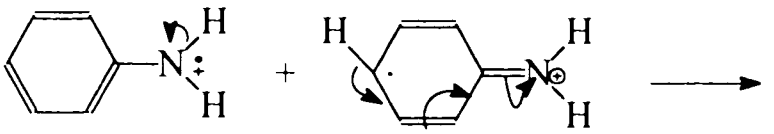

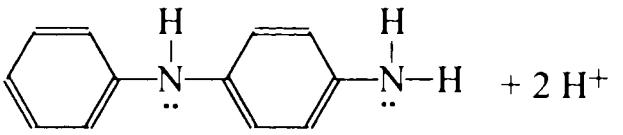

The oxidation potential of the dimer is less positive than the monomer. Thus the dimer is further oxidized and reacts with either another aniline radical cation in solution or with oligomeric or growing polymeric radical cations in a chain propagation step.

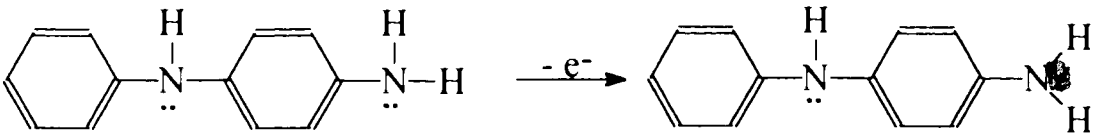

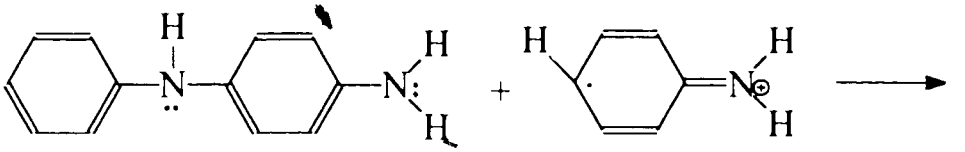

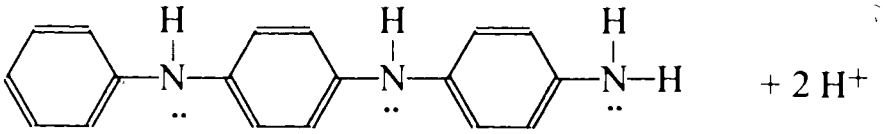

In the present study, polyaniline was synthesized by chemical oxidative polymerization of aniline in aqueous HCl solution, using ammonium peroxydisulfate as the oxidant according to Ref. [37]. Based on the kinetic salt effect [38], the reaction rate of reactant ions having the same sign is increased by increasing the ionic strength of the solution. Conversely, ions of opposite charge react slower in solution the higher the ionic strength of the solution. Therefore polyaniline was polymerized in the presence of dissolved LiCl in order to obtain polyaniline with high molecular weight. In this case, the addition of LiCl increases the ionic strength of the solution and therefore reaction between the anilinium ion and the peroxydisulfate ion is hindered while the chain propagation step, which involves the reaction of two radical cations, is enhanced. This leads to a smaller number of initiation reactions as well as an increase in the chain propagation reaction. The molecular weight of the polymer is therefore increased.

3.2. Processable Polyaniline

Polyaniline obtained by the above synthesis is in the emeraldine salt form, having Cl^- ions as counter ions in order to maintain electronic neutrality.

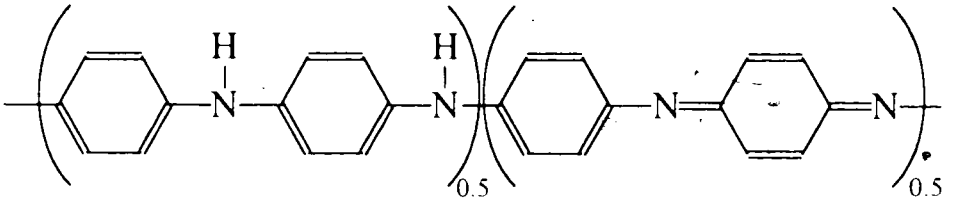

Emeraldine base

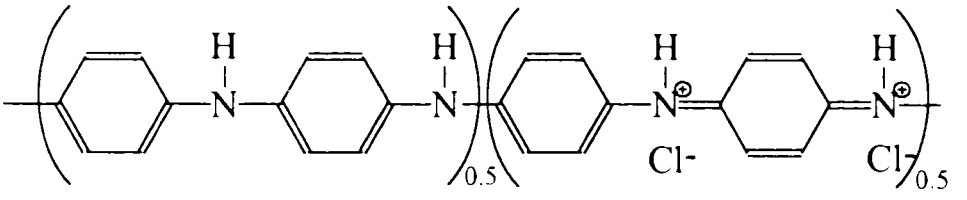

Emeraldine Salt

The emeraldine salt may be deprotonated upon stirring in NH_4OH solution to give the emeraldine base which is black in colour with a metallic lustre.

A major impediment to the development of conducting organic polymers is the intractability of these materials. Several methods have been reported to dissolve and process polyaniline [39-41]. For example, emeraldine base can be solubilized in N-methyl-pyrrolidinone, pyrrolidine, or in concentrated sulphuric acid and other strong acids. The processability of a doped, conducting form of polyaniline in common non-polar or weakly polar solvents was not reported unitl 1992 when Cao *et al.* [42] reported that polyaniline can be doped and simultaneously solubilized using functionalized protonic acid solutes. The functionalized protonic acids are generally denoted as $H^+(M^-R)$ where H^+M^- is the protonic acid group (e.g. sulfonic acid, carboxylic acid or phosphonic acid, etc.) and R is an organic functionality. The acid protonates the imine nitrogens of polyaniline and the (M^-R) group serves as the counter ion. In the conducting polymer community, this process is known as "doping" since it converts an insulating conjugated polymer to a conducting material. The R group is chosen to be compatible with non-polar or weakly polar organic solvents so that it solubilizes the polyaniline in these solvents in a similar manner to how a surfactant solubilizes oil in water. Among the variety of R groups reported, dodecylbenzenesulfonic acid (DBSA) and (±)-10-camphorsulfonic acid (CSA) showed best results [42]. Polyaniline doped by DBSA (PANI-DBSA) was reported to be soluble in toluene, xylene, decalin, chloroform, chlorobenzene, and polyaniline doped by CSA (PANI-CSA) was reported to be soluble in *m*-cresol, benzyl alcohol, chloroform and DMSO.

The method for inducing solution processability by using camphorsulfonic acid

was adopted in this thesis. The resulting PANI-CSA complex was dissolved in chloroform to yield a blue-green solution. A fine precipitate of undissolved polymer was also observed. In contrast, PANI-CSA dissolved completely in *m*-cresol to yield a dark green solution (5 mg/mL). However, due to the high viscosity of *m*-cresol polymer solution, casting films from this solvent was very slow. A binary solvent mixture of *m*-cresol and chloroform was therefore used in order to hasten the film preparation process. High quality, homogeneous films of conducting polyaniline were readily obtained from this solution.

3.3. Spectroscopic Characterization of PANI

Figure 3.2 shows the FT-IR spectrum of the emeraldine base obtained in the form of a KBr pellet (compressed powder). The IR peaks observed agree well with reported values [43,44]. The assignments of these vibrational signals are shown in Table 3.1.

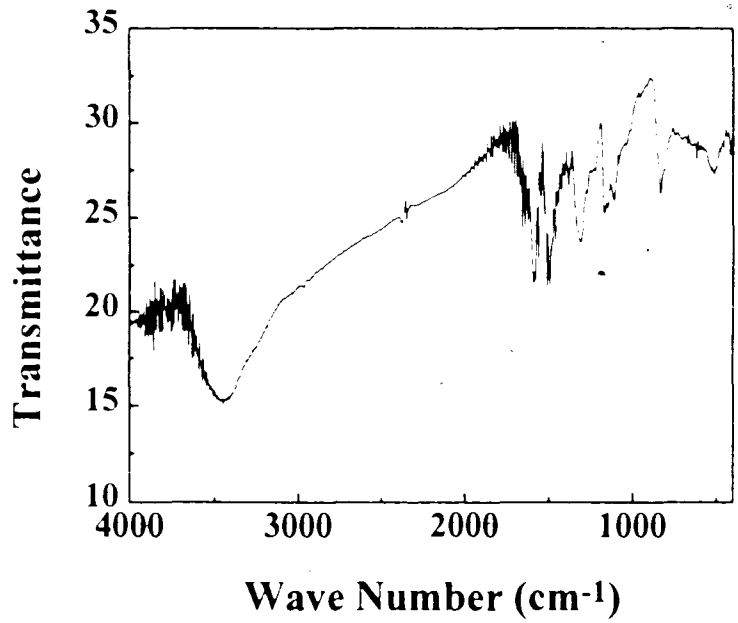

Figure 3.2 IR spectrum of PANI base.

Wave number (cm^{-1})	Peak Assignment
3456	N-H Stretch for 2° amine
3252	Hydrogen bonded NH band
2970	C-H stretch
1590	non-symmetric C_6 ring stretching (quinoid)
1505	non-symmetric C_6 ring stretching (benzoid)
1308	C-N stretch for 2° aromatic amine
1152	in-plane C-H bending
956	out-of-plane C-H bending
834	out-of-plane C-H bending

Table 3.1 Assignment of IR signals of polyaniline

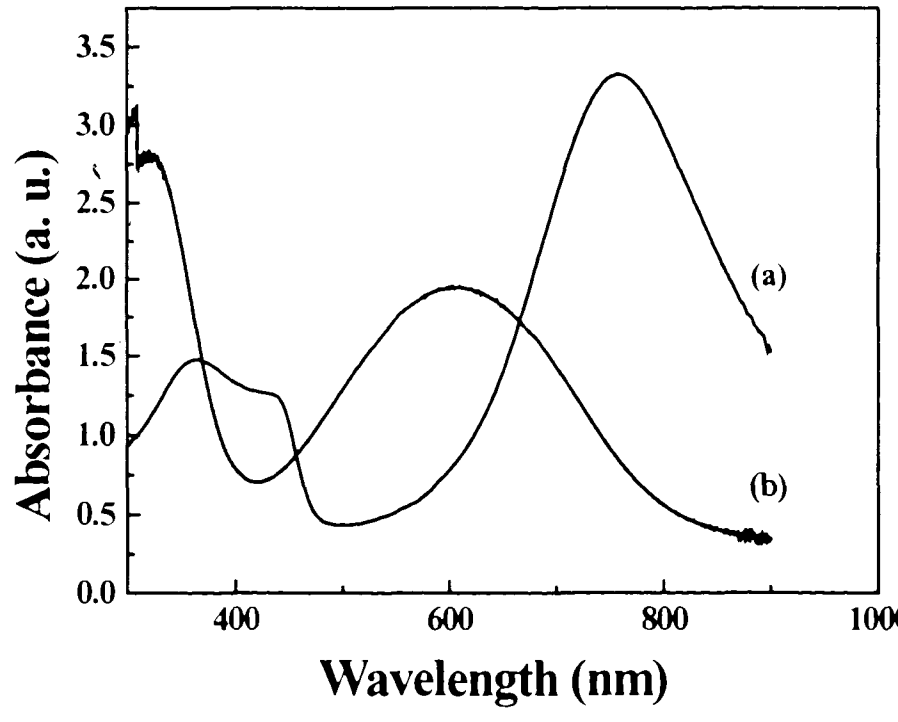

Figure 3.3 UV-Vis spectrum of (a) camphorsulfonic acid-doped polyaniline (PANI-CSA) film cast from *m*-cresol/chloroform solution, and (b) polyaniline base film cast from NMP solution.

Figure 3.3 shows the UV-vis absorption spectrum of polyaniline emeraldine base and camphorsulfonic acid-doped polyaniline in the form of a film cast from NMP and *m*-cresol/chloroform solution, respectively. The absorption at ~ 600 nm for the PANI base is assigned to the n - π * transition and the absorption at 330 nm is assigned to the π - π * transition [45]. For the camphorsulfonic acid doped-polyaniline, the absorption at 427 nm is due to the presence of localized semiquinone groups, i.e. polarons. The absorption at ~ 760 nm is due to the trapped exciton centred on quinoid moieties or due to delocalized free electron states.

3.4. Electrochemistry of Polyaniline

The aqueous electrochemistry of polyaniline films polymerized by electrochemical methods and the role of the conditions of polymerization on the film properties have been studied extensively [30-35]. Due to the lack of processability of the chemically synthesized polyaniline emeraldine salt, the electrochemistry of the chemically synthesized polymer was studied using an electrode prepared by impregnating the polyaniline salt solid into glass filter paper and subsequently wrapping a Pt gauze around it as described in the Experimental Section (Section 2.4.3.). However, the amount of polyaniline used in this method is not easily controlled. Figure 3.4(a) shows the cyclic voltammogram of the polyaniline emeraldine salt synthesized in our laboratory. With the development of processable polyaniline doped by camphorsulfonic acid, the electrochemistry of PANI can be studied easily by casting the polymer solution onto a Pt electrode to yield a homogeneous film with controllable thickness. Figure 3.4(b) shows a cyclic voltammogram of the camphorsulfonic acid doped polyaniline (PANI-CSA) in

0.5M H_2SO_4.

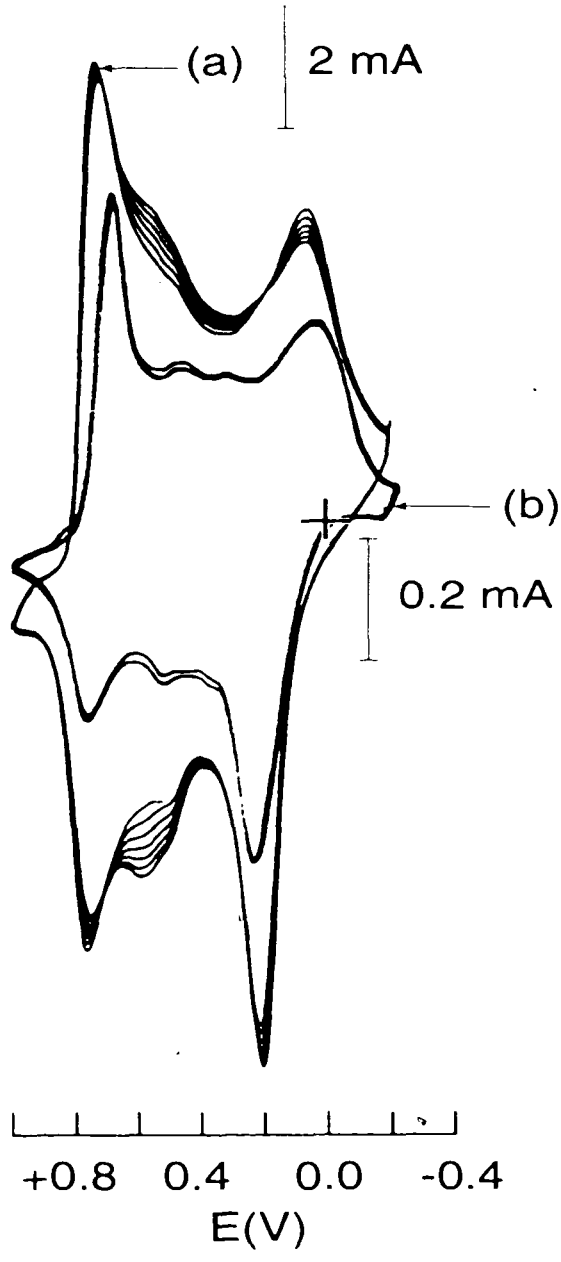

Figure 3.4 Cyclic voltammogram of (a) PANI salt in the form of a powder impregnated into a piece of glass filter paper and wrapped with a Pt gauze, (b) PANI-CSA film cast on a Pt electrode. Both are in 0.5 M H_2SO_4. Scan rate was 100 mV/s.

The electrochemistry of the PANI-CSA is identical to PANI-HCl. It consists of two sets of redox peaks. The first set of redox peaks occurs at ~ +0.15 V (vs. SCE). This set of peaks corresponds to the oxidation (and re-reduction) of the insulating leucoemeraldine

to the emeraldine form [46]:

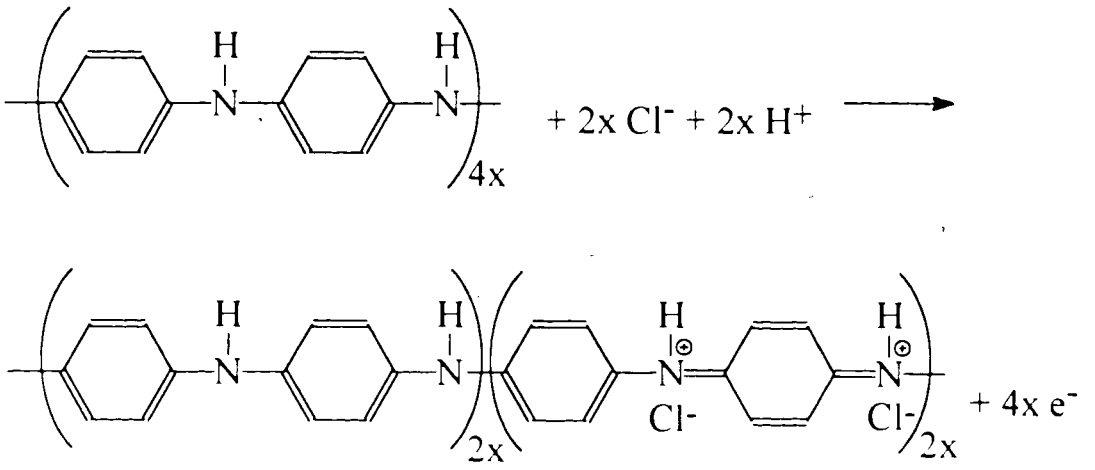

The second set of redox peaks appears at ~ +0.75 V (vs.SCE) and is associated with the oxidation (and re-reduction) of the emeraldine form to pernigraniline [46]:

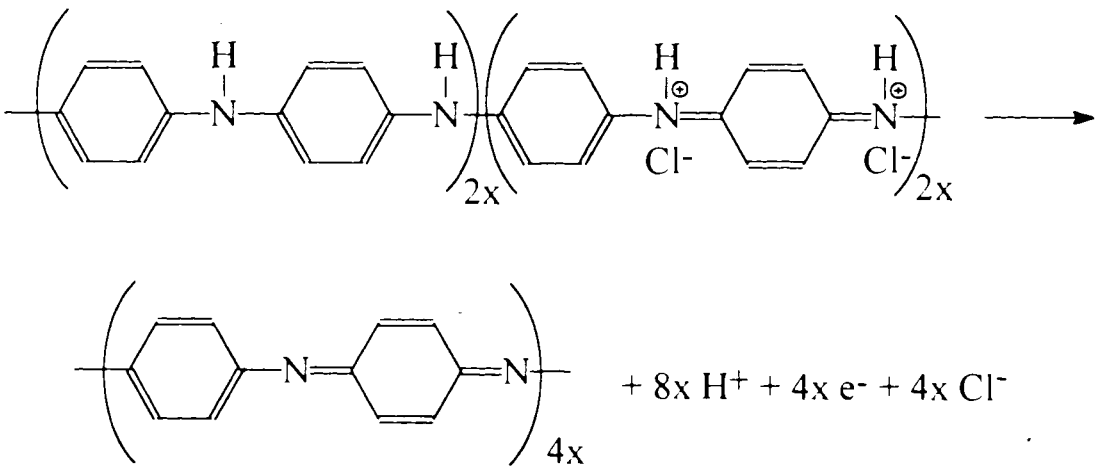

The electrochemistry of polyaniline changes gradually with continuous cycling (Figure 3.1). In addition to the two sets of redox peaks attributed to reversible redox chemistry of the polymer, a third set of peaks was observed to grow at ~ +0.5 V vs. SCE. This set of peaks increases steadily with increasing number of potential cycles as reported by other

researchers. Kobayashi *et al.* attributed the growth of this peak to redox reaction of benzoquinone groups [47]. Stilwell and Park suggested that these peaks could be due to the redox reactions of benzoquinone, *p*-aminophenol and/or the dimer *p*-aminodiphenylamine [48]. However, Genies *et al.* suggested that it is due to the phenazine insertion reaction, leading to a cross-linked polymer [49]. S.-M. Park *et al.* proposed the formation of a nitrene cation as an intermediate species during the growth of polyaniline (as shown below) [48]:

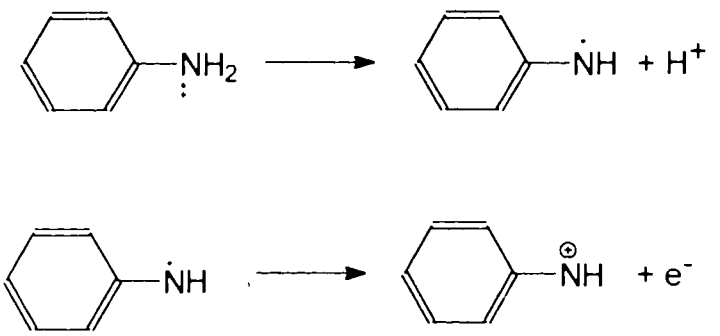

Depending on the reaction conditions, the nitrene cation can be polymerized to give polyaniline or can react with H_2O to give *p*-aminophenol and thereafter hydrolyzed to give benzoquinone. The presence of the nitrene cation also supports the formation of phenazine-type oligomers as a cross-linked product as suggested by Genies *et al.* [49]. The processes involved in the third set of redox peaks in polyaniline electrochemistry are summarized by the reactions shown in Scheme 3.1. [48]. Despite the fact that polyaniline can degrade upon continuously cycling, the stability of the polyaniline may be maintained if the experimental conditions are strictly controlled. It was reported that a relative stabilizing effect can be achieved if the anodic potential is kept less positive of +0.7 V (vs.SCE) [47]. Kobayashi *et al.* also reported very stable electrochromic behavior of up to 10^6 cycles when the potential was cycled between -0.2 V and +0.6 V (vs. SCE)

[47].

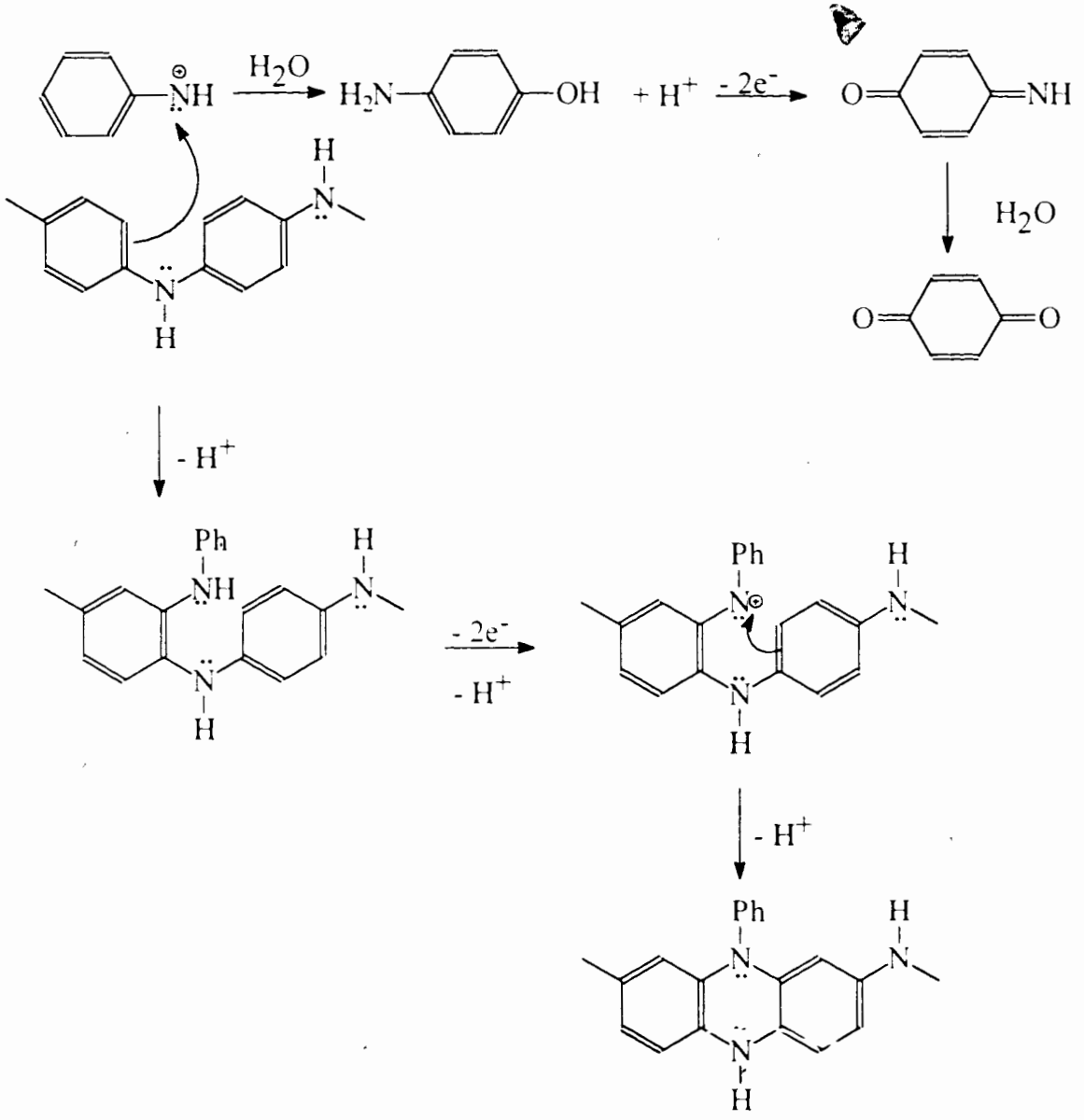

Scheme 3.1 Summary of reactions involving the degradation of polyaniline

3.5. Conductivity of Polyaniline

As described in Chapter 1 (Section 1.2.), conductivity through polyaniline can be attained either by protonic doping or redox doping. Redox doping can be achieved by a

chemical oxidant or by applying an appropriate electrochemical potential. In order for polyaniline to be considered as a matrix for an oxygen electrocatalyst, it must be conductive in the potential region of the oxygen reduction reaction. Therefore, an *in-situ* determination of the dependence of the electrical resistance of polyaniline versus electrochemical potential was carried out. Wrighton *et al.* reported the construction of a microband array of electrodes for *in-situ* determination of resistance of polymer films at different electrochemical potentials [50-52]. The array of microelectrodes were fabricated on a SiO_2 layer grown on a single crystal Si substrate by use of standard microfabrication techniques. Due to the difficulties in fabrication of the microband electrodes described by Wrighton, Zotti *et al.* reported a simple and reusable 2-band electrode which can be fabricated more easily [26]. A similar 2-band electrode was also constructed in this thesis work. The procedures for constructing this electrode were described in the Experimental Section (Section 2.4.2). Figure 3.5 shows the dimensions of the 2-band electrode constructed in our laboratory.

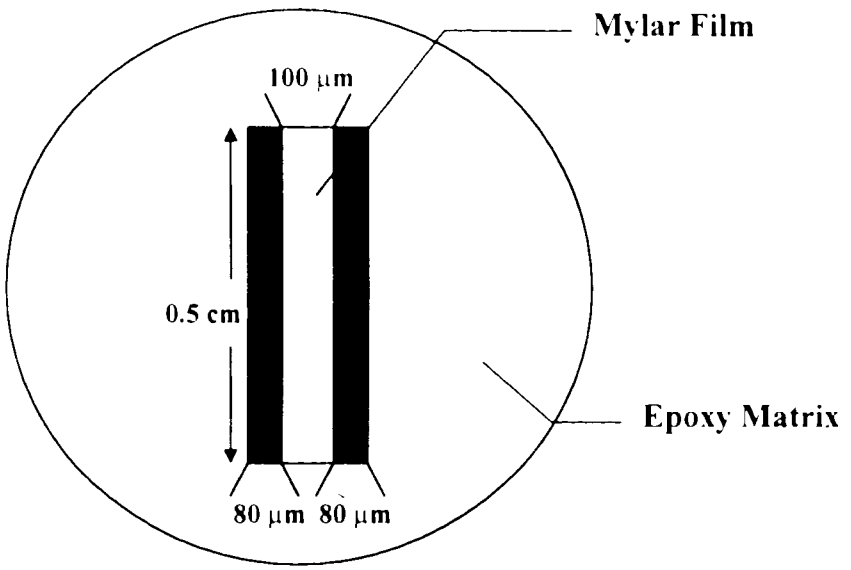

Figure 3.5 Top view of a 2-band Pt Electrode.

The two Pt band electrodes were separated by a layer of insulating Mylar film. To measure the conductivity profile of the polymer as a function of electrochemical potential, a film of polyaniline doped by camphorsulfonic acid was cast from the *m*-cresol/chloroform solution to cover both of the electrodes as shown in Figure 3.6.

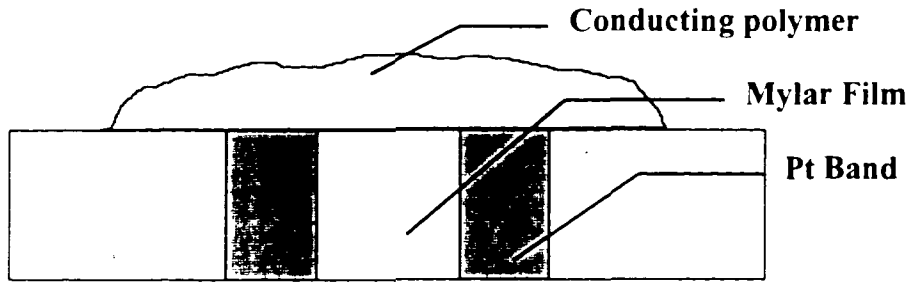

Figure 3.6 Cross-sectional view of the two-band Pt electrode with polymer deposited on it.

The electrical connectivity formed between the two electrodes by the presence of conducting polymer was examined by cyclic voltammetry. The electrodes were connected as in Figure 3.7.

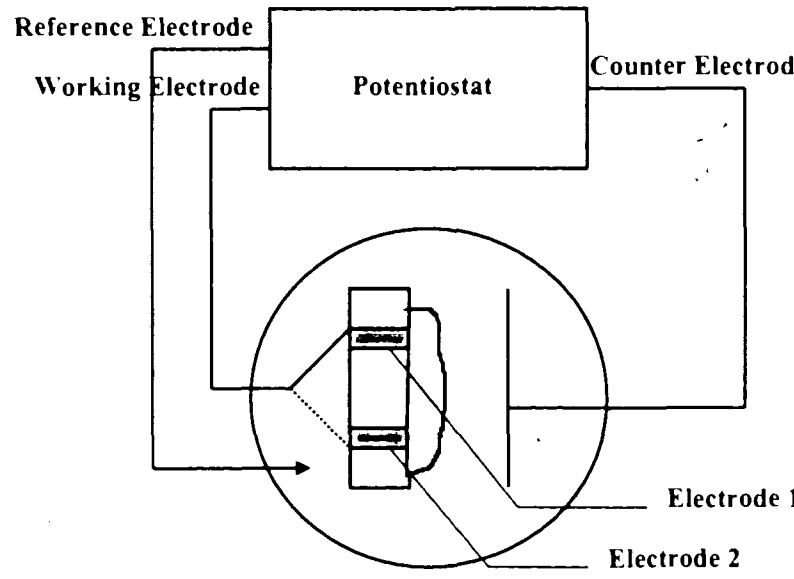

Figure 3.7 Circuit Diagram for the two-band electrode.

Figure 3.8(a) shows the cyclic voltammogram of PANI-CSA cast on the two-band electrode when only Electrode 1 was used as the working electrode. Figure 3.8(b) shows the cyclic voltammogram of PANI-CSA when only Electrode 2 was used as the working electrode under the same conditions. Figure 3.8 (c) shows the cyclic voltammogram of the PANI-CSA on the band electrode when both Electrode 1 and Electrode 2 were used simultaneously as the working electrode.

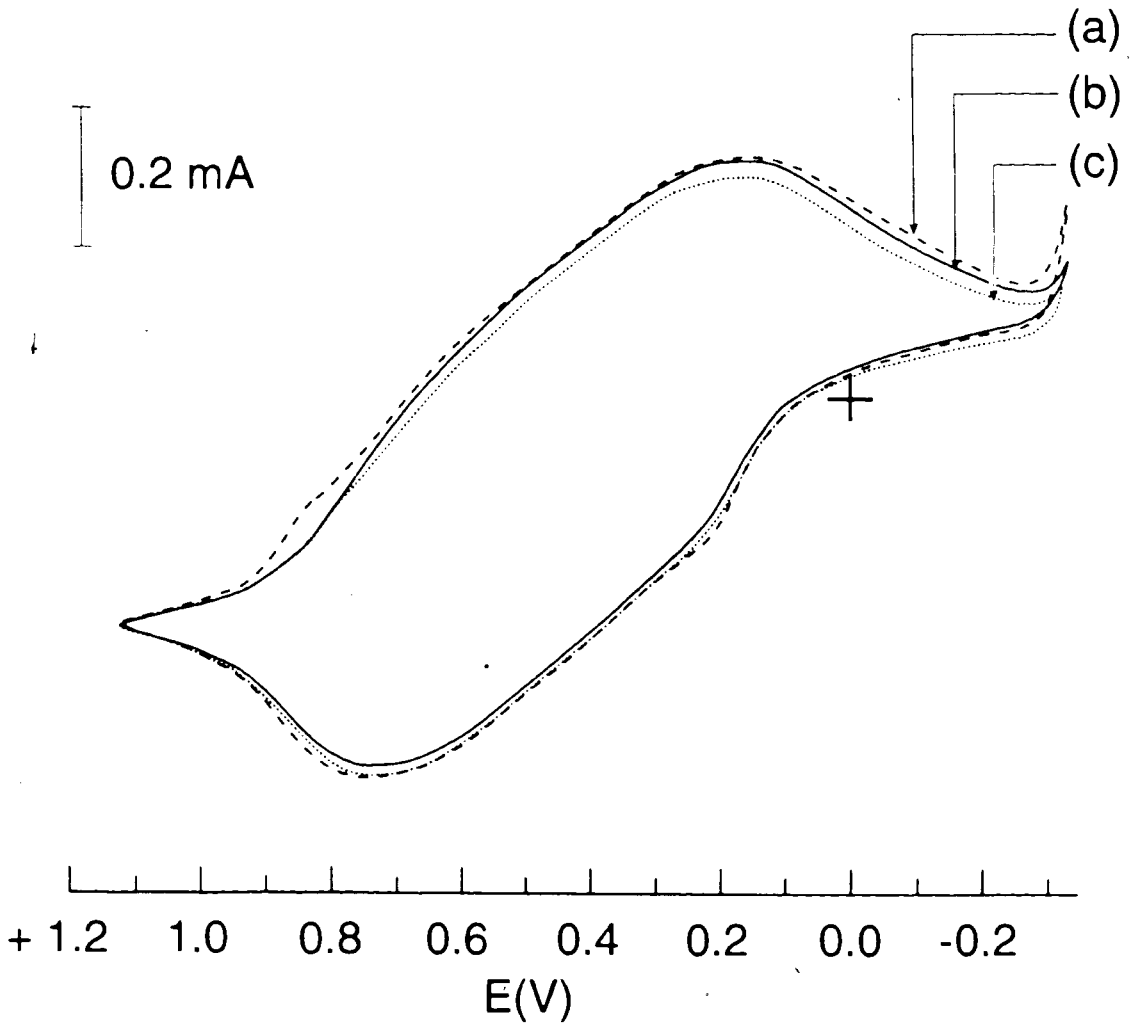

Figure 3.8 Cyclic voltammogram of PANI-CSA on the 2-band Pt electrode obtained in 0.5M H_2SO_4 at a scan rate of 100 mV/s, when the working electrode was (a) Electrode 1, (b) Electrode 2, and (c) both Electrode 1 and Electrode 2.

One can see that the cyclic voltammograms are very similar. This suggests that either one

of the electrodes was able to oxidize or reduce all the polymer spanning the 2 band electrodes when a potential was applied. This requires that the polymer spanning the 2 electrodes is conducting and therefore connects the 2 electrodes electronically. If there was no connection between the two electrodes, the cyclic voltammograms of the individual electrodes would have been different according to the amount of polymer present on that electrode. Moreover, if both of the electrodes were connected at the same time as the working electrode, the area under the cyclic voltammogram should have equalled to the sum of the area under the cyclic voltammograms of the individual electrodes. Therefore, it can be concluded that the PANI-CSA was conductive enough to connect the two-band electrode in this case. After verifying the connectivity between the two electrodes, the *in-situ* conductivity measurement of conductivity as a function of applied electrode potential was investigated as shown in the schematic diagram in Figure 3.9.

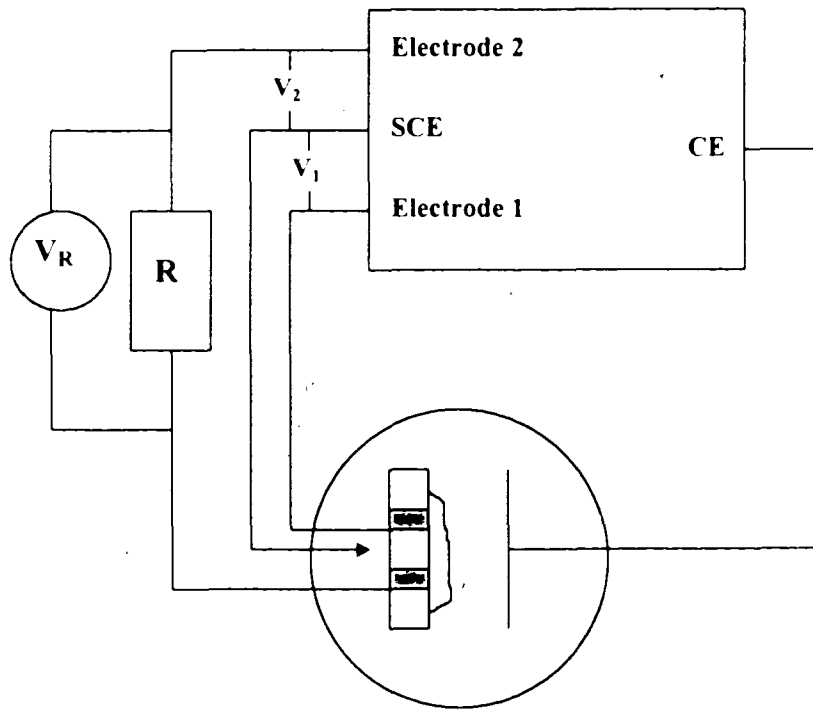

Figure 3.9 Schematic Diagram of the operation of the in-situ measurement of conductivity as a function of electrochemical potential.

Both of the electrodes were brought to an appropriate potential with respect to the SCE reference electrode. After attaining equilibrium, a small d.c. voltage difference (20 mV) was applied to Electrode 2. For example, both electrodes were brought to +1.0V vs. SCE, then Electrode 2 was brought up to +1.02V vs. SCE while Electrode 1 was kept at +1.0V vs. SCE. The potential difference between the two electrodes results in a flow of current across the polymer. Due to the small magnitude of the generated current, a large resistor R (1 kΩ) was connected in series with Electrode 2 and the voltage across the resistor was recorded. The magnitude of the current flow is an indication of the conductivity of the polymer - the more conductive the polymer, the higher the current flow across the polymer. Since $V_R = iR$, the potential difference across the resistor R was used as an indication of the conductivity of the polymer. Figure 3.10 shows the potential difference across resistor R as a function of electrochemical potential.

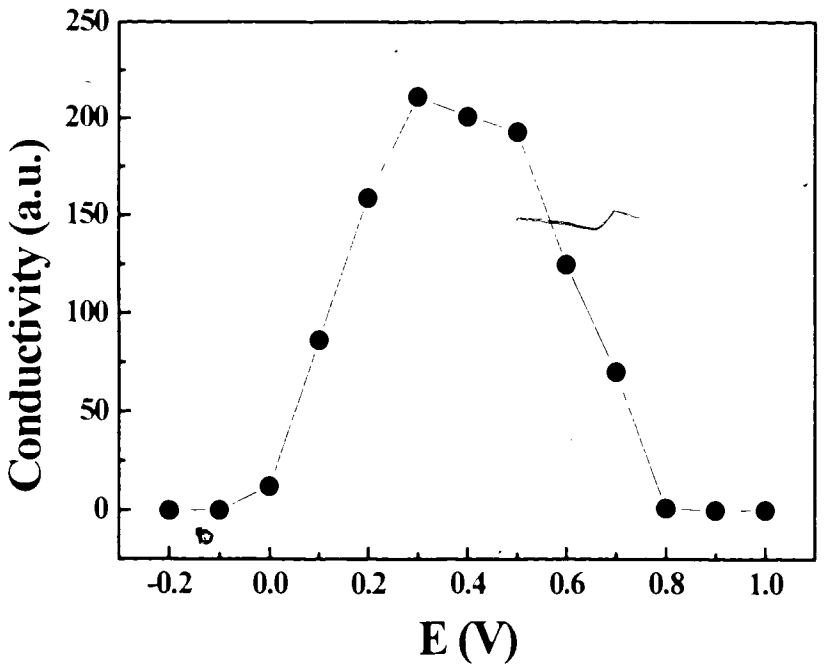

Figure 3.10 The conductivity of PANI-CSA as a function of electrochemical potential.

The PANI-CSA was found to be electronically conducting between 0.0 V and +0.7 V vs. SCE with maximum conductivity between +0.2 V and +0.5 V vs. SCE. This is in agreement with the published results in the literature [50]. Since the onset of the oxygen reduction reaction is ~ +0.6V vs. SCE, PANI-CSA is suitable to be used as a conductive matrix for Pt for the study of the oxygen reduction reaction.

3.6. Conclusions

Polyaniline was synthesized by the chemical polymerization of aniline in 1.0 M HCl. The polyaniline base was found to be soluble in N-methyl-2-pyrrolidinone while the emeraldine HCl salt of the polyaniline was insoluble in common organic solvents. Processable polyaniline solution was prepared by doping polyaniline base with camphorsulfonic acid and solubilizing it in *m*-cresol/chloroform solvent mixture. The polymer was characterized both by spectroscopic techniques and electrochemical techniques. The variation of the conductivity of polyaniline as a function of applied electrochemical potential was studied using a two-band Pt electrode constructed in our laboratory. Polyaniline was found to be conductive from 0.0 V to +0.7 V vs. SCE. With the versatility of the polymerization process, the processability of PANI-CSA, and the conductivity window of polyaniline, it was concluded that polyaniline is a good candidate to be used as a conductive matrix for Pt in the studies of the oxygen reduction reaction.

Chapter 4

Incorporation of Pt into Polyaniline-Modified Electrodes

The synthesis of polyaniline by chemical oxidative polymerization of aniline and the formation of processable solutions of polyaniline doped by camphorsulfonic acid was discussed in the last chapter. Films cast from such solutions were chosen as a matrix for depositing electrocatalyst. The incorporation of Pt into the matrix is discussed in this chapter. The incorporation of electrocatalyst was achieved by the electrochemical method and the electrodes obtained were evaluated for their morphology and electrocatalytic activity. Finally, in the last section, the diffusion properties of oxygen in the polymer matrix are described.

4.1. Electrochemical Deposition of Pt into PANI-CSA Films

Deposition of metal particles into polymer matrices is of general interest in the field of electrocatalysis [13-18,53]. Literature methods for preparing polymer modified electrodes involve polymerization of monomers, either chemically or electrochemically, onto the substrate electrode directly. Kao and Kuwanan dispersed Pt into poly(vinylacetic acid) (PVAA) for the electrocatalytic generation of hydrogen [53]. The PVAA films were formed on a glassy carbon substrate electrode by refluxing in the monomer solution. Holdcroft and Funt deposited Pt into polypyrrole for the electrocatalytic reduction of O_2 [18]. Kao also deposited Pt into polyaniline for the reduction of hydrogen and oxidation of methanol [16]. They reported that a three dimensionally dispersed Pt system was obtained. In both studies, the conducting polymers were grown on the substrate electrode by electropolymerization. However, this technique is inconvenient because polymer

synthesis has to be performed for fabrication of each polymer modified electrode. Moreover, the polymer matrices formed from electropolymerization are technically limited by the type of electrode substrates.

In this work, polyaniline was synthesized chemically instead of electropolymerizing it directly onto the substrate electrode. A polymer solution was obtained which was readily cast onto a wide variety of electrode substrates and electrode geometries. This provided a convenient and practical method to prepare polymer modified electrodes in a reproducible manner. In order to incorporate Pt into the polymer films, the method of electrochemical reduction of K_2PtCl_6 was adopted, because it has been previously reported that this method allows Pt to be dispersed homogeneously into polymer matrices [16]. The Pt loading was determined by monitoring the amount of charge passed for the reduction of Pt (IV) to Pt(0). It was also assumed that this is a complete four-electron reduction step (Eqn. 4.1). The calculations used to determine the Pt content are shown below:

$$Pt(IV) + 4e^- \longrightarrow Pt(0) \qquad \text{[Eqn. 4.1]}$$

$$\textit{Pt loading (grams)} = \frac{QM_{Pt}}{4Ne} \qquad \text{[Eqn. 4.2]}$$

where Q = cathodic charge passed in C

M_{Pt} = atomic mass of Pt (195.08g/mol)

N = Avogadro's Number (6.02×10^{23})

e = electronic charge (1.62×10^{-19} C)

$$Pt\ loading\ (\mu g/cm^2) = \frac{Pt\ loading\ (grams) \times 10^6}{A} \qquad \text{[Eqn. 4.3]}$$

where A = geometric area of the electrode (cm^2)

The electrodeposition process is described below. A polyaniline modified electrode was immersed in a 1 mM K_2PtCl_6 solution and the electrode was connected to a coulometer in order to record the cathodic charge. The electrode was cycled between +0.5 V and -0.3 V vs. SCE. The growth of Pt could be observed by the increase in the hydrogen evolution peak on Pt at around -0.2 V vs. SCE in the cyclic voltammograms (Figure 4.1). The PANI-CSA modified electrode containing electrochemically deposited Pt was denoted **PANI-CSA/Pt**.

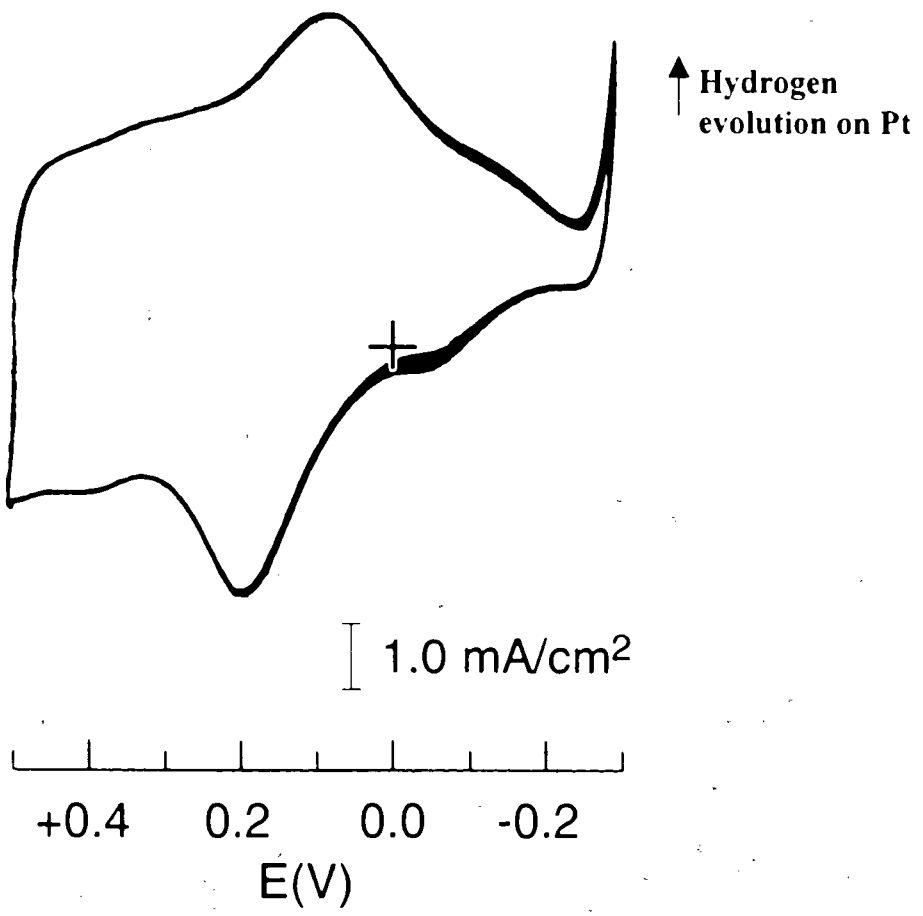

Figure 4.1 Cyclic voltammogram showing the incorporation of Pt into a PANI-CSA modified glassy carbon electrode. The potential was cycled between +0.5 V and -0.3 V vs. SCE, scan rate = 100 mV/s, in 1 mM K_2PtCl_6/0.5 M H_2SO_4.

Due to the large background charge associated with reduction of polyaniline itself, the charge for the reduction of K_2PtCl_6 was determined by subtracting the cathodic charge associated with the reduction of PANI in 0.5M H_2SO_4 in the absence of K_2PtCl_6.

Figure 4.2 shows the cyclic voltammograms of polyaniline modified electrodes before and after electrodeposition of Pt in O_2 saturated 0.5 M H_2SO_4.

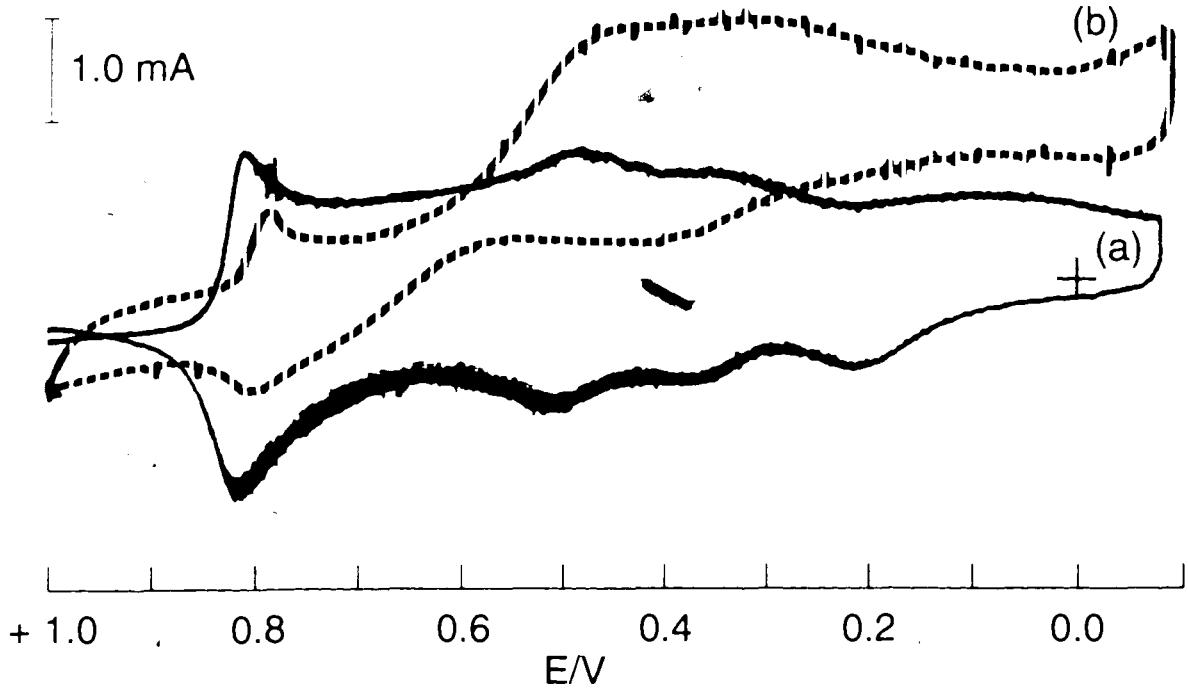

Figure 4.2 Cyclic voltammogram of PANI-CSA modified glassy carbon electrode (a) before and (b) after incorporation of Pt (film thickness = 0.44 μm, Pt loading = 23 μg/cm^2), in O_2 saturated 0.5 M H_2SO_4, scan rate = 5 mV/s.

It can be seen that in the absence of Pt, a typical cyclic voltammogram of polyaniline was obtained. After deposition of Pt, the cathodic current increased due to the reduction of O_2 on Pt. A rotating disk experiment was performed on the PANI-CSA/Pt modified electrode and the results are shown in Figure 4.3.

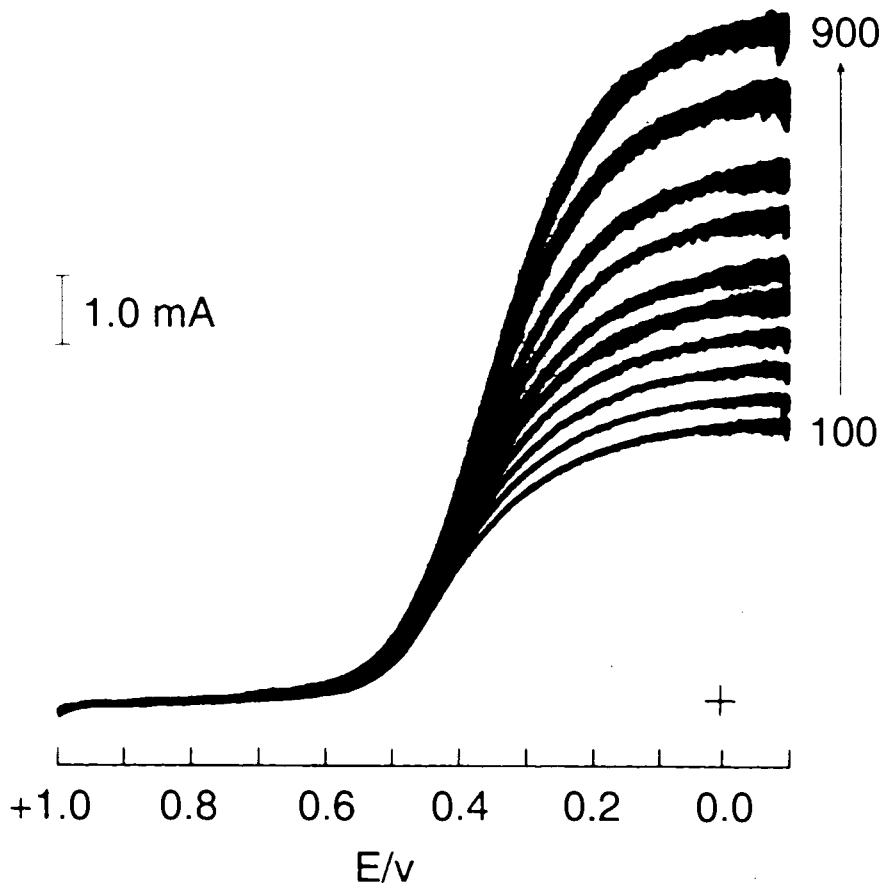

Figure 4.3 Rotating disk voltammograms of a PANI-CSA/Pt modified glassy carbon electrode (film thickness = 0.44 μm, Pt loading = 23 μg/cm^2) in O_2 saturated 0.5 M H_2SO_4, scan rate = 5 mV/s. Rotation speeds: 100, 120, 150, 200, 250, 300, 400, 500, 700 and 900 rpm.

The onset of the oxygen reduction reaction was observed at ~ +0.6 V vs. SCE and a plateau region was observed for all rotation speeds. The limiting current was observed to increase with the rotation speed. A Levich plot (i_l vs. $\omega^{1/2}$) for the oxygen reduction reaction at a PANI-CSA/Pt modified glassy carbon electrode in an O_2 saturated 0.5 M H_2SO_4 solution is shown in Figure 4.4. A linear relationship between the limiting current for the oxygen reduction reaction, i_l, and the square root of the rotation speed, $\omega^{1/2}$, was obtained.

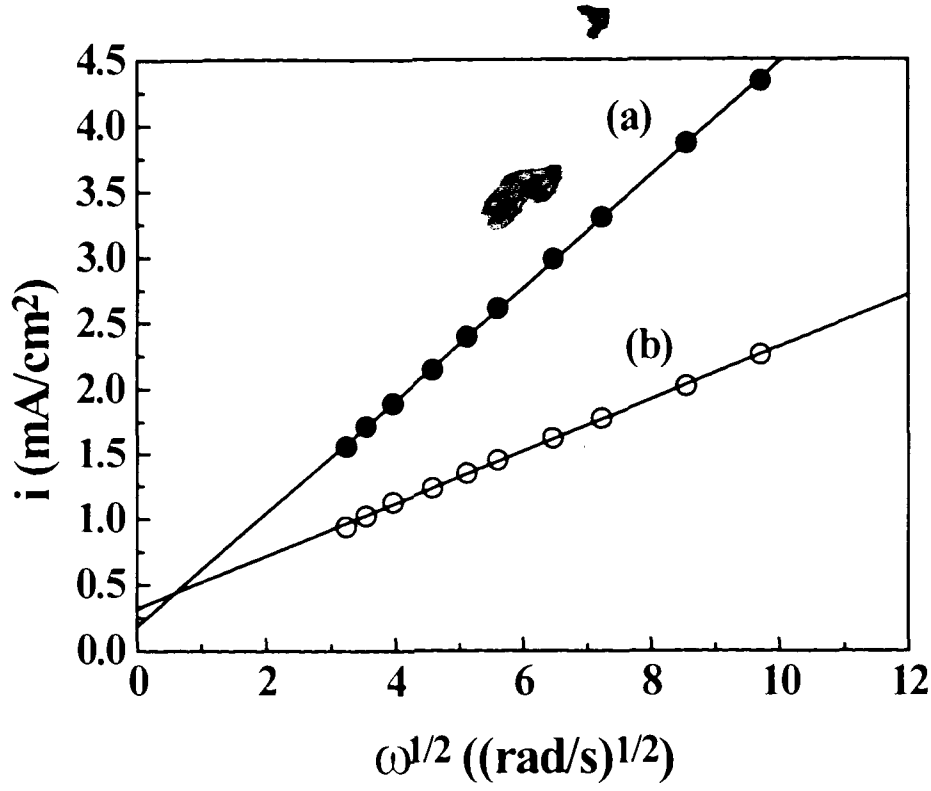

Figure 4.4 Levich plot for O_2 reduction reaction at (a) a bare Pt electrode, (b) a PANI-CSA/Pt(23 μg/cm^2) modified glassy carbon electrode, in O_2 saturated 0.5M H_2SO_4, scan rate = 5mV/s.

For comparison, the Levich Plot for the oxygen reduction reaction at a Pt rotating disk electrode in an O_2 saturated 0.5 M H_2SO_4 solution is shown. The Levich plots for both electrodes are linear. In another study, Holdcroft and Funt reported a curved Levich plot for oxygen reduction at a Pt incorporated polypyrrole modified electrode [18]. They attributed the curvature to diffusion limitation of O_2 through the polypyrrole film, i.e. O_2 reduction is limited by the rate of diffusion of O_2 to Pt particles through the film and not by the rate it is brought up to the polymer/electrolyte interface. A linear Levich plot in this case suggests that the reactant gas was not impeded from reaching the electrocatalyst due to poor diffusion through the film. Two possible scenarios can lead to this observation: (1). The Pt was dispersed homogeneously through the bulk of the polymer

but polyaniline is sufficiently permeable to enable rapid diffusion of O_2 to the Pt particles; or (2), the Pt particles were deposited on the surface of the polymer film, i.e. at the polymer/electrolyte interface so that O_2 has only to diffuse through the electrolyte solution in order to reach the catalytic electrode surface. In the latter, polyaniline is acting merely as an electrically conductive layer which provides the electrons a conductive pathway between the glassy carbon substrate electrode and the Pt particles. This scenario should be very similar to a pure Pt electrode because the diffusion properties of the solution species through the polymer do not affect the current. In order to determine which situation was present, the depth profile of the PANI-CSA/Pt electrode was studied by Auger Electron Spectroscopy.

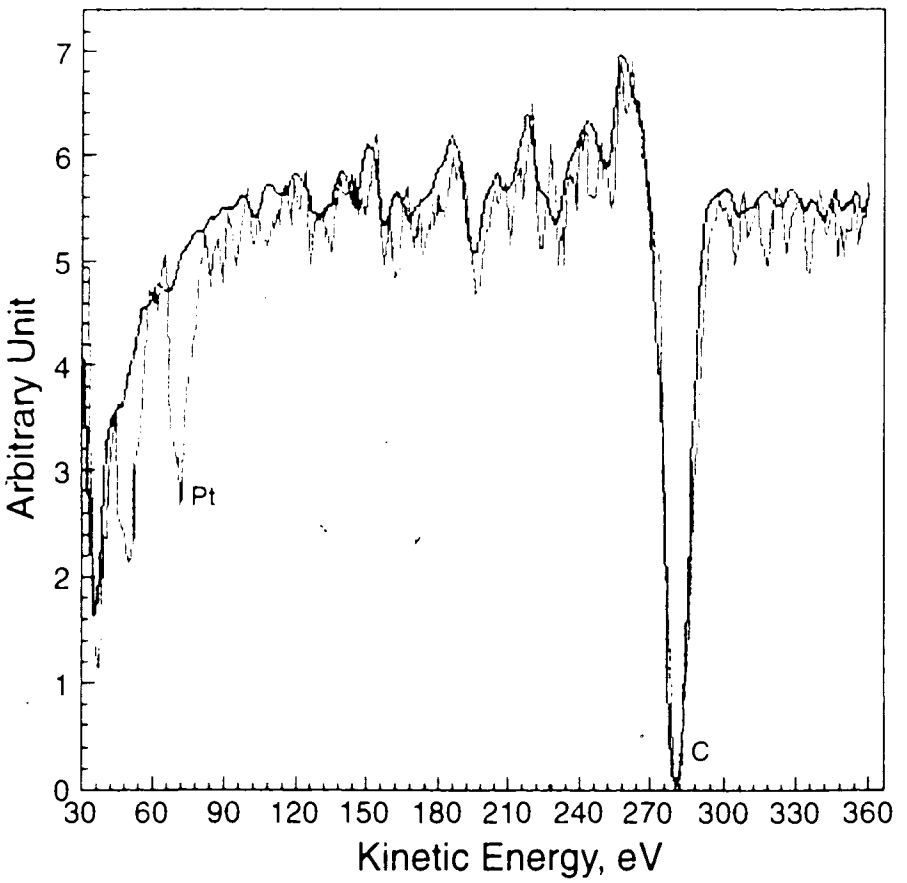

Figure 4.5 Auger electron spectrum of a PANI-CSA/Pt modified electrode before (gray line) and after 20 seconds sputtering (black line).

Auger electron spectra were obtained for the surface of the PANI-CSA/Pt film prepared as described in section 4.1. A large Pt peak at 64 eV and a carbon peak at 273 eV were observed on the sample substrate before sputtering the films (Figure 4.5). Then the polymer surface was sputtered with an Ar^+ ion beam for 20 seconds in order to remove the top layers of the polymer surface. Twenty seconds is a relatively short sputtering time, as a comparison, it took ~ 20 minutes of continuous sputtering to completely etch the 2000 nm film. From the time required to etch through a film of 2 μm, it was estimated that about 30-40 nm of the polymer film was removed during the 20-second sputtering process. It appears that the Pt particles were mainly deposited on the top 30-40 nm of the polymer film. The spatial distribution of Pt in this electrode is illustrated in Figure 4.6.

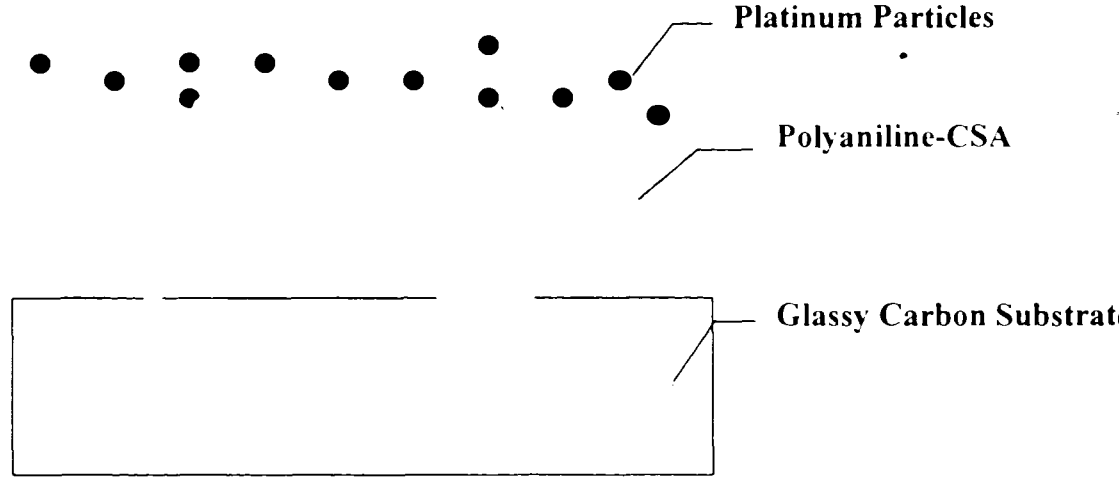

Figure 4.6 Proposed spatial distribution of Pt in the PANI-CSA/Pt modified electrode. Pt was incorporated by electrochemical reduction of K_2PtCl_6 at a PANI-CSA modified electrode.

An important conclusion from these experiments is that polyaniline is sufficiently conductive in the potential region required for oxygen reduction reaction to provide an electronic pathway between the substrate electrode to the electrocatalyst. If it was not,

then the Pt particles would have been electrically isolated from the glassy carbon current collector and no electrocatalytic activity would have been observed. Thus, PANI satisfies one of the requirements in the design of matrices for the electrocatalytic reaction of a solution species, even though a three-dimensionally dispersed catalytic system was not obtained in the present case.

The electrocatalytic activity of these catalytic films was investigated further and compared to other modified electrodes. The catalytic property of the PANI-CSA/Pt electrode was first compared to a bare glassy carbon electrode onto which the same amount of Pt was deposited, as illustrated in Figure 4.7 (i.e. the conducting polymer matrix was absent).

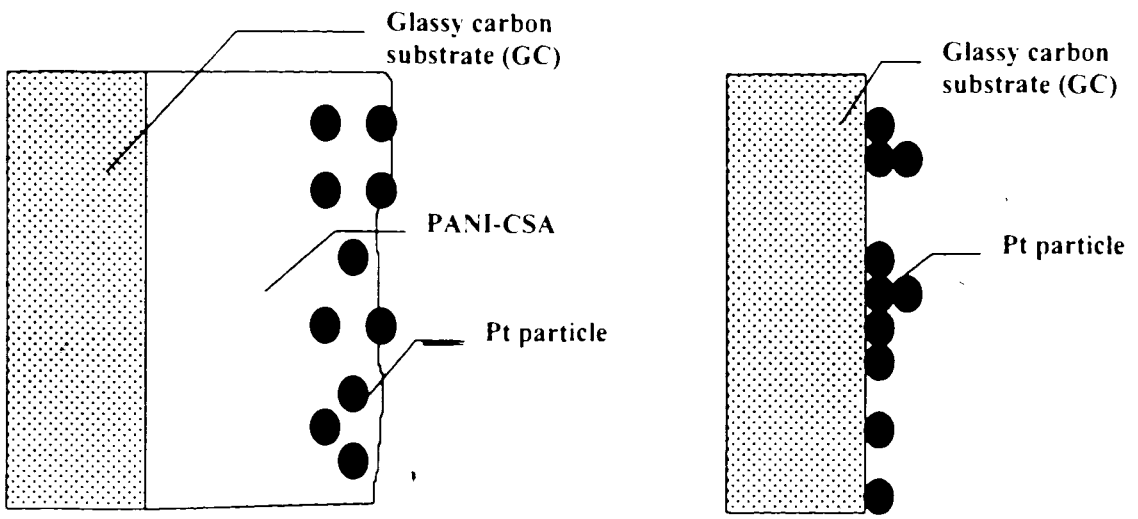

Figure 4.7 Schematic illustration of two Pt-modified electrodes examined for electrocatalytic reduction of O_2: (a) PANI-CSA/Pt (23 μg/cm^2) electrode; (b) GC/Pt (24 μg/cm^2) electrode.

In these studies, the same mass of Pt was deposited on both a polyaniline modified glassy carbon electrode and a bare glassy carbon electrode by electrochemical reduction of K_2PtCl_6, using potential cycling between +0.5 V and -0.3 V (SCE). Their electrocatalytic activities towards the oxygen reduction reaction were compared using

rotating disk voltammetry. Figure 4.8 shows the Levich plots for these two electrodes for O_2 reduction in an O_2-saturated 0.5 M H_2SO_4 solution. It can be seen that the current for the oxygen reduction reaction is higher in the case of Pt deposited onto the polyaniline-modified electrode. Since the diffusion coefficient and the concentration of O_2 in the electrolyte are the same in both cases, and the same amount of catalyst was deposited in each case, the increase in current is indicative of an increase in the active surface area of the Pt catalyst. It is postulated that the Pt microparticles in the polyaniline penetrate the polymer film to a certain extent (but less than 30-40 nm), hence exposing a larger surface of the catalyst to the electrolyte and the reactants. This shows preliminary evidence that an increase in the active surface area of the catalyst is achieved by its dispersion into a polymer matrix.

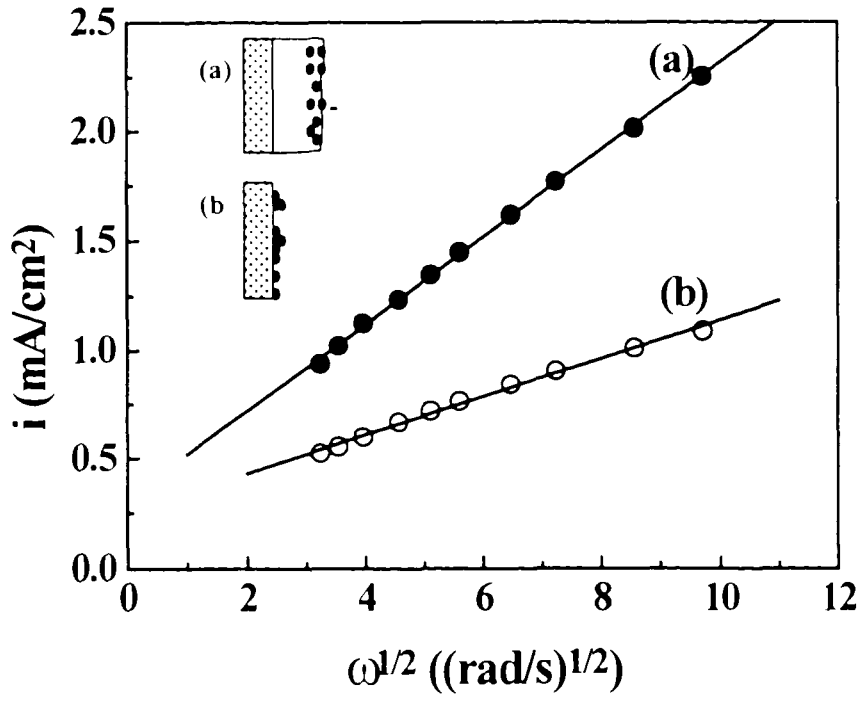

Figure 4.8 Levich plots for O_2 reduction at (a) PANI-CSA/Pt (23 μg/cm^2) modified GC electrode, (b) a bare GC onto which 24 μg/cm^2 Pt has been electrodeposited. O_2 saturated 0.5 M H_2SO_4, scan rate = 5 mV/s.

4.2. Permeability of Oxygen Through PANI-CSA Films

Pt microparticles were deposited mainly on the surface of the PANI-CSA electrode as described above. Although this resulted in an increase in the active surface area of the Pt, a three-dimensionally dispersed catalytic system was desired in order to maximize the active surface area of the Pt as illustrated in Figure 4.9. If this type of electrode were achieved, then the ability of the solution species to diffuse through the polymer would play a major role in the rate of electrocatalysis. If the diffusion of the reactant through the matrix were not fast enough, Pt microparticles deep inside the matrix would not be fully utilized.

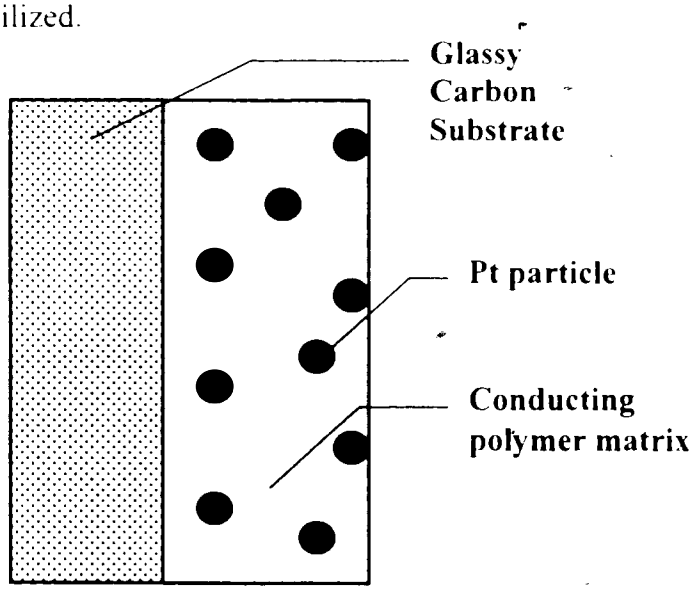

Figure 4.9 Illustration of polymer modified electrode with Pt homogeneously dispersed throughout the polymer film.

In order to investigate O_2 mass transport through the PANI-CSA films, a Pt rotating disk electrode was used, onto which a thin film of PANI-CSA was cast. Rotating disk electrode voltammetric experiments were carried out in oxygen-saturated 0.5 M H_2SO_4 at a scan rate of 5 mV/s. Figure 4.10 shows the Levich plot for oxygen reduction at a polyaniline-modified Pt electrode in O_2 saturated 0.5 M H_2SO_4. The Levich plot for

oxygen reduction at a bare Pt electrode under the same conditions is shown for comparison. In contrast to the linear plot for the bare Pt electrode, the plot for the PANI-CSA-modified Pt electrode deviates from linearity at higher rotation speeds, indicating that the diffusion of O_2 to the Pt substrate electrode is impeded by the polyaniline film.

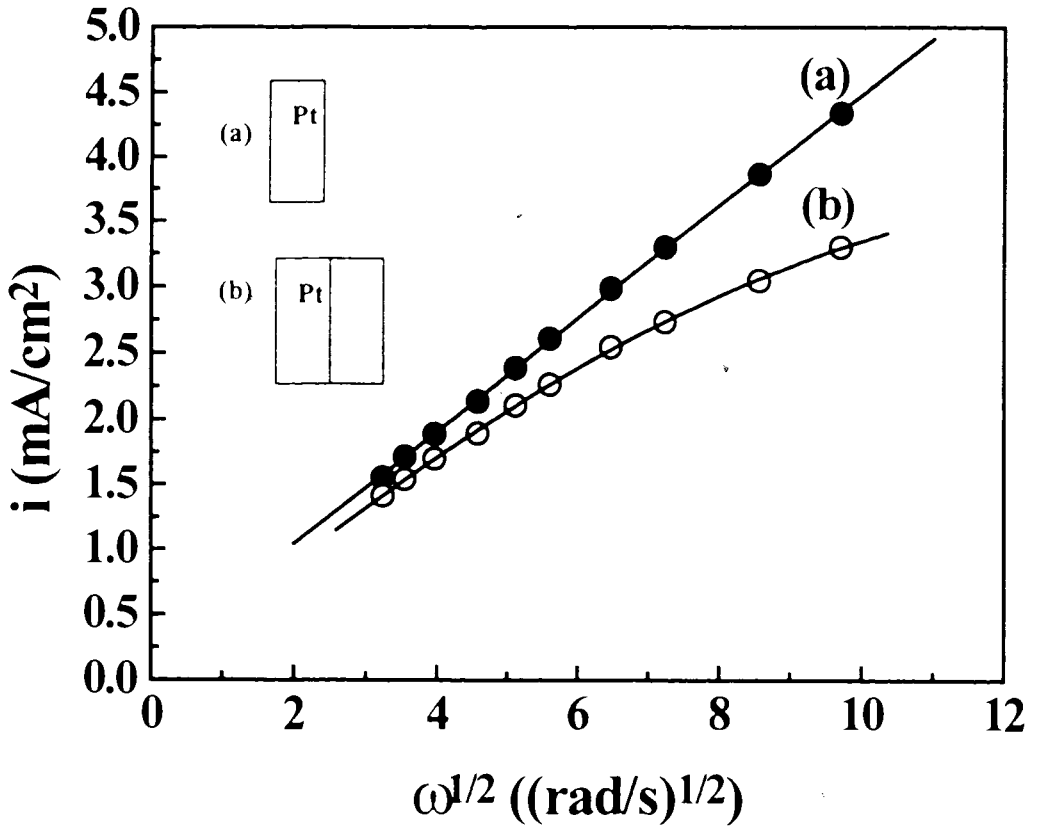

Figure 4.10 Levich plot for oxygen reduction reaction at: (a) a bare Pt electrode, (b) a PANI-CSA (0.9±0.1μm)-modified Pt electrode in O_2 saturated 0.5M H_2SO_4, scan rate = 5mV/s.

The permeability, D_fC_f, of the polymer film towards O_2 diffusion can be obtained by plotting 1/i vs. $1/\omega^{1/2}$. This is called a Koutecky- Levich plot. The relationship between the measured current and rotation speed is given in Chapter 1. For a planar, rotating disk electrode with a reaction species in solution, the limiting current at high overpotentials is given by Eqn.1.5.

$$i_L = 0.62nFAC_o D^{2/3} \upsilon_k^{-1/6} \omega^{1/2} \qquad \text{[Eqn. 4.4]}$$

For a polymer modified electrode, the limiting current measured is given by Eqn. 1.7.

$$\frac{1}{i} = \frac{1}{i_k} + \frac{1}{i_f} + \frac{1}{i_L} \qquad \text{[Eqn.4.5]}$$

Expanding Eqn.4.5 by substitution gives:

$$\frac{1}{i} = \frac{1}{i_k} + \frac{d}{nFD_f C_f} + \frac{1}{0.62nFAC_o D^{2/3} \upsilon_k^{-1/6} \omega^{1/2}} \qquad \text{[Eqn. 4.6]}$$

where i = measured current (A),

i_k = kinetic current (A),

i_f = diffusion current through the film (A),

i_L = diffusion current through the electrolyte (A),

D_o = diffusion coefficient of reactant in the electrolyte (cm^2s^{-1})

C_o = concentration of reactant in the electrolyte (mol cm^{-3})

D_f = diffusion coefficient of reactant in the film (cm^2s^{-1}),

C_f = concentration of reactant in the film (mol cm^{-3})

d = thickness of the polymer film (cm),

n = number of electrons involved,

F = Faraday's Constant ($Cmol^{-1}$),

ω = electrode rotating speed (rad s^{-1})

ν_k = kinematic viscosity

The Levich plot (i vs. $\omega^{1/2}$) obtained from Eqn. 4.4 is independent on the

thickness of the polymer film. From Eqn. 4.5, we can see that the measured current is composed of the kinetic current, i_k, the diffusion current through the polymer film, i_f, and the diffusion current through the electrolyte solution, i_l. The slope of the Koutecky-Levich plot gives information on the mass transport of the reactant species in the electrolyte while the intercept of the plot gives information about the permeability, D_fC_f, of the same species through the polymer film. The diffusion current through the polymer film, i_f, is inversely proportional to the thickness of the film, i.e., the thicker the polymer film, the smaller the diffusion current. Figure 4.11 shows the Koutecky-Levich plots for oxygen reduction of polyaniline modified Pt electrodes possessing different polymer thickness.

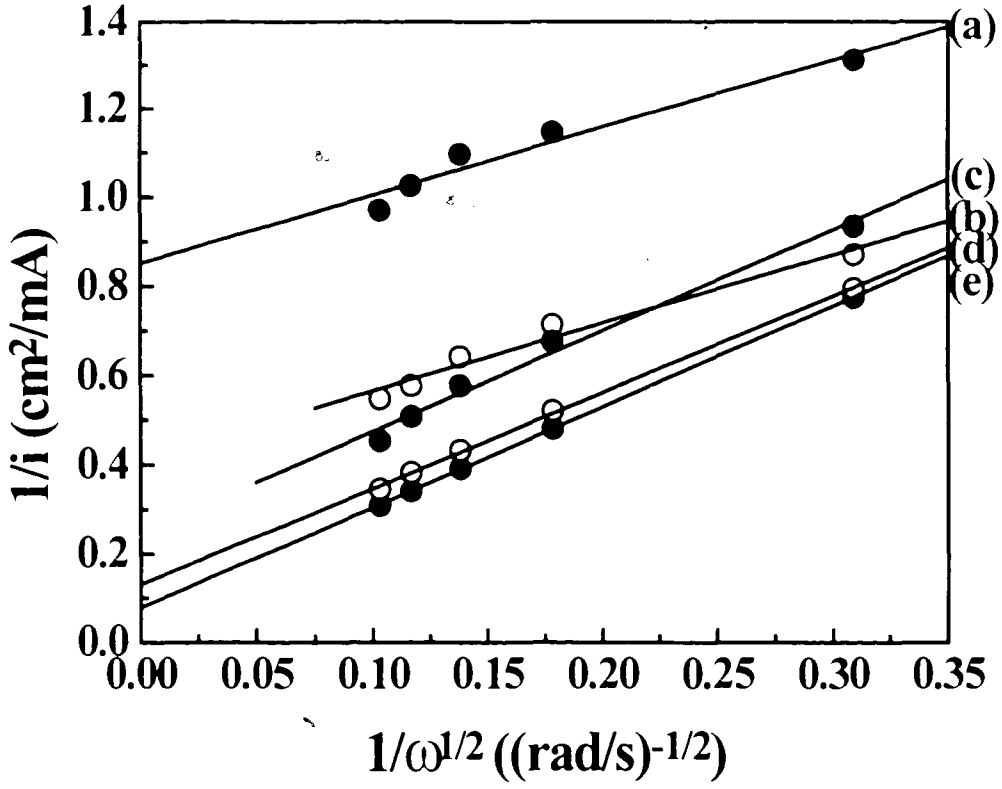

Figure 4.11 Koutecky-Levich plot for oxygen reduction at a PANI-CSA modified Pt electrode (area = 0.159cm^2), in O_2-saturated 0.5 M H_2SO_4; scan rate = 5 mV/s; thickness of films : (a) 2.4 μm, (b) 1.9 μm, (c) 1.5 μm, (d) 1.0 μm, (e) 0.5 μm.

One can see that although polyaniline modified Pt electrodes yield curved Levich plots, the plot of 1/i against $1/\omega^{1/2}$ yields straight lines. From Figure 4.11, it can be observed that the thicker the film, the larger the intercept, which corresponds to a smaller oxygen reduction current. The permeability of the PANI-CSA was determined by plotting the intercepts of the Koutecky-Levich plots against the film thickness (Figure 4.12). From the slope of this graph, which is equal to $1/nFAD_fC_f$ (Eqn. 4.3), the O_2 permeability, D_fC_f, of PANI-CSA films in 0.5 M H_2SO_4 was calculated to be 1.18 x 10^{-12}mol cm^{-1} s^{-1}. The permeability of O_2 in a 0.5 M H_2SO_4 solution was reported as 20.3 x 10^{-12} mol cm^{-1} s^{-1} [64]. The permeability of O_2 in the PANI-CSA films is only 1/20 that 0.5 M H_2SO_4 solution.

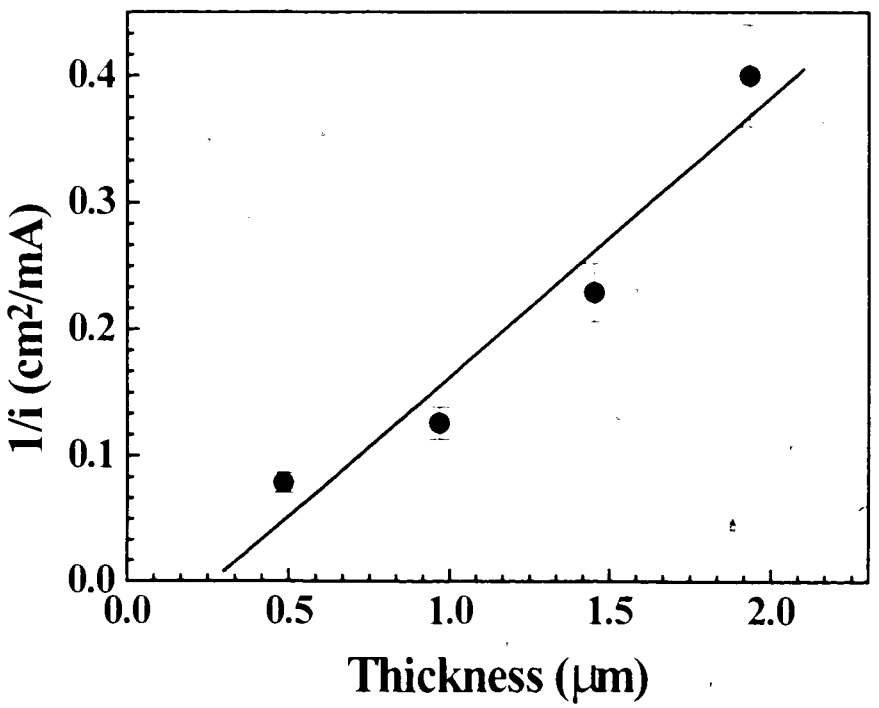

Figure 4.12 Plot of 1/i (obtained from the intercept of Koutecky-Levich plots in Figure 4.11) vs. the polymer film thickness for O_2 reduction in O_2-saturated 0.5 M H_2SO_4.

4.3. Conclusions

It has been demonstrated that polyaniline doped by camphorsulfonic acid (PANI-CSA) is sufficiently conductive to be used as a matrix for dispersed electrocatalytic Pt. Although the Pt deposited onto the PANI-CSA films by electrochemical means was mainly localized on the top surface of the polymer film, i.e., at the polymer/electrolyte interface, the electrocatalytic activity of the Pt was proven to be greater than for the same quantity of Pt electrodeposited on glassy carbon electrode. This suggests that the active surface area of the Pt particles is increased by deposition onto the polymer substrate, perhaps because of the more porous structure of the polymer compared to the glassy carbon substrate. The permeability of the PANI-CSA film was determined to be 1.18 x 10^{-12} mol cm^{-1} s^{-1} (which is about 1/20 of the permeability of O_2 in a 0.5 M H_2SO_4 solution). In the next chapter the possibility of improving the permeability of oxygen is investigated and the results will be compared to Nafion which is a solid polymer electrolyte being used in fuel cells.

Chapter 5

Polyaniline-Nafion Composites

In this chapter, the formation and characterization of polyaniline and Nafion composites are studied and discussed. Also, the diffusion parameters of oxygen through the composites are compared with the pure camphorsulfonic acid doped polyaniline (PANI-CSA). In addition, Pt was deposited into some of these composites and the catalytic activity of the resultant films was evaluated and is discussed in Chapter 6.

5.1. Preparation of Composites of Polyaniline and Nafion

As demonstrated in Chapter 4, a drawback in using polyaniline as a matrix for Pt is the limitation of the reactants accessing the catalyst particles. If the diffusion of O_2 into the film is relatively slow, the Pt microparticles will not be fully utilized even if a three-dimensionally dispersed system was attained. Therefore, the diffusion properties of the film must be improved.

Recently, researchers studying fuel cell technology found that most of the Pt in the catalyst layer is not utilized; only ~10% of the Pt catalyst particles are actually in simultaneous contact with the reactant, the electrolyte, and the current collector [56,57]. They found that utilization of the Pt particles can be greatly enhanced by impregnating a polymer electrolyte, such as Nafion, into the catalyst layer. This extends the three dimensional reaction zone by increasing the active surface area of Pt in contact with the electrolyte. As a result, Pt loadings can be greatly reduced. Other advantages of having Nafion in the catalyst layer include the higher proton conductivity because of the pendent sulfonic acid groups and higher oxygen solubility due to the higher fluorine content. Hence, the reactants are found to have a better access to the catalyst through the

incorporation of Nafion. Another important issue in utilizing matrices for electrocatalysts is the electrical conductivity of the matrix which determines the efficiency of shuttling electrons from the catalyst to the current collector. Polyaniline has been demonstrated in the previous chapter to be a good candidate for this purpose; therefore, a system which combined the advantages of both Nafion and polyaniline were pursued in this study.

Chemical and electrochemical methods of preparing conducting polymer/Nafion composites have been described in the literature. For example, C.-H. Hsu [58] prepared a PANI/Nafion composite by placing a thick film of Nafion membrane between flanges on the side arms of two glass containers where one side contained aniline while the other contained an oxidant solution. Polyaniline was formed when aniline and oxidant combined in the Nafion membrane upon diffusion from both sides. Kuwabata *et al.* electropolymerized aniline in a Nafion solution [59], and Orata *et al.* electropolymerized aniline onto a Nafion modified electrode [60]. While these studies provide useful information on the characteristics of PANI/Nafion composites, they appear impractical for industrial applications.

In contrast, Barthet *et al.* [61] developed a simple chemical method of preparing PANI/Nafion composite films where Nafion powder was dissolved in a N-methyl-2-pyrrolidinone (NMP) solution of PANI (polyaniline base) and direct doping of PANI by Nafion was observed. This method was repeated and in contrast to the report, the Nafion powder was not soluble in NMP. However, it was found that a 5% Nafion solution (in water/alcohol mixture) when added to the polyaniline base in NMP did result in doping of PANI. The advantage of this technique is that it yields a solution of PANI/Nafion ready for solution casting. A series of composite solutions with different PANI:Nafion

content were prepared and were characterized by UV-Vis spectroscopy and electrochemical techniques.

5.2. Characterization of PANI-Nafion Composites

5.2.1. UV-Vis Spectroscopy

Figure 5.1 shows the UV-Vis spectra of PANI-Nafion composite films comprised of different weight percentages of PANI and Nafion. The UV-Vis absorbances of the 5% and 10% PANI solutions were low due to the low concentration of the PANI in the original casting solution.

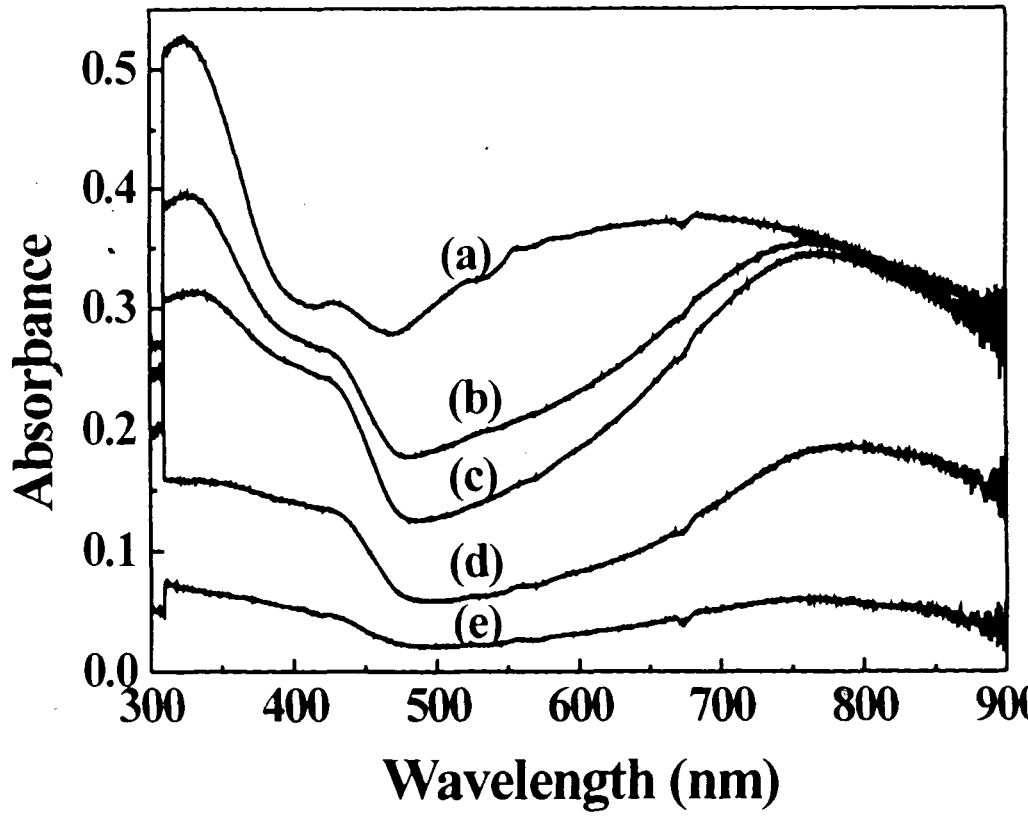

Figure 5.1 UV-Vis spectrum of PANI-Nafion composites films, (a) PANI (25%wt)-Nafion, (b) PANI(20%wt)-Nafion, (c) PANI(15%wt)-Nafion, (d) PANI(10%wt)-Nafion, (e) PANI(5%wt)-Nafion.

The broad peaks centred at 427 m and ~760 nm indicate that the PANI base was fully doped by the Nafion solution. As the weight percentage of PANI was increased, the lower energy absorption peak blue shifted to 650 nm indicating the presence of the insulating base form of the polymer. When polyaniline is in the conducting emeraldine salt form, the molar ratio of the dopant to the phenyl nitrogen repeating unit is 0.5 as shown below:

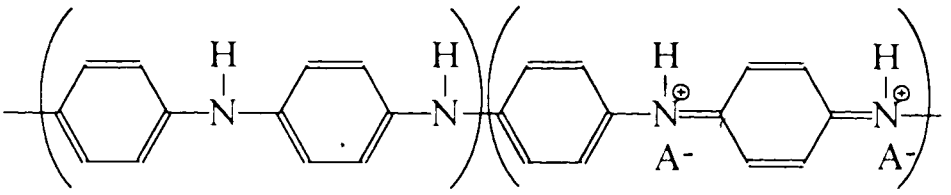

Emeraldine Salt

According to this, it was calculated that for composites of polyaniline content > 14 wt.%, there are insufficient sulfonic acid groups associated with Nafion to completely dope the polyaniline base. Therefore, the UV-vis spectra of the PANI(5 % wt)-Nafion and PANI(10 % wt)-Nafion composite films showed characteristic absorption peaks for the doped form of polyaniline whereas spectra of the composites films containing 15%, 20% and 25% of polyaniline indicated the presence of undoped polyaniline in addition to the doped polyaniline salt.

5.2.2. Electrochemical Characterization of PANI-Nafion Composites

Figure 5.2 shows the cyclic voltammograms of polyaniline-Nafion composite films on a Pt electrode in 0.5 M H_2SO_4. The potential was cycled between +1.0 V and -0.1 V vs. SCE at a scan rate of 100 mV/s.

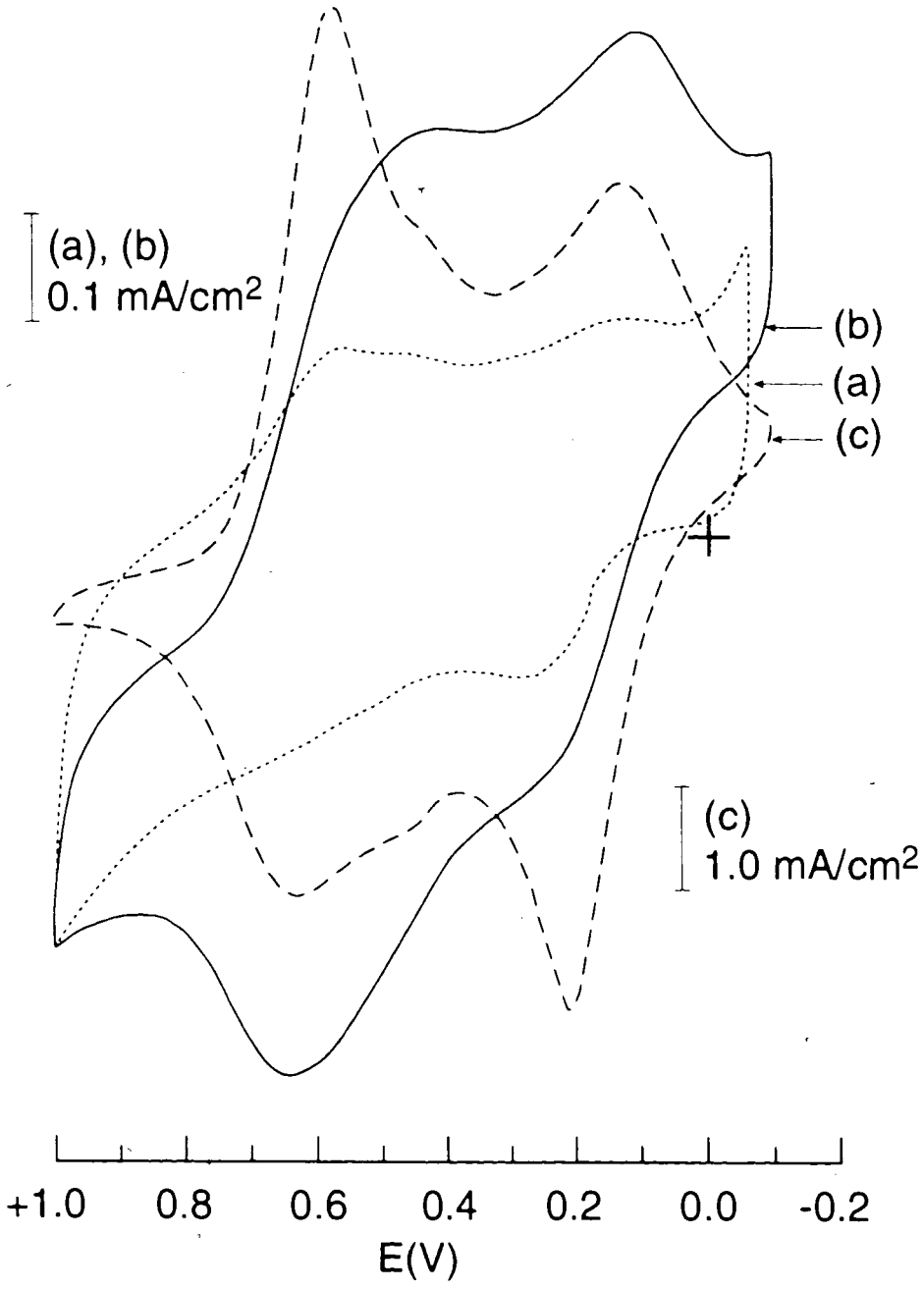

Figure 5.2 Cyclic Voltammograms of composite films in 0.5 M H_2SO_4 (a) PANI(5%wt)-Nafion, (b) PANI(10%wt)-Nafion, (c) PANI(15%wt)-Nafion, scan rate = 100 mV/s.

The electroactivity of the PANI-Nafion films increased with increasing polyaniline content. This behaviour is also observed by Barthet *et al.* [61]. The large excess of Nafion in the PANI(5%wt)-Nafion composite most likely surrounds and insulates regions of the conducting polyaniline, so that the electroactivity is substantially less than anticipated.

When the polyaniline content increased, percolation of polyaniline conducting domains is achieved and the electrochemistry is more pronounced. The cyclic voltammograms of the PANI(20%wt)-Nafion and PANI(25%wt)-Nafion were not obtained due to the poor adhesion of the films to the Pt electrode. The 20 wt% and 25 wt% films were observed to peel off the electrode when immersed in the electrolyte solution. Furthermore, the PANI(15%wt)-Nafion, PANI(20%wt)-Nafion and PANI(25%wt)-Nafion solutions were observed to precipitate upon standing and films cast from these solutions showed significant phase segregation as shown in Figure 5.3. This figure shows a picture of a film cast from a PANI(15%wt)-Nafion solution. Discrete regions of polyaniline (dark) and Nafion (clear) are clearly observed.

A proposed morphology of the PANI-Nafion composites can be represented by Figure 5.4. With sufficient polyaniline content, the polymer is interconnected to form a conductive network in the composite.

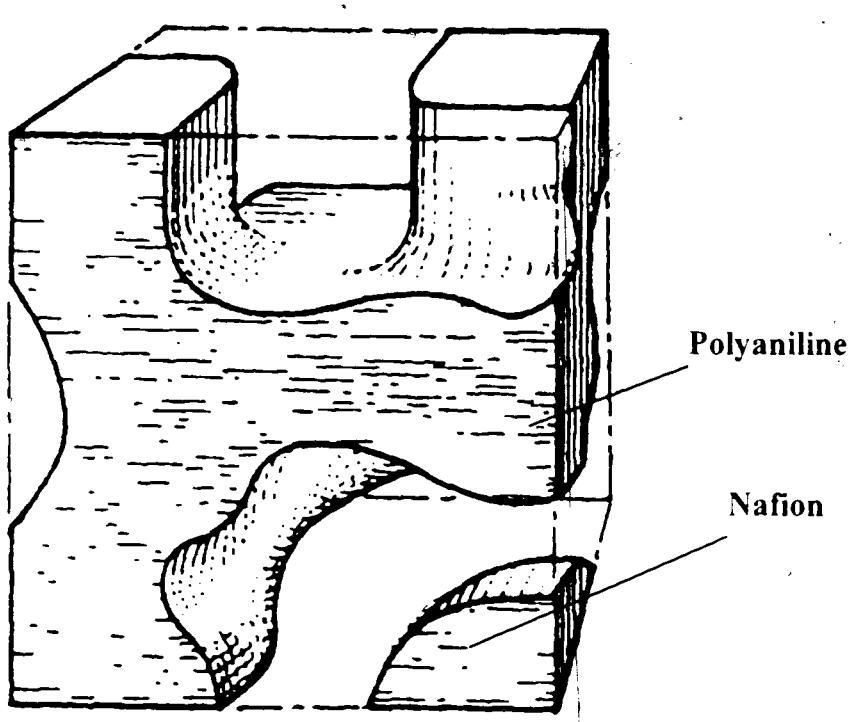

Figure 5.4 Proposed morphology of PANI-Nafion composites [adopted from Ref. 62]

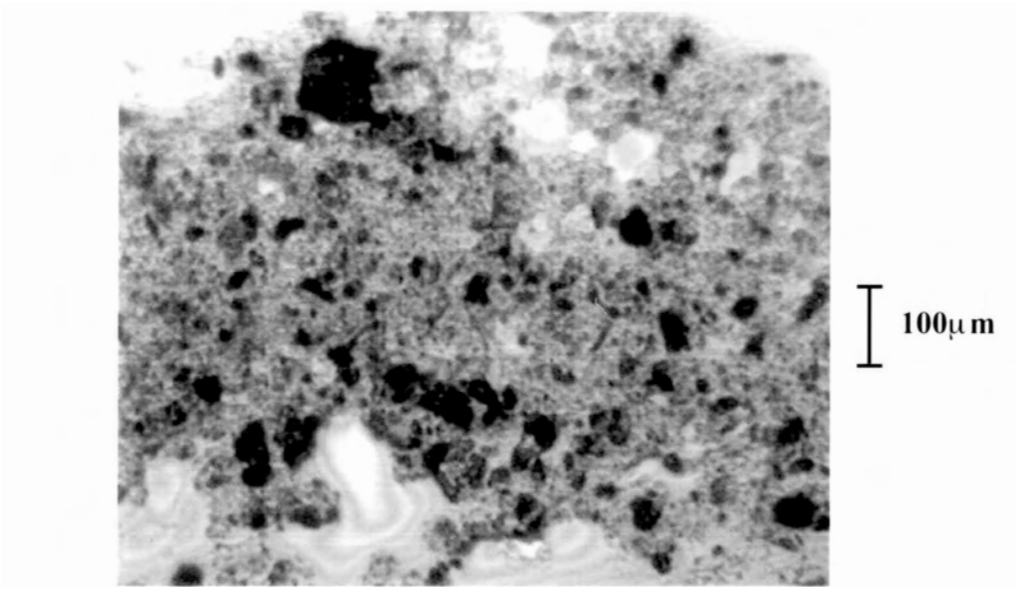

Figure 5.3 Optical micrograph of a PANI(15%wt)-Nafion composite films.

5.2.3. Conductivity of PANI-Nafion Composites

The dependence of the conductivity of the polyaniline-Nafion composites on the electrochemical potential was studied using the 2-band electrode as described in Chapter 3 (Section 3.5). A thin film of PANI(15%wt)-Nafion composite was cast onto the 2-band electrode so that the polymer film spanned both electrodes. The electrical connectivity of the two electrodes through the polymer film was determined by performing cyclic voltammetry on the electrodes. First, a cyclic voltammogram was obtained by making one of the band electrodes the working electrode (Figure 5.5(b)). Then another cyclic voltammogram was obtained by making the other electrode the working electrode (Figure 5.5 (c)).

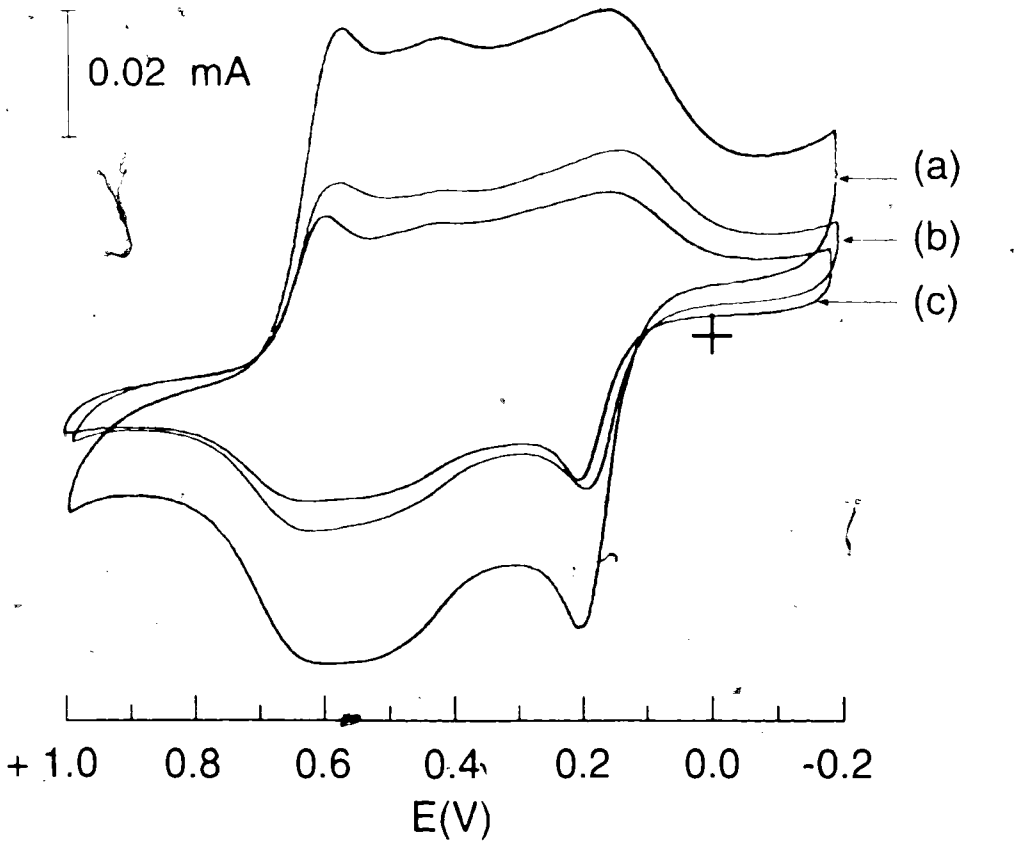

Figure 5.5 Cyclic voltammograms of a PANI(15%wt)-Nafion composite film on a two-band electrode in 0.5 M H_2SO_4 at a scan rate of 100 mV/s (a) Electrode 1 and 2 connected together as the working electrode, (b) Electrode 1 connected as the working electrode, (c) Electrode 2 connected as the working electrode.

The two band electrodes were then connected together as the working electrode and a cyclic voltammogram was obtained. Figure 5.5(a) shows the cyclic voltammogram obtained when the two electrodes were used simultaneously as the working electrode. The charge passed is almost twice as large as those obtained for the individual electrodes. It was concluded, therefore, that the two electrodes were not electrically connected by the polyaniline-Nafion composite film, that is, the lateral electrical conductivity of the film was not continuous over the 100 μm distance between the two electrodes. Nevertheless, as will be shown later in this thesis, the films are sufficiently conductive over micron dimensions that they can serve as conductive matrices for electrocatalysis.

5.3. Effect of Nafion Content on Film Permeability

The motivation for the addition of Nafion into the matrix was to increase the permeability of the matrix toward oxygen. The permeability of a series of PANI-Nafion composites with different Nafion content was studied using a Pt disk substrate electrode as described in Chapter 4 (Section 4.2.). Rotating disk voltammetry was performed at the PANI-Nafion modified Pt electrodes in an O_2 saturated 0.5 M H_2SO_4 solution using rotation speeds between 100 rpm and 900 rpm.

Figure 5.6 shows the Levich plot for the reduction of oxygen at a PANI(5%wt)-Nafion and a PANI(10%wt)-Nafion composite modified electrode. Shown for comparison are the Levich plots for O_2 reduction at Pt electrode modified with camphorsulfonic acid doped polyaniline (PANI-CSA), a Nafion-modified Pt electrode and a bare Pt electrode. The 15%, 20% and 25% composite films cracked and peeled off upon rotation in the electrolyte solution and therefore detailed analysis of voltammetric data was not carried out on these composite films. As expected, the bare Pt electrode

exhibits the highest current density because the current is limited only by the rate at which O_2 is brought up to the electrode surface. The PANI(5%wt)-Nafion film exhibits a very similar current density as a Nafion modified electrode which is not surprising since the PANI(5% wt)-Nafion film comprises mainly of Nafion (95%). The current density for oxygen reduction decreased as the polyaniline content is increased to 10%. The PANI-CSA film showed the lowest rate of O_2 reduction at Pt. This clearly shows that polyaniline is less permeable to O_2 than Nafion. The Levich plots of the polymer modified electrodes deviate from linearity at higher rotation speed providing further evidence of diffusion limitation in these films.

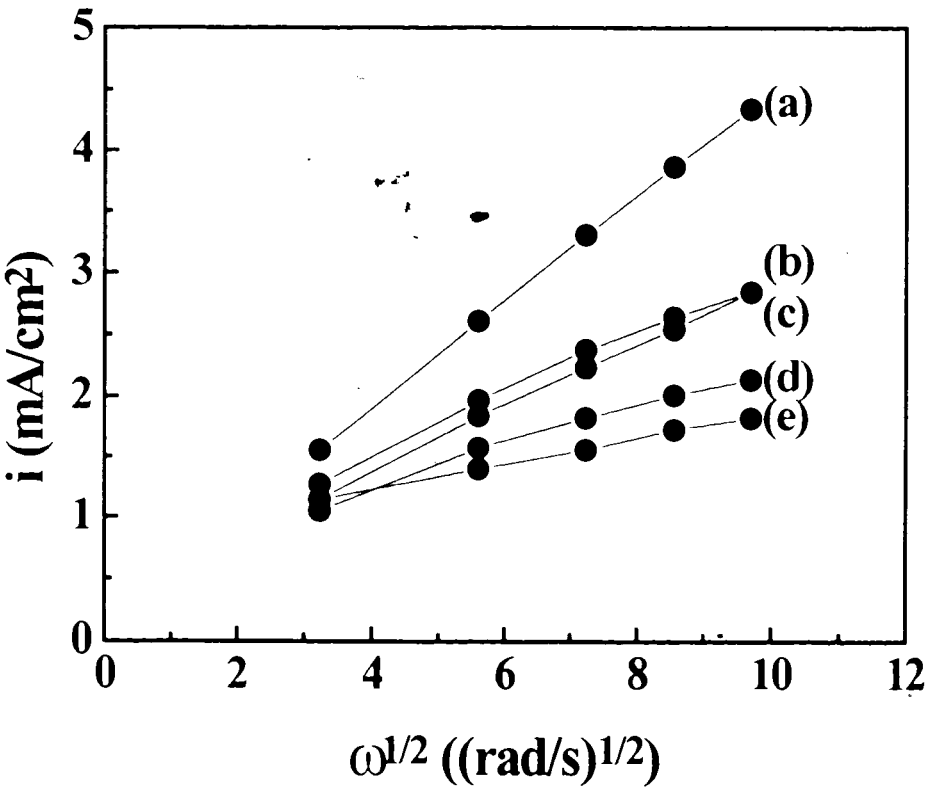

Figure 5.6 Levich plot for oxygen reduction at (a) bare Pt electrode, (b) PANI(5%wt)-Nafion, (c) Nafion, (d) PANI(10%wt)-Nafion, (e) PANI-CSA, modified Pt electrode in O_2 saturated 0.5 M H_2SO_4, scan rate = 5 mV/s.

A comparison of the permeability of these films may be obtained by plotting 1/i against $1/\omega^{1/2}$ as shown in the Koutecky-Levich plot (Figure 5.7) for O_2 reduction at a PANI(5%wt)-Nafion, a PANI(10%wt)-Nafion , a PANI-CSA, a Nafion modified electrodes, and a bare Pt electrode.

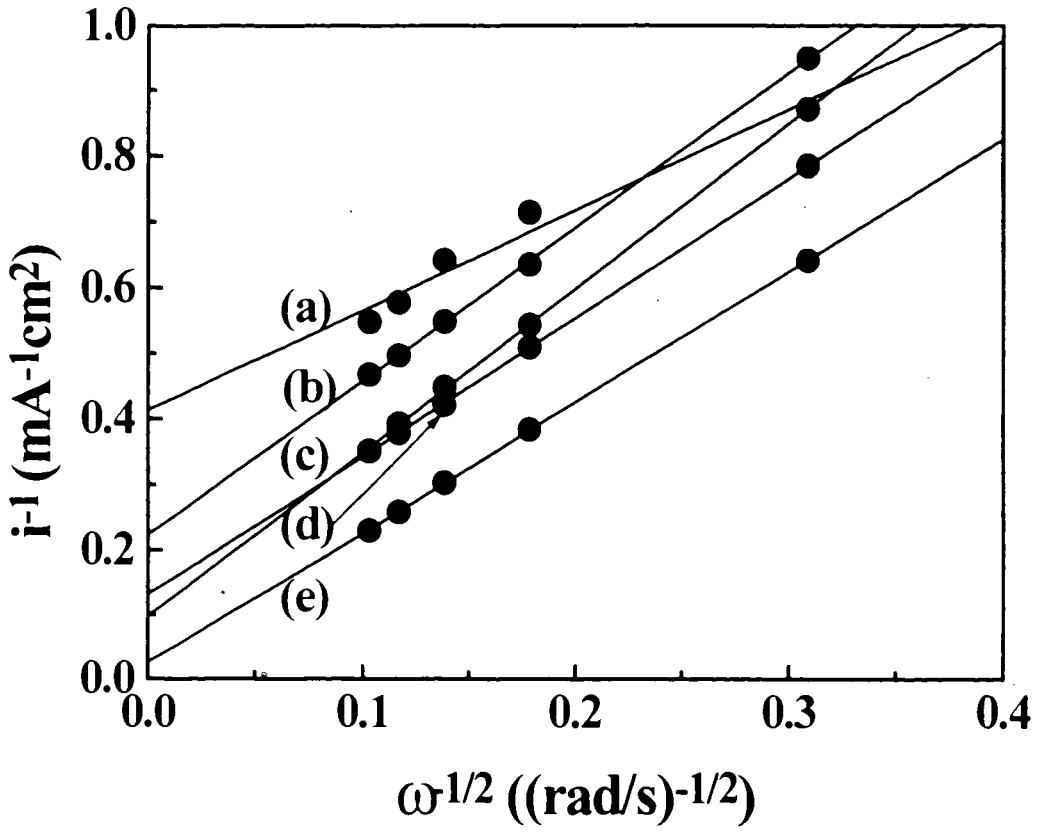

Figure 5.7 Koutecky-Levich plots for modified Pt electrodes constructed using data in Figure 5.6: (a) PANI-CSA, (b) PANI(10%wt)-Nafion, (c) Nafion, (d) PANI(5%wt)-Nafion and (e) a bare Pt electrode in O_2 saturated 0.5 M H_2SO_4, scan rate = 5 mV/s.

The intercept of a Koutecky-Levich plot comprises of the reciprocal of both the kinetic current and the O_2 diffusion current through the composite films (Eqn. 1.7).

$$\left(\frac{1}{i}\right)_{intercept} = \frac{1}{i_k} + \frac{1}{i_f} \qquad \text{[Eqn. 5.1]}$$

Expanding Eqn.5.1 gives:

$$\left(\frac{1}{i}\right)_{intercept} = \frac{1}{i_k} + \frac{d}{nFD_f C_f} \quad \text{[Eqn. 5.2]}$$

Assuming that the kinetic current, i_k, is large at high over-potential, and $1/i_k$ is negligible, the permeability, D_fC_f, of the polymer composite films is inversely proportional to the intercept of the Koutecky-Levich plot. Therefore, as can be seen from Figure 5.7, the PANI-CSA has the largest intercept (i.e. lowest permeability) and with increasing Nafion content, the permeability was observed to increase.

5.4. Permeability of O_2 Through PANI(10%wt)-Nafion Films

The permeability of the PANI(10%wt)-Nafion composite films towards oxygen was investigated as a function of film thickness, d. Further studies on the PANI(5%wt)-Nafion composite films were not performed because there was concern that there was insufficient polyaniline to form a homogeneous conductive network even though they show higher permeability compared to the PANI(10%wt)-Nafion films.

The permeability of a PANI(10%wt)-Nafion film was studied using a bare Pt rotating disk electrode as previously described, and voltammetry was performed using PANI(10%wt)-Nafion films of thickness 1.4 μm, 2.2 μm, 2.7 μm, 3.4 μm and 4.1 μm. Figure 5.8 shows the Levich plots of these PANI(10%wt)-Nafion modified electrodes obtained from the rotating disk voltammetry in 0.5 M H_2SO_4 saturated with O_2. It can be seen that the limiting current for oxygen reduction reaction decreases with increasing thickness due to the diffusion limitation of O_2 through the composite films.

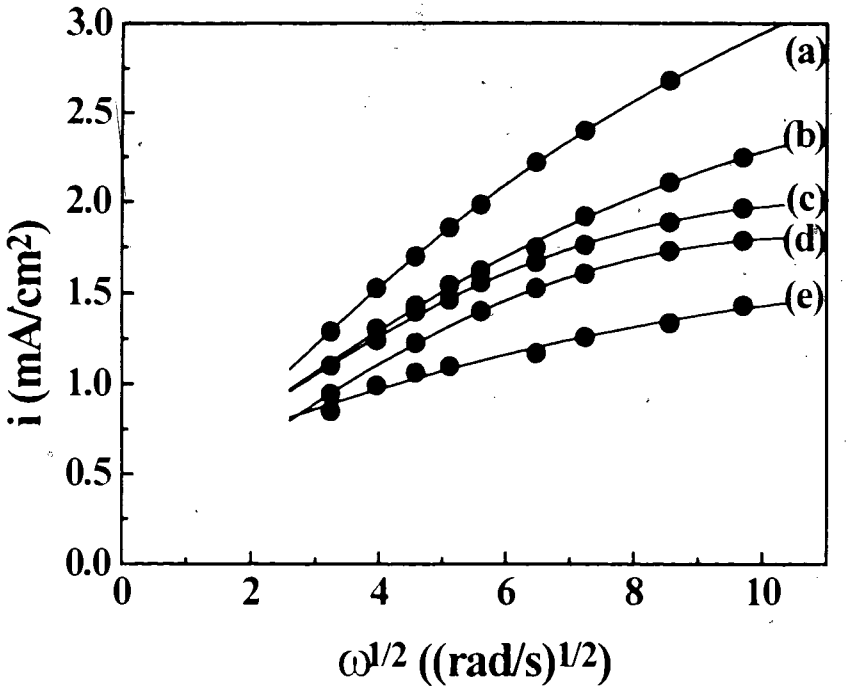

Figure 5.8 Levich plots of PANI(10%wt)-Nafion films with varying film thickness, (a) 1.4 μm, (b) 2.2 μm, (c) 2.7 μm, (d) 3.4 μm, (e) 4.1 μm, in O_2 saturated 0.5 M H_2SO_4.

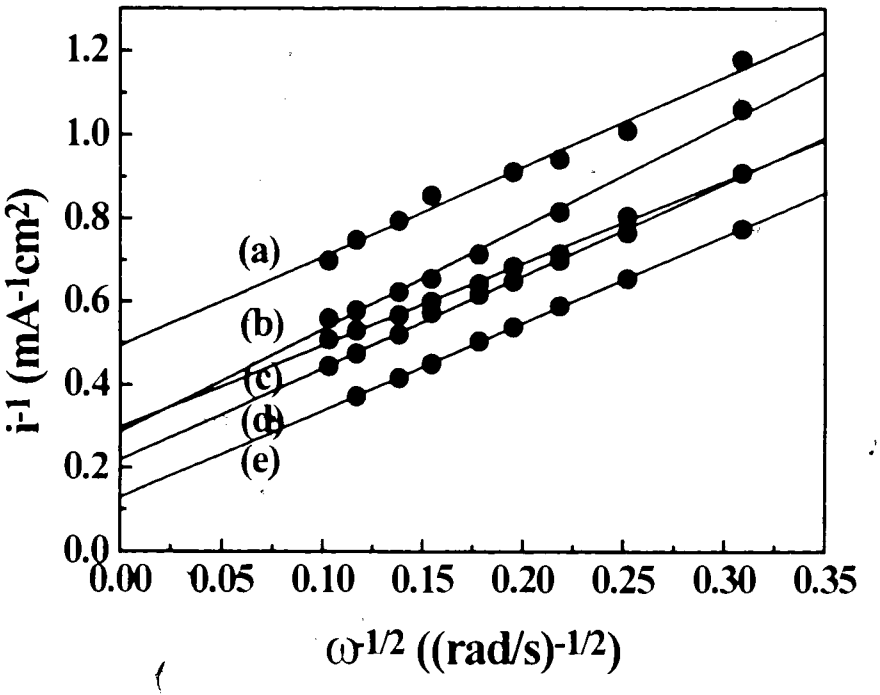

Figure 5.9 Koutecky-Levich plots of PANI(10%wt)-Nafion films with varying thickness, (a)4.1 μm, (b) 3.4 μm, (c) 2.7 μm, (d) 2.2 μm, (e) 1.4 μm. O_2 saturated 0.5 M H_2SO_4.

The permeability, D_fC_f, of the PANI(10%wt)-Nafion films towards O_2 can be obtained by plotting 1/i vs. $1/\omega^{1/2}$ (Koutecky-Levich Plot). These were plotted in Figure 5.9 for oxygen reduction at these electrodes. The intercepts of the Koutecky-Levich plots which comprise of the reciprocal of both the kinetic current and the O_2 diffusion current, were then plotted against the film thickness (Figure 5.10). From the slope, the permeability of the PANI(10%wt)-Nafion composite film was determined to be 1.74×10^{-12} mol cm^{-1} s^{-1}. Comparing this value with the one obtained for camphorsulfonic acid doped polyaniline film (1.18×10^{-12} mol cm^{-1} s^{-1}), incorporation of Nafion into the film resulted in a 47% increase in permeability.

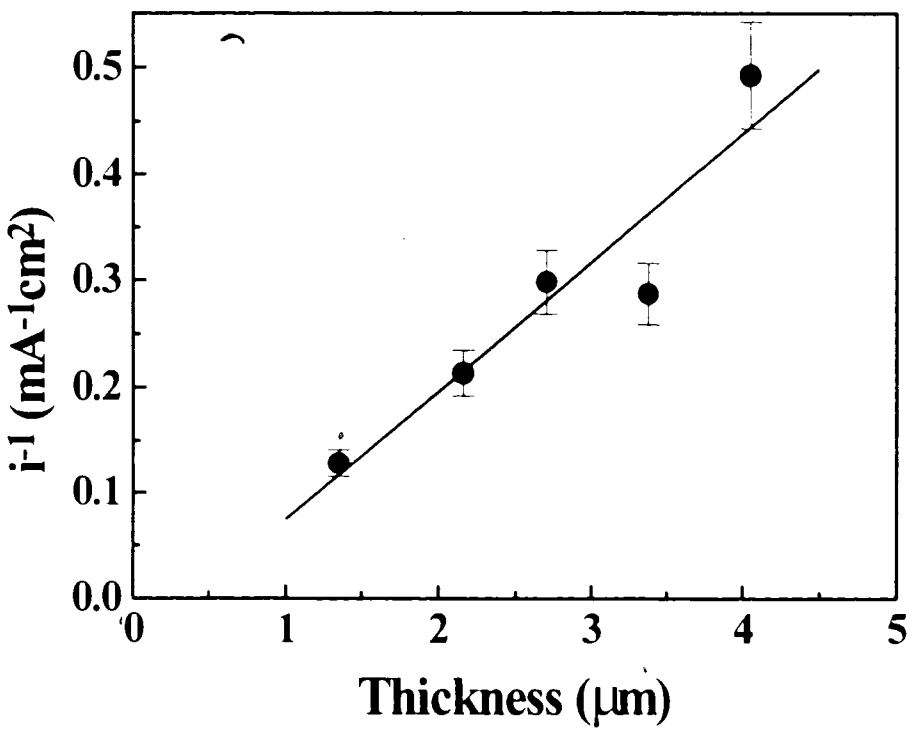

Figure 5.10 Plot of 1/i (obtained from the intercept of the Koutecky-Levich plot) vs. thickness of the PANI(10%wt)-Nafion films.

Temperature (°C)	Medium	Permeability of O_2 ($x10^{12}$ mol cm^{-1} s^{-1})	Reference
25	Recast Nafion in 0.5M H_2SO_4	3.4	63
25	Recast Nafion in 0.5M H_2SO_4	6.3	64
20	Nafion Membrane	1.73	.65
25	0.5M H_2SO_4	20.3	64
25	H_2O	38.3	66
20	PTFE	3.7	67
20	PANI-CSA	1.18	this work
20	PANI(10%wt)-Nafion	1.74	this work

Table 5.1 Permeability of oxygen in several media

Table 5.1 shows the permeability of O_2 in different media as a further comparison. There is a large variation in the permeability of O_2 in Nafion in the literature. This is largely due to the difference in morphology of Nafion, e.g., recast films vs. membranes. A recast Nafion film is obtained by casting Nafion solution onto the substrate electrode whereas Nafion membranes are prepared by compression molding under elevated temperature. Furthermore, different research groups use different methods for determining the thickness of the Nafion film. In the case of Nafion membrane, a micrometer can be used to determine the thickness. However, for a recast Nafion film, which is usually deposited onto a solid substrate, the thickness of the film is usually calculated from the density of the Nafion and the volume of liquid Nafion used. This allows only an estimate of film thickness and leads to discrepancies in the permeability value obtained by different research groups when different estimates of densities of Nafion are used. For example,

Watanabe *et al.* [63] calculated the thickness of the Nafion film from the mass of polymer added and the electrode surface area assuming a dry Nafion density of 1.98 g cm^{-3}. Alternatively, Gottesfeld *et al.* [64] took the swelling of the Nafion film in aqueous solution into account and assumed a hydrated Nafion density of 1.58 g cm^{-3}. For the PANI(10%wt)-Nafion composite, the density was estimated using a direct ratio of PANI and Nafion densities. Assuming 1.3 g cm^{-3} for the density of PANI [19], and 1.98 g cm^{-3} for the density of Nafion, the density of PANI(10%wt)-Nafion composite was calculated as follow:

$$\mathbf{d_{PANI(10\%wt)\text{-}Nafion} = 10\% \times d_{PANI} + 90\% \times d_{Nafion}}$$

$$\mathbf{d_{PANI(10\%wt)\text{-}Nafion} = 1.9\ g\ cm^{-3}}$$

This density value was used to determine the permeability of PANI(10%wt)-Nafion films and a value of 1.7×10^{-12} mol cm^{-1} s^{-1} was obtained. If 1.58 g cm^{-3} was used for the density of Nafion, the density of PANI(10%wt)-Nafion would be 1.55 g cm^{-3} and the permeability of the PANI(10%wt)-Nafion composite calculates to be 2.1×10^{-12} mol cm^{-1} s^{-1} accordingly.

Comparing the permeability of the PANI(10 wt%)-Nafion composite with the aqueous acid (0.5 M H_2SO_4), it is about 1/10 of the permeability of H_2SO_4; however, the PANI-Nafion composites appear to have a permeability towards O_2 in the same order of magnitude as Nafion.

5.5. Conclusions

A polyaniline-Nafion composite was prepared by direct doping of polyaniline base solution in NMP by Nafion solution (5% w/w). The permeability of O_2 through

these PANI-Nafion composites was studied and it was found that the higher the Nafion content, the higher the permeability of O_2 through the composites. However, phase segregation was observed in the composites with PANI weight content greater than 10% and the mechanical stability of films cast from the high PANI content solutions was very poor. Permeability studies were focused on the PANI(10%wt)-Nafion composites and it was determined to be 1.7×10^{-12} mol cm^{-1} s^{-1} which when comparing with the camphorsulfonic acid doped polyaniline (PANI-CSA), shows a 47% increase. It has also been shown that the permeability of the PANI(10%wt)-Nafion composite is in the same order of magnitude as Nafion.

Chapter 6

Methods of Incorporating Pt into PANI-Nafion Composites

6.1 Electrochemical Deposition of Pt

Pt microparticles were deposited into PANI-Nafion films cast on electrodes by electrochemical reduction of K_2PtCl_6 as described in Chapter 4. In order to achieve this, the potential of the modified electrodes was cycled between +0.5 V and -0.3 V (vs.SCE). The cathodic charge was monitored and used to calculate the amount of Pt deposited. The PANI-Nafion modified electrode into which Pt is electrochemically deposited is denoted by **PANI-Nafion/Pt**. The presence of Pt was confirmed by Auger Electron Spectroscopy as described in Section 2.6, by observance of the characteristic Pt peak at 64 eV. The depth profile of Pt in the PANI-Nafion/Pt electrode was also determined by Auger Electron Spectroscopy by continuous sputtering of the film with an Ar^+ ion beam. Figure 6.1 shows the depth profile of this electrode.

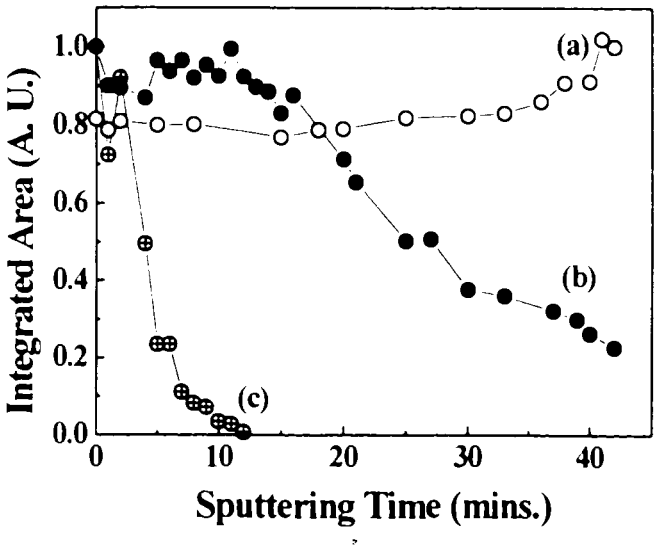

Figure 6.1 Depth Profile of a PANI-Nafion/Pt electrode obtained by Auger Electron Spectroscopy, (a) Carbon, (b) Fluorine, (c) Platinum.

The Pt signal decreased to undetectable level after 12 minutes of sputtering. The fluorine signal, corresponding to the Nafion concentration profile started to decrease after 16 minutes while the carbon signal started to increase. No sharp boundary between the polymer film and the substrate graphite could be identified from the carbon or fluorine signals. This may be due to the relatively rough surface topology of the graphite substrate. Nevertheless, it can be seen that the Pt particles are not localized at the surface of the composite to the extent observed for the pure camphorsulfonic acid doped polyaniline films, onto which Pt was electrochemically deposited. In the latter case, no Pt was observed after 20 seconds of sputtering under similar conditions. However, a Pt concentration gradient is still observed for the PANI-Nafion composite film indicating that Pt was not dispersed completely into the polymer matrix, i.e. a homogeneously dispersed catalytic system was still not achieved yet.

The electrocatalytic activity of a PANI-Nafion/Pt electrode was studied using rotating disk voltammetry as previously described. Levich plots for O_2 reduction were obtained from the data. Figure 6.2 shows the Levich plot for oxygen reduction reaction in 0.5 M H_2SO_4 at a PANI-Nafion modified electrode onto which 3.1 $\mu g/cm^2$ of Pt was electrochemically deposited.

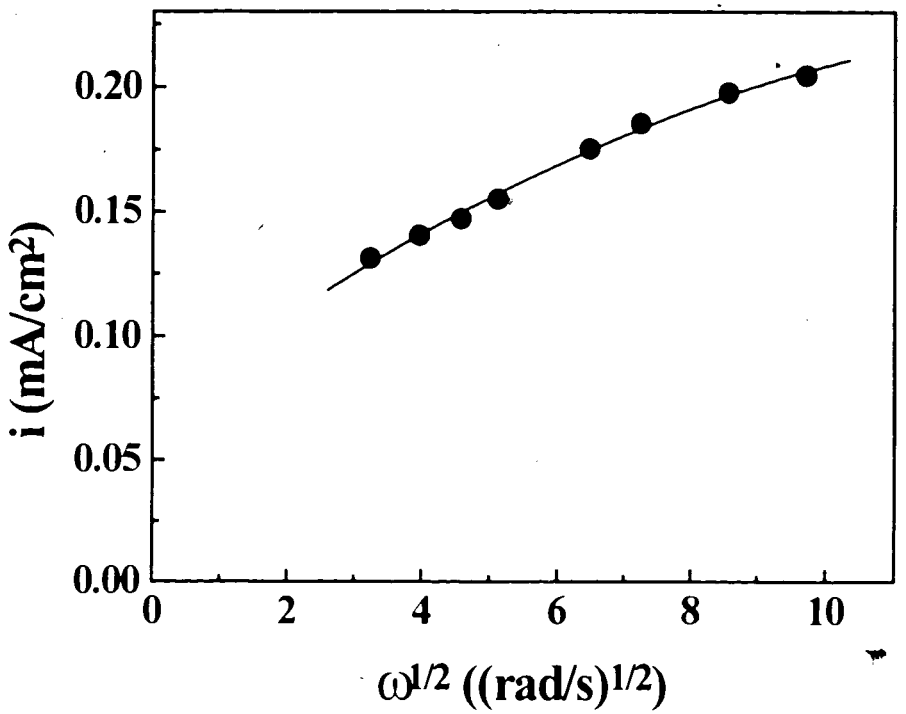

Figure 6.2 Levich plot for oxygen reduction at a PANI-Nafion/Pt modified glassy carbon electrode in O_2 saturated 0.5 M H_2SO_4, scan rate = 5 mV/s, film thickness = 2.4 μm, Pt loading = 3.1 μg/cm².

The curvature of the Levich Plot is further confirmation that Pt particles are not confined to the surface of the polymer film because in that case a linear Levich plot would be expected. The curvature is interpreted to indicate that Pt particles are embedded in the film to a certain extent and oxygen has to diffuse through the matrix in order to reach the catalyst sites. While these data appear qualitatively consistent with such a model, a quantitative comparison of the rate of reduction of O_2 at these films provides more striking information. This is shown in Figure 6.3 which shows Levich plots for oxygen reduction at a PANI-Nafion/Pt and a PANI-CSA/Pt modified glassy carbon electrode. In both cases, Pt was deposited electrochemically and the Pt loadings were similar. The PANI/CSA films are slightly thinner but this should be irrelevant because Pt is largely

deposited at the surface as described in Chapter 4 so that the film does not impede O_2 reduction.

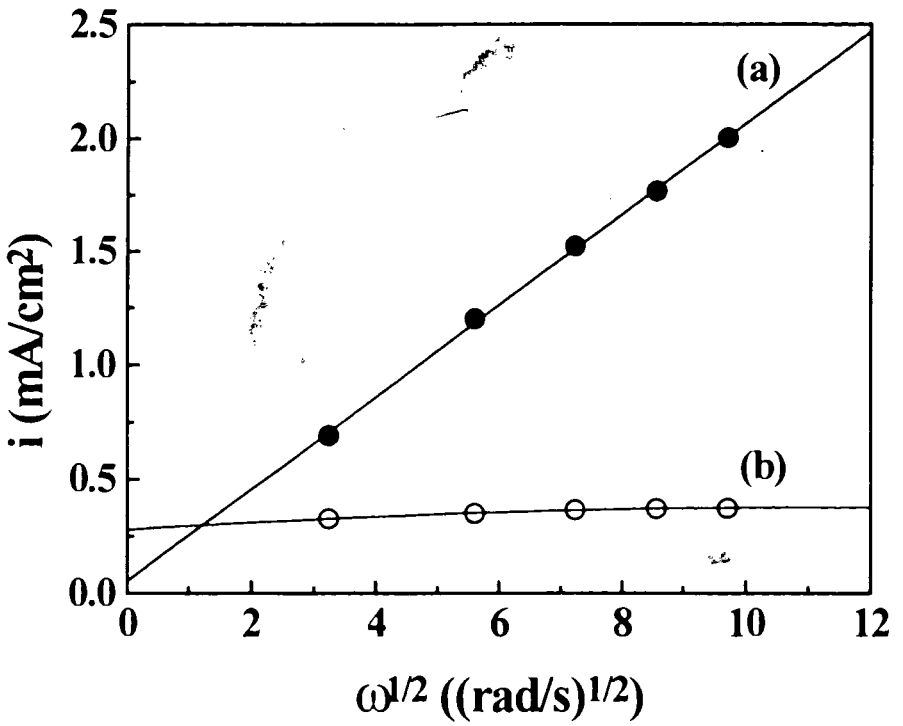

Figure 6.3 Levich Plot of (a) PANI-CSA/Pt (film thickness = 0.44 μm, 23 μg/cm²); (b) PANI-Nafion/Pt (thickness = 1.5 μm, Pt loading = ~24 μg/cm²), in O_2 saturated 0.5 M H_2SO_4, scan rate = 5 mV/s.

Under these conditions, the PANI-CSA/Pt film has a much higher activity towards O_2 reduction than the corresponding PANI-Nafion/Pt electrode even though an enhancement in electrocatalytic activity was expected from the PANI-Nafion composite electrode due to the higher dispersion of Pt into the matrix. These results were completely reproducible upon repeated analysis on film preparation. Postulations on the reason behind the poor catalytic activity are given later in this chapter.

6.2 Addition of Platinum Black

Although the method of incorporating Pt into the polymer film by the electrochemical reduction of K_2PtCl_6 has been widely accepted and used by other researchers in similar applications for the purpose of research, a three-dimensionally catalytic system with Pt homogeneously dispersed in the matrix was not attained in our experiments using the electrochemical deposition method.

From the Auger electron spectroscopic data, it was concluded that the Pt microparticles were mainly located on the surface of the camphorsulfonic acid doped polyaniline (PANI-CSA) matrix. Even though the diffusional properties of the composite are superior to pure PANI, Pt microparticles were not incorporated throughout the matrix. Moreover, electrochemical reduction of K_2PtCl_6 may not be practical for large scale industrial applications due to its high cost. Therefore, other methods of Pt deposition were investigated in this thesis.

Pt black is a commercial product consisting of very finely divided Pt particles having a large surface area. Pt black was added to a solution of Nafion and the solution was sonicated to provide a homogeneous suspension of Pt black.

Figure 6.4 shows the Transmission Electron Microscopic (TEM) and Scanning Electron Microscopic (SEM) pictures of a PANI(10 wt %)-Nafion-Pt Black (11.9 $\mu g/cm^2$) film.

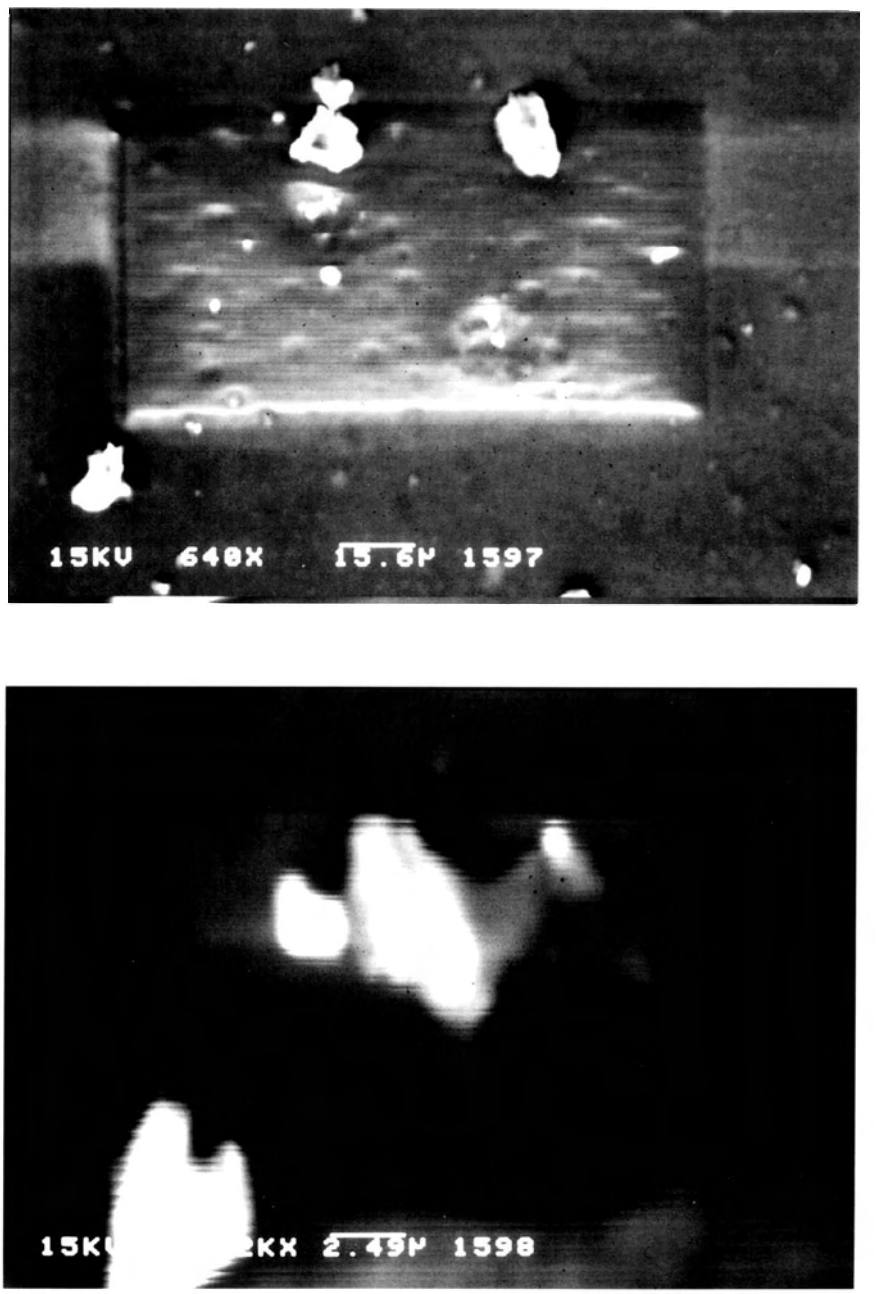

Figure 6.4 (a) SEM of a OANI(10 wt%) Nafion-Pt Black electrode

Figure 6.4 (b) TEM of a PANI(10 wt%)-Nafion-Pt Black electrode

As seen in the TEM picture, the Pt black particles aggregate together to form bigger clusters of Pt (1 μm-7 μm) although the individual Pt black particles are very small (<500 Å). Smaller aggregates (100 nm -500 nm) were also found dispersed in the matrix. Figure 6.5 shows the cyclic voltammograms of a Nafion modified glassy carbon electrode containing 25 $\mu g/cm^2$ of Pt black in N_2 and O_2 purged 0.5 M H_2SO_4. Oxygen reduction was observed under O_2 environment at ~+0.6 V vs. SCE. Bearing in mind that Nafion is electrically insulating, the observation that oxygen is reduced indicates that the Pt microparticles are interconnected some way. This could be achieved by the Pt particles touching the surface of the glassy carbon electrode as a result of extensive sedimentation. As can be seen from the TEM micrograph, it is possible that the large Pt clusters might have sedimented on the glassy carbon surface, and the oxygen reduction observed was due to these Pt clusters which have electrical contact to the current collector. O_2 reduction can occur at these catalytic sites and this is likely the reason why O_2 current was observed in the Nafion-Pt black composite film. In fact, if the Pt particles were dispersed homogeneously through the film, no O_2 reduction should be observed because the catalyst would be electrically isolated.

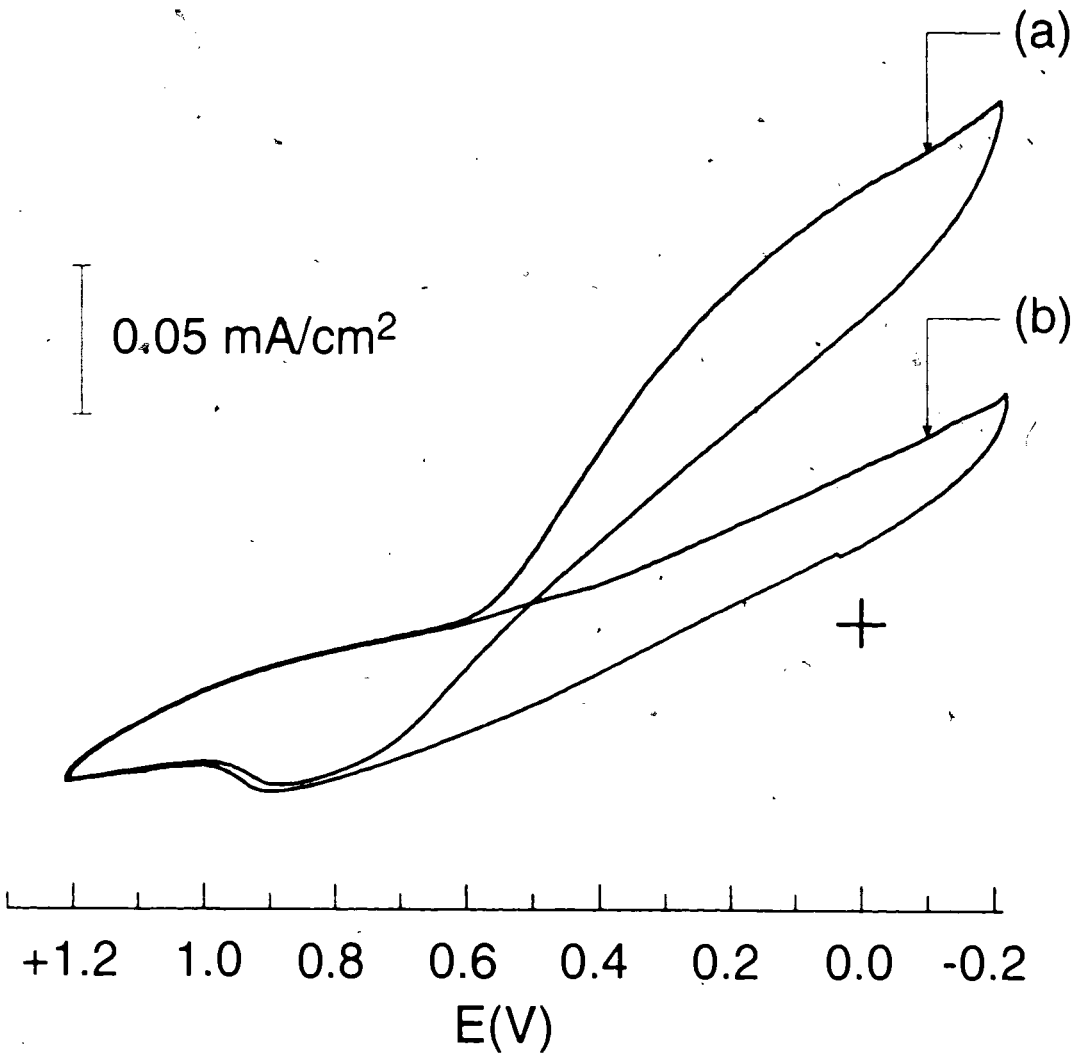

Figure 6.5 Cyclic voltammogram of Nafion-Pt Black modified GC electrode (Pt loading = 25 μg/cm², thickness = 5.7 μm) in 0.5 M H_2SO_4, (a) under O_2 and (b) under N_2, scan rate = 5 mV/s. Nafion-Pt black composite was prepared by mixing Pt black and liquid Nafion (5 wt%, EW1100).

Following this preliminary experiment, the same Nafion-Pt Black slurry solution was added to a N-methyl-2-pyrrolindinone (NMP) solution of polyaniline base to determine the effect of PANI. The components of this mixture were controlled to yield a PANI(10 wt %)-Nafion composite solution. Electrodes modified by solution casting of this PANI-Nafion-Pt Black composite are denoted by **PANI(10 wt %)-Nafion-Pt Black**. Figure 6.6 shows the cyclic voltammogram of a PANI(10 wt %)-Nafion-Pt Black electrode under N_2 and O_2.

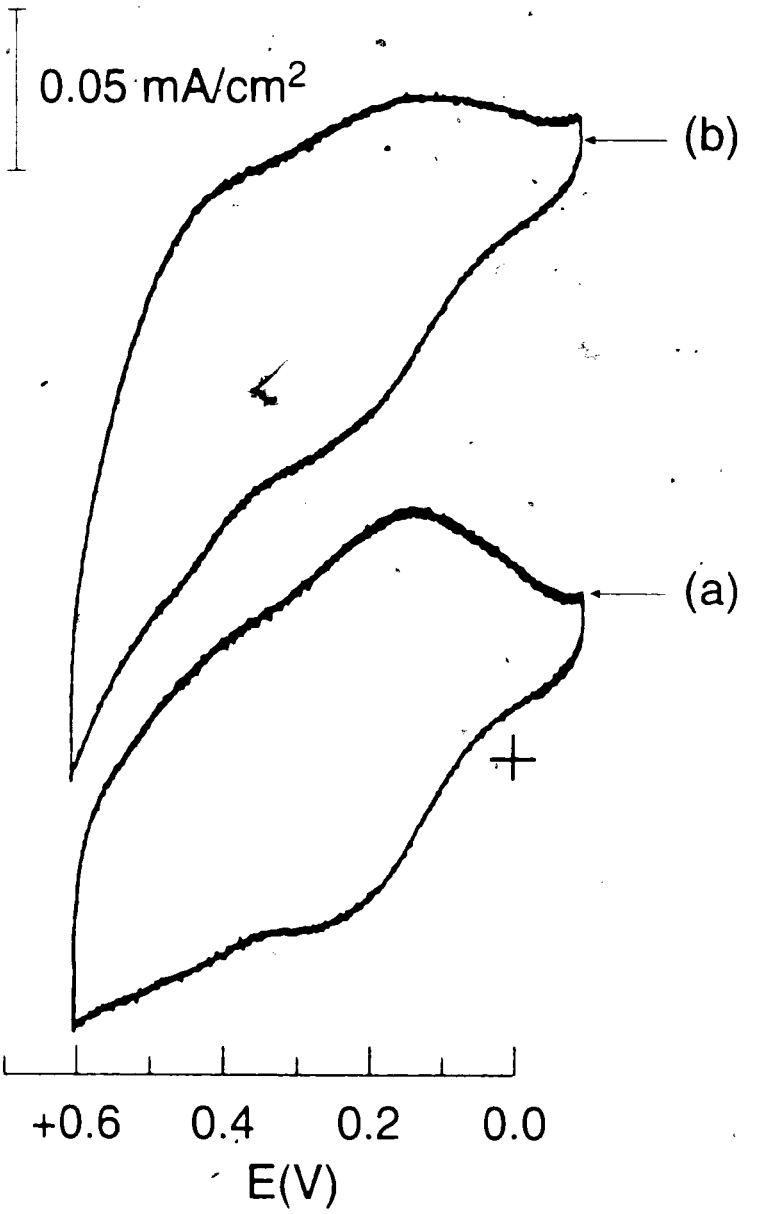

Figure 6.6 Cyclic voltammogram of PANI(10% wt)-Nafion-Pt Black modified GC electrode in 0.5 M H_2SO_4, (a) under N_2, (b) under O_2. Pt loading = 11.9 μg/cm², thickness = 3.1 μm , scan rate = 5 mV/s.

The cathodic potential limit was set at +0.6V vs. SCE to minimize the degradation of polyaniline. The redox peak at ~ +0.15V, due to the polyaniline, was observed both in the N_2 and O_2 environment. However, the cathodic current in the O_2 environment was much higher than in the N_2 environment. This is due to reduction of oxygen at Pt black particles. Comparing this electrode with the Nafion-Pt Black electrode, the increase in

cathodic current due to oxygen reduction is higher in the PANI(10 wt %)-Nafion-Pt black modified electrode. It is clear that the addition of polyaniline enhances the oxygen reduction reaction in this instance. In the Nafion-Pt black mixture, the small aggregates are electrically isolated and do not participate in the oxygen reduction reaction. With the addition of conducting polyaniline, the oxygen reduction reaction at the Pt clusters at the glassy carbon substrate can still occur, but at the same time, the smaller aggregates were also being connected electrically to the current collector by the polyaniline, and hence oxygen reduction can also occur at these Pt particles. Therefore, the addition of polyaniline enhances the Pt utilization and the cathodic current observed for oxygen reduction was higher than the Nafion-Pt Black modified electrode.

The sedimentation and aggregation of Pt black particles in solutions of Nafion that were observed might indicate that the quantity of Pt is too high to attain stable dispersions. A smaller quantity of Pt might reduce the extent of aggregation of Pt black particles, and increase the active surface area of the catalyst. Therefore a series of solutions with different Pt black loading were prepared. Figure 6.7 shows the cyclic voltammograms of a series of Nafion-Pt black modified electrodes in the presence of O_2

The cyclic voltammograms show that the oxygen reduction current decreases with decreasing loading as expected. Oxygen reduction reaction was still observed at loading as low as 4.5 $\mu g/cm^2$ but the cathodic currents were much smaller and the overpotential for O_2 reduction are quite large.

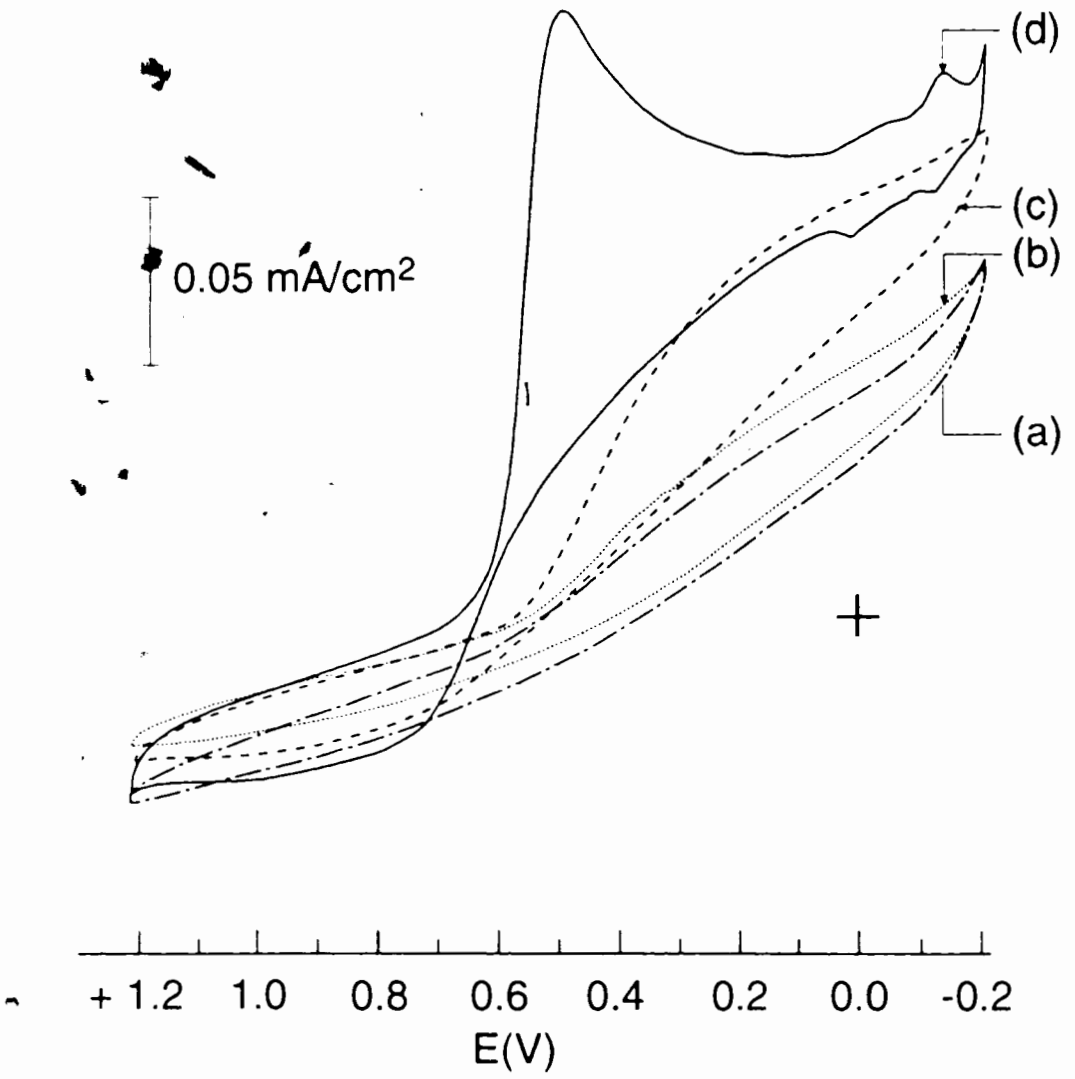

Figure 6.7 Cyclic voltammogram of PANI-Nafion-Pt Black with the following Pt Black loading: (a) 4.5 μg/cm², (b) 9.1 μg/cm², (c) 13.6 μg/cm², (d) 18.1 μg/cm², in O_2 saturated 0.5M H_2SO_4, scan rate = 5 mV/s.

Hence, from the experiment with Pt black, it can be concluded that the Pt black particles tend to aggregate in liquid Nafion and the active surface area of the catalyst is not being maximized even though this promotes activity when no activity was anticipated. Comparing the electroactivity of the Nafion-Pt black before and after the addition of polyaniline shows that the presence of polyaniline enhanced the utilization of

Pt black due to its electrically conducting nature which provides a conductive pathway for the smaller Pt aggregates.

6.3 Chemical Reduction of K_2PtCl_6 in Solutions of Nafion

In addition to simple mixture of Pt black with commercial solutions of Nafion, other methods of incorporating Pt have been published in the literature. For example, Millet *et al.* soaked a Nafion membrane in a solution containing a cationic Pt precursor, $Pt(NH_3)_4Cl_2$ [68]. The H^+ in the Nafion membrane ion-exchanged with $Pt(NH_3)_4Cl_2$ which was subsequently chemically reduced by $NaBH_4$ to Pt metal. The amount of Pt deposited is relatively small. In the present study, K_2PtCl_6 was first reduced in a commercial solution of Nafion and the resultant suspension was added to a polyaniline solution: K_2PtCl_6 was dissolved in a commercial solution of Nafion which contains water and aliphatic alcohols. The solution was refluxed for one hour, during which K_2PtCl_6 was reduced to Pt(0) by the reducing power of the alcohols. A grey suspension of Pt was observed. Electrodes of Nafion containing Pt were prepared by solution casting. Electrodes modified by this solution are denoted by **Nafion-Pt**. PANI-Nafion-Pt composites were obtained by adding the Nafion-Pt suspension to a NMP solution of PANI base. PANI base was immediately doped by the liquid Nafion as evidenced by its colour change from deep blue to dark green. Cast films were evaluated for electrocatalytic activity towards oxygen reduction reaction. The PANI-Nafion films with Pt chemically deposited by this method are denoted by **PANI-Nafion-Pt**. Figure 6.8 shows the TEM and SEM micrographs of PANI(10 wt %)-Nafion-Pt films prepared by depositing Pt chemically in liquid Nafion prior to doping of PANI. The SEM picture

indeed indicates that the Pt particles are distributed homogeneously in the matrix. The size of the particles range from 1 μm-4 μm. From the TEM picture, it can be observed that the larger particles observed in the SEM micrographs are actually composed of smaller spherical particles (~100 nm in diameter). In comparing these micrographs with those obtained on films prepared by simple mixing of liquid Nafion-PANI with Pt black and subsequent solution casting (Figure 6.4), it is clear that the aggregate size of Pt particles is smaller compare to the Pt black aggregates. Furthermore, the Pt particles appear to be more homogeneously dispersed.

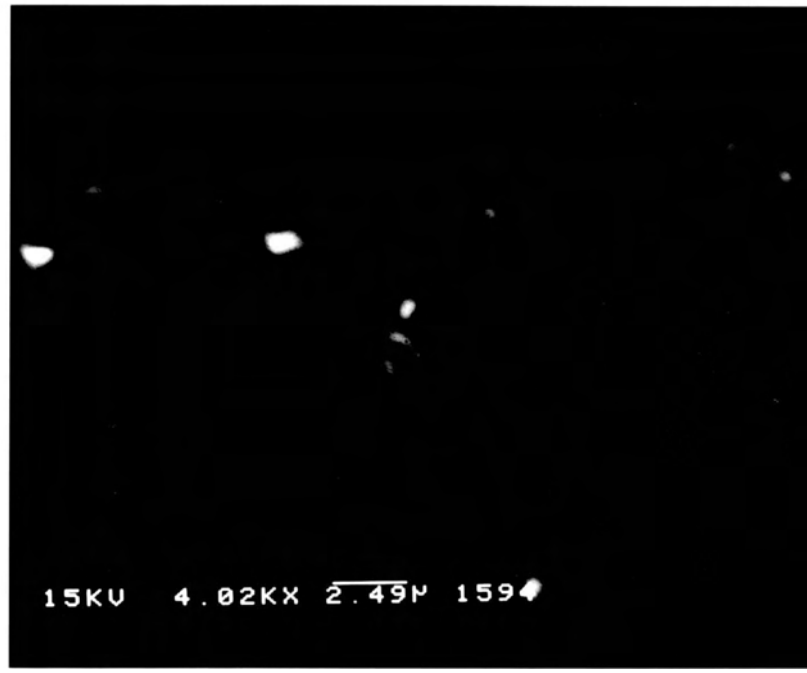

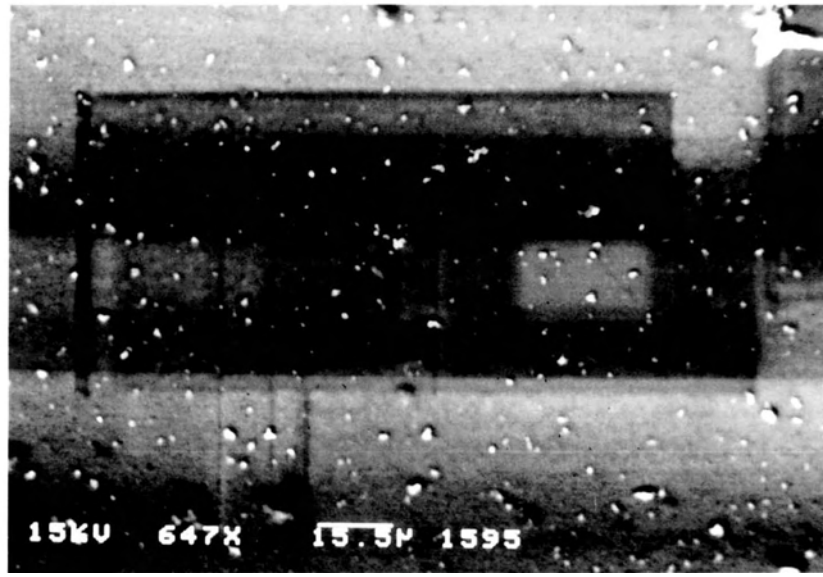

Figure 6.8 (a) SEM of PANI (10 wt %)-Nafion-Pt electrode.

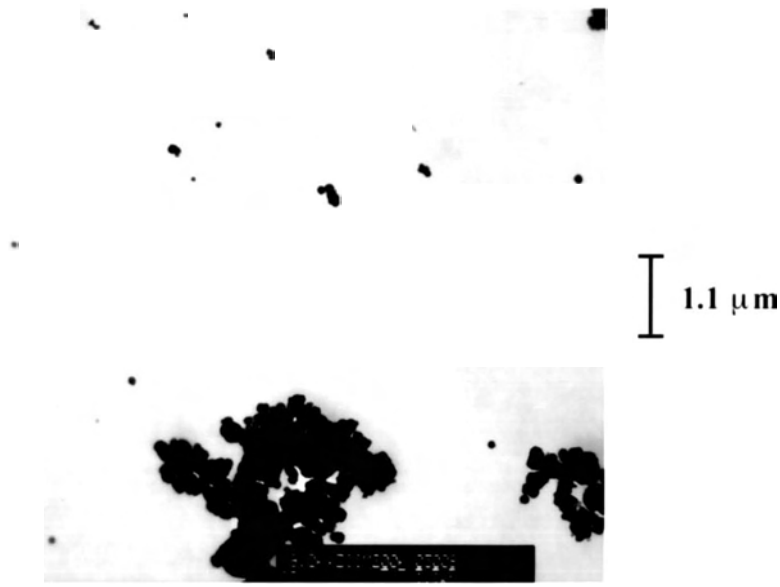

Figure 6.8 (b) TEM of PANI (10 wt%)-Nafion-Pt electrode.

The depth profile of Pt in the PANI-Nafion-Pt electrode was also determined by Auger electron spectroscopy by continuous sputtering of the film with an Ar^+ ion beam. With a Pt loading of 3 $\mu g/cm^2$, no Pt signal was detected in this sample even after 384 minutes of sputtering. Comparing the total time of sputtering of this PANI-Nafion-Pt sample with the PANI-Nafion/Pt sample (Figure 6.1), the thickness of the PANI-Nafion-Pt sample is much thicker than the PANI-Nafion/Pt sample (it only took 42 minutes to sputter through the PANI-Nafion/Pt sample). With similar Pt loading (~3 $\mu g/cm^2$) in both cases, the Pt signal was observed in the PANI-Nafion/Pt sample because most of the Pt particles were situated in the top 30% of the total film thickness. In the case of PANI-Nafion-Pt, the Pt signal is below the detectable limit which indicates that the Pt particles were homogeneously dispersed throughout the film, i.e. the concentration of Pt across the total thickness of the film is consistently low. This could be illustrated by the concentration gradient of Pt in a PANI-Nafion/Pt electrode and a PANI-Nafion-Pt electrode (Figure 6.9). These results provide indirect evidence that the Pt particles are homogeneously dispersed throughout the polymer composite matrix.

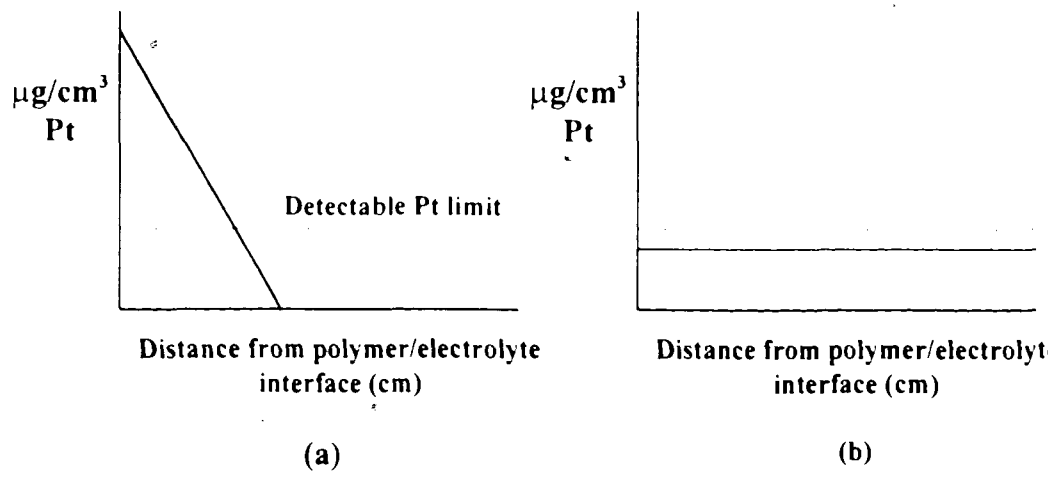

Figure 6.9 Pt concentration gradient in (a) a PANI-Nafion/Pt electrode, (b) a PANI-Nafion-Pt electrode.

Figure 6.10 shows the rotating disk voltammograms of a Nafion-Pt modified GC electrode in an oxygen saturated solution without electrode rotation and at 900 rpm.

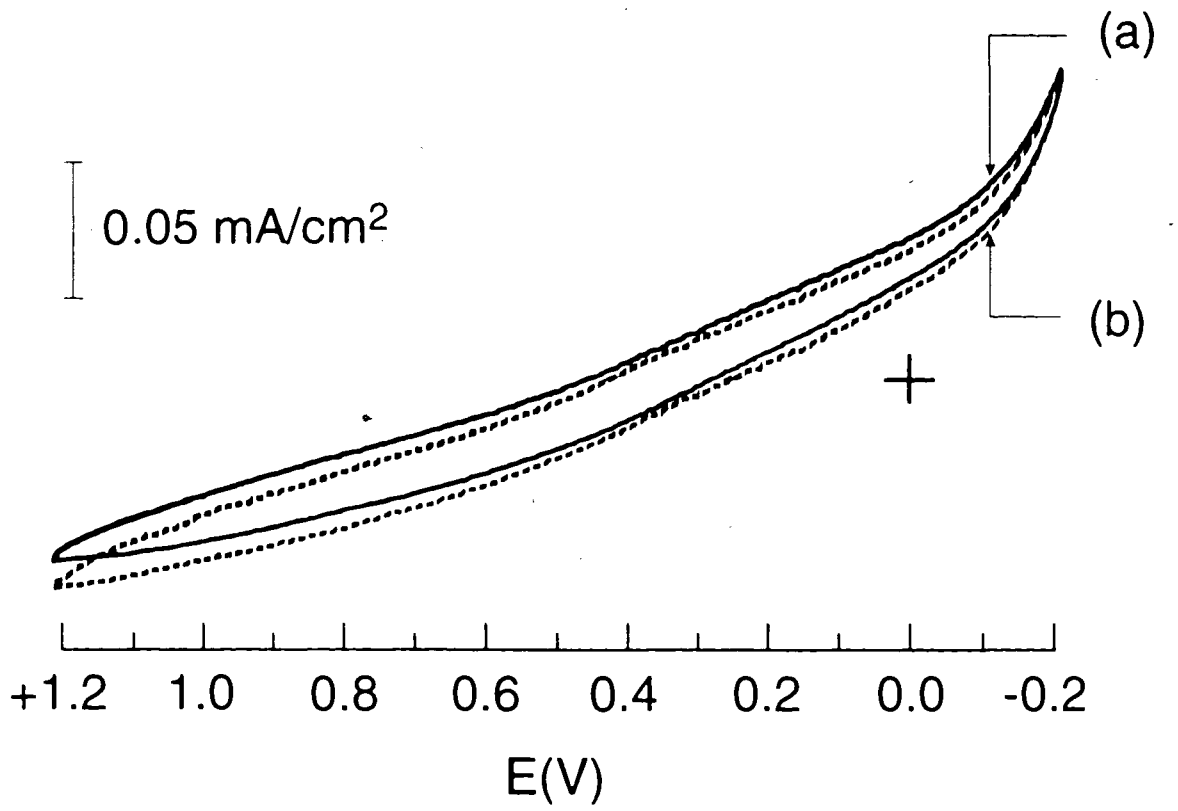

Figure 6.10 Cyclic voltammograms of a Nafion-Pt modified electrode (thickness = 8.5 μm, Pt loading = 34 μg/cm^2) electrode (a) at 900 rpm (solid line) and (b) at 0 rpm (dotted line) in O_2 saturated 0.5 M H_2SO_4, scan rate = 5 mV/s.

The electrocatalytic activity towards O_2 reduction is observed to be negligible. This suggests that the majority of the Pt particles in the matrix are not in electrical contact with the substrate electrode. This is achieved when the particles are homogeneously dispersed in the electronically non-conducting matrix.

Figure 6.11 shows the rotating disk voltammogram of a PANI (10 wt %)-Nafion-Pt modified glassy carbon electrode under the same conditions (the Pt loading and the thickness of the films were also kept similar to Nafion-Pt films for comparison). The cathodic potential was set at +0.6V vs. SCE in order to minimize degradation of

polyaniline. The increase in the cathodic current at different rotation speed clearly shows that the addition of the conducting polyaniline enhances the reduction of oxygen compared to the Nafion-Pt modified electrode in which PANI was absent.

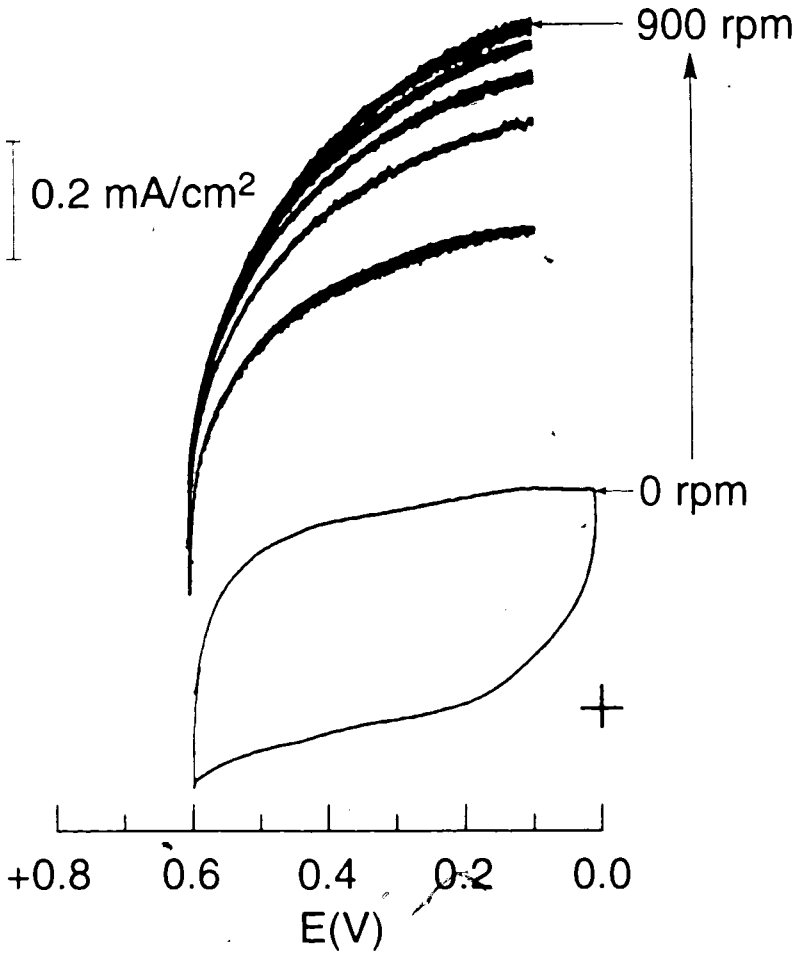

Figure 6.11 Rotating disk voltammograms of a PANI-Nafion-Pt electrode (thickness = 9.3 μm, Pt loading = 33 μg/cm^2) in O_2 saturated 0.5 M H_2SO_4, scan rate = 5 mV/s, rotation rates of 0, 100, 300, 500, 700, and 900 rpm.

As shown in Figure 6.10 and described in subsequent paragraphs, the electrocatalytic activity towards oxygen reduction was negligible for Nafion-Pt electrodes prepared by chemical deposition of Pt into Nafion solutions. This is due to the fact that Pt particles are homogeneously dispersed into an electronically insulating matrix. The effect of incorporating a conducting polymer into the matrix in order to facilitate electrical

connectivity between Pt particles was found to be very dramatic in this case. Figure 6.12 shows Levich plots for oxygen reduction at a PANI(10 wt %)-Nafion-Pt electrode prepared by casting of PANI(10 wt %)-Nafion-Pt composite, in comparison with a PANI(10 wt %)-Nafion-Pt Black electrode, in which Pt was deposited by simply mixing of Pt black and Nafion solutions.

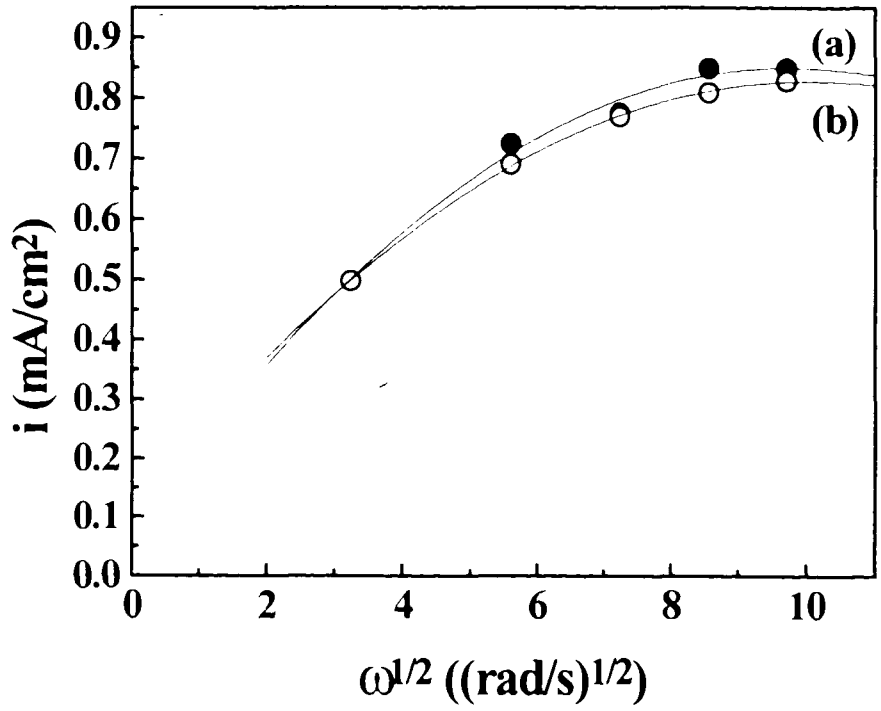

Figure 6.12 Levich plot for oxygen reduction at (a) PANI-Nafion-Pt Black electrode (thickness = 3.1 μm, Pt loading = 11 μg/cm²); (b) PANI-Nafion-Pt electrode (thickness = 3.1 μm, Pt loading = 11 μg/cm²), in O_2 saturated 0.5 M H_2SO_4, scan rate = 5 mV/s.

Although the electrocatalytic activity towards oxygen reduction at a Nafion-Pt electrode (Pt chemically deposited in Nafion solution) is negligible compared to the Nafion-Pt Black electrode (mixing of Pt black with Nafion solution), the electrocatalytic activity towards oxygen reduction reaction after incorporating the conducting polymer is almost identical for the two electrodes. The difference in electrocatalytic activity towards oxygen

reduction between the Nafion-Pt and Nafion-Pt electrodes appears to due to the difference in the spatial distribution of the Pt particles. In an electronically insulating matrix such as Nafion, the electrical connectivity between the catalyst particles and the current collector is the main issue. The Pt deposited chemically in Nafion solutions ia found to be smaller in size and appear not to settle at the surface of the glassy carbon substrate whereas the Pt black aggregates tend to settle at the glassy carbon surface. This provides an explanation why the Nafion-Pt Black electrode has a much higher electrocatalytic activity towards oxygen reduction than the Nafion-Pt electrodes. However, upon incorporation of conducting polyaniline, electrical connectivity between the Pt particles and the current collector is established in either case and therefore the electrocatalytic activity of the PANI-Nafion-Pt electrodes and the PANI-Nafion-Pt Black electrodes is similar. In situations where mass transport to the polymer films is increased, such as in fuel ccell application, it is expected that the PANI-Nafion-Pt electrodes will out-perform the PANI-Nafion-Pt Black electrodes for similar Pt loadings because the Pt in PANI-Nafion-Pt electrodes do not show extensive sedimentation and therefore the active surface area of the catalyst will be larger.

6.4 Discussion of the Electrocatalytic Activity of the Modified Electrodes Studied

The chemical reduction of K_2PtCl_6 in Nafion solutions yields a homogeneous suspension of Pt particles in the PANI-Nafion composite solution. Electrocatalytic films obtained from this solution mixture consist of Pt homogeneously dispersed throughout

the matrix as illustrated by the SEM micrograph in Figure 6.8, therefore a three dimensionally dispersed catalytic system was achieved. The electrocatalytic activity of this electrode (PANI-Nafion-Pt) was compared with the previously studied electrodes. Figure 6.13 shows the Levich plots for oxygen reduction reaction at a PANI-CSA/Pt electrode (Pt electrochemically deposited on a precast camphorsulfonic acid doped polyaniline film); a PANI-Nafion/Pt electrode (Pt electrochemically deposited on a precast PANI(10 wt %)-Nafion film); and a PANI-Nafion-Pt electrode (Pt incorporated by chemical reduction in Nafion solution prior to doping and solution casting).

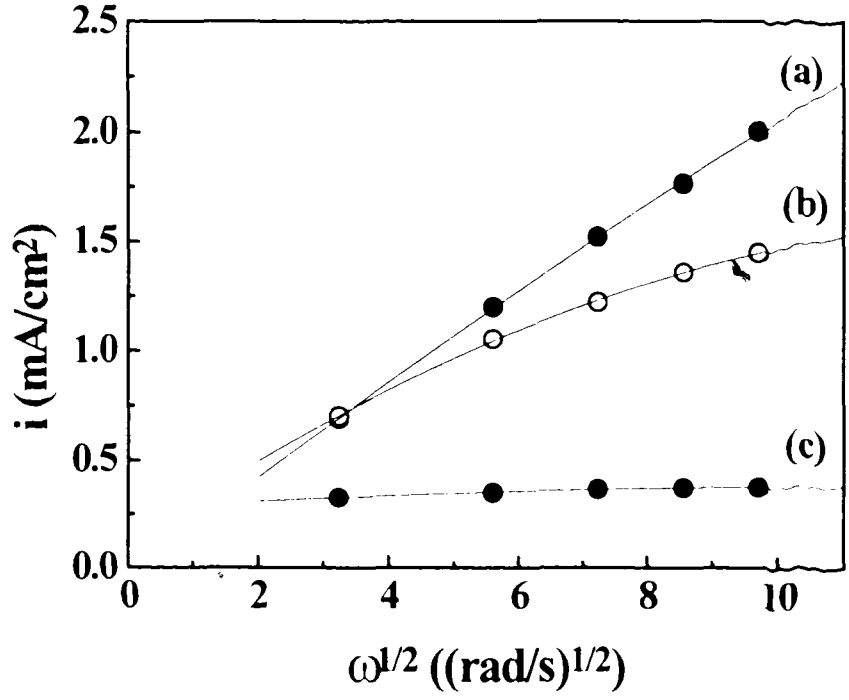

Figure 6.13 Levich plot for (a) PANI-CSA/Pt (film thickness = 0.44 μm, 23.1 μg/cm²); (b) PANI-Nafion-Pt (thickness = 3.1 μm, Pt loading 21 μg/cm²); (c) PANI-Nafion/Pt (thickness = 1.5 μm, Pt loading ~24 μg/cm²), in O_2 saturated 0.5 M H_2SO_4, scan rate = 5 mV/s.

As described previously, the Levich plot for oxygen reduction at the PANI-CSA modified electrode with Pt localized mainly at the polymer/electrolyte interface (Section 4.1.) is linear showing that the oxygen is not impeded by the polymer film. The PANI-

Nafion-Pt electrode containing homogeneously dispersed Pt yields a Levich plot which deviates from linearity at higher rotation rate. This is expected in a polymer modified electrode where the reactant has to diffuse through the polymer film in order to reach the catalyst particles in the matrix. At low rotation speeds, the electrocatalytic current for O_2 reduction at the PANI-Nafion-Pt is comparable to, if not higher than, the PANI-CSA/Pt modified electrode. This indicates that the area of the Pt particles available for oxygen reduction reaction may be larger in the PANI-Nafion-Pt electrode. However, at higher rotation rates, the limiting current for oxygen reduction reaction on the PANI-Nafion-Pt electrode becomes smaller than that in PANI-CSA/Pt electrode because the current is limited by the diffusion of oxygen through the composite film in the PANI-Nafion-Pt electrode in which Pt is dispersed within the matrix, whereas there is no mass transport limitation of oxygen in the PANI-CSA/Pt modified electrode.

The low electrocatalytic activity for O_2 reduction at the PANI-Nafion/Pt electrode in which Pt was incorporated by electrochemical deposition into a precast PANI-Nafion film is an unexpected result especially since the PANI-Nafion-Pt electrodes in which Pt is deposited chemically yields high catalytic activity. It is noted that the matrix for these two modifying films are identical, the only difference is in the method of incorporating Pt into the matrix. It has been previously documented that the dispersion of the Pt is affected by the deposition method. Kost and Kuwana reported a three-dimensionally dispersed catalytic system of Pt in polyaniline in their study of methanol oxidation [16]. The Pt particles were deposited by the electrochemical reduction of K_2PtCl_6 into a electropolymerized polyaniline film. The Pt particles were observed to grow along the polyaniline fibrils. The particles were found to be spherical, ~ 100 nm in diameter and

quite narrow in size distribution. In our work, as observed by TEM micrographs of PANI-Nafion-Pt films in Figure 6.8, the size of the Pt particles/clusters varied considerably (100 nm - 4 μm) due to the aggregation of small particles (~100 nm). Some of the larger Pt clusters may span across large regions of the film.

The proposed spatial distribution of Pt particles in a PANI-Nafion/Pt electrode in which Pt is electrochemically deposited is represented by Figure 6.14.

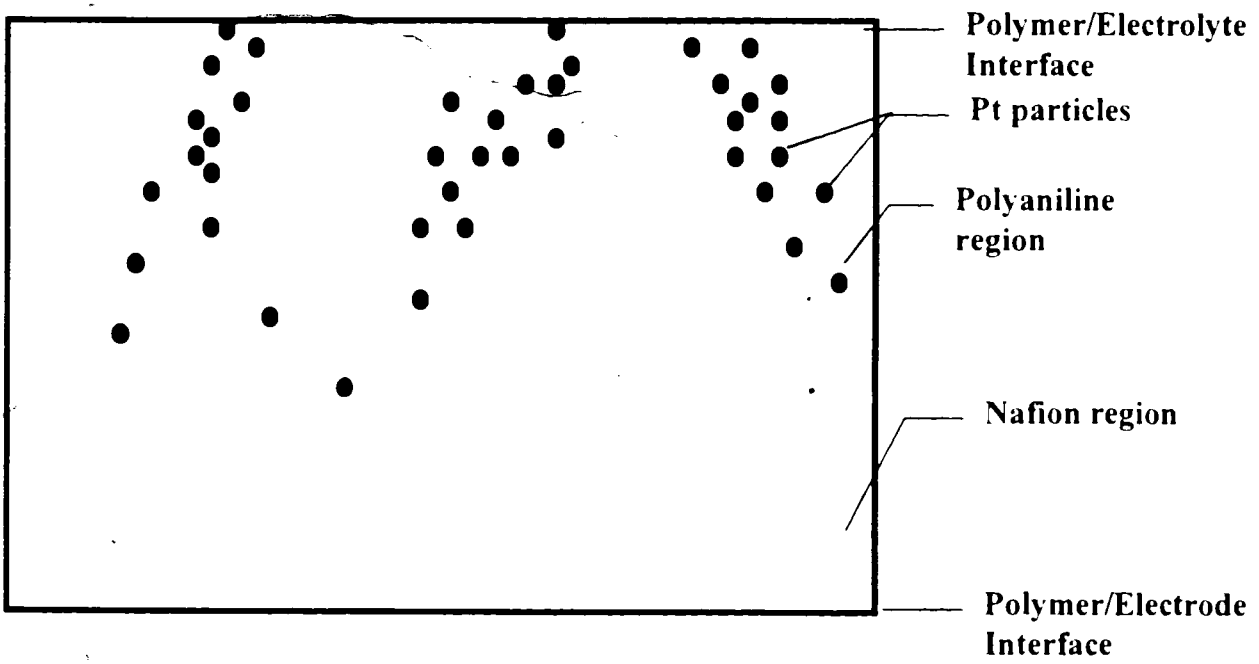

Figure 6.14 Proposed spatial distribution of Pt in a PANI-Nafion/Pt electrode (Pt incorporated by electrochemical deposition onto a precast PANI-Nafion film).

The Pt particles are assumed to grow along the conductive channels of PANI. Therefore the Pt particles deposited inside these polyaniline regions have no direct exposure to Nafion which is important in enhancing O_2 diffusion through the film.

In the case of chemical incorporation of Pt, Pt (IV) is reduced in Nafion solution and the particles are smaller, and the composite solution is less prone to sedimentation. As a result, Pt clusters/particles distribute more homogeneously in the matrix. The

proposed spatial distribution of Pt in a PANI-Nafion-Pt electrode is represented by Figure 6.15.

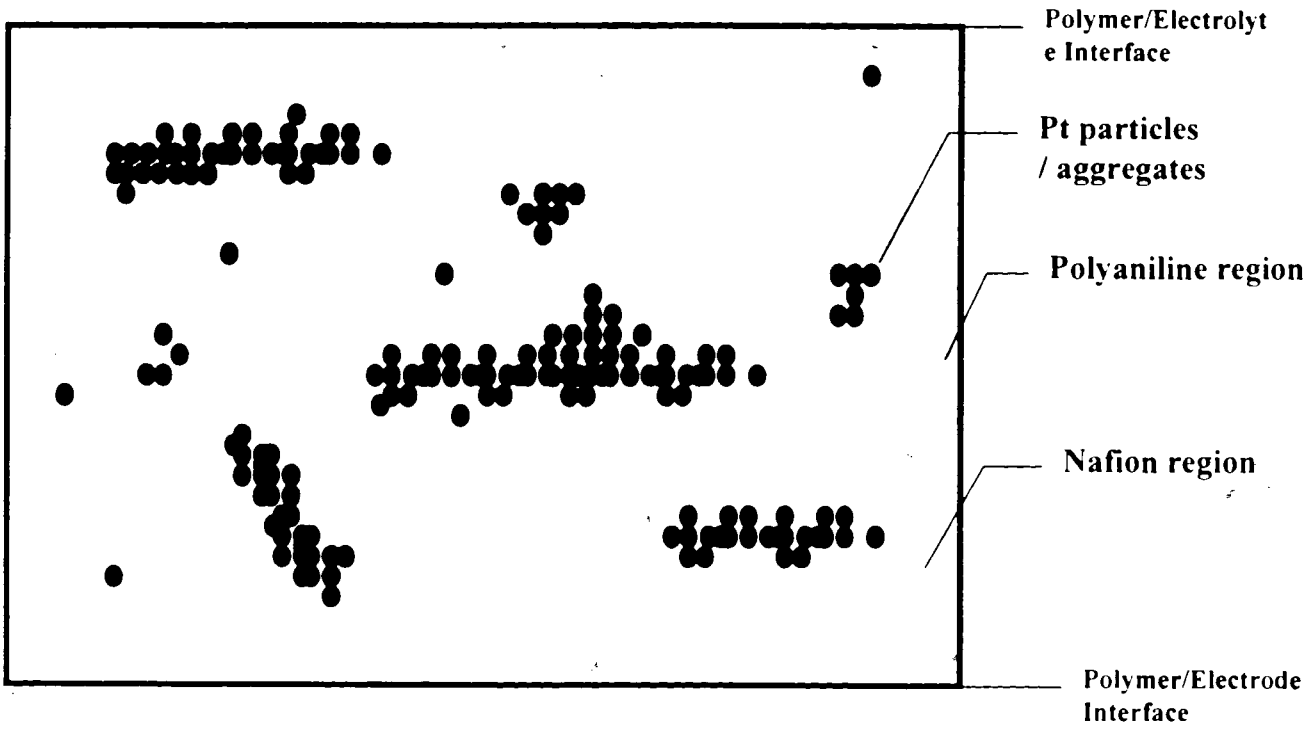

Figure 6.15 Proposed spatial distribution of Pt in a PANI-Nafion-Pt electrode (electrode prepared by reducing K_2PtCl_6 chemically in Nafion solution prior to doping of PANI).

In order to design catalytic systems which facilitate efficient electrochemical reactions, the catalyst/electrolyte/reactant interface needs to be maximized. Since electrochemical reactions have to occur at this three-phase interface, and no reaction will occur without either one of the three phases. In the oxygen reduction reaction studied in this work, the catalyst, Pt, the electrolyte, H_2SO_4, and the reactants, proton and oxygen, have to come together for reaction to occur. In this case, the O_2 permeability in Nafion is much higher than in PANI (Table 5.1). Therefore, it is advantageous to have Pt particles located in close proximity to the Nafion. However, in the PANI-Nafion/Pt electrode in which Pt is incorporated in an electrochemical step, the Pt particles are assumed to be

located mainly inside the PANI region and therefore may not be in direct contact with Nafion. Although the permeability of the PANI-Nafion composite is higher than the pure PANI-CSA polymer, O_2 still has to diffuse through the less diffusive PANI regions to reach Pt catalyst. In contrast, Pt particles incorporated by chemical reduction in Nafion solution, aggregate to form relatively large clusters of 1-4 μm in size. These are of sufficient size to span both Nafion and conductive PANI regions (Figure 6.15). Those Pt particles in contact with PANI and in close proximity to Nafion will yield the highest electrocatalytic activity because both electrical connectivity and O_2 permeability requirements are met. It is clear that the electrocatalytic activity is strongly affected by the method of catalyst deposition and the spatial distribution of the catalyst in the matrix. Thus some catalytic films are very active while others are not, even though the chemical compositions of the various films appear similar.

6.5 Stability of PANI-Nafion-Pt Modified Electrodes

Among all the polymer modified electrodes studied, the PANI-Nafion films containing chemically deposited Pt were deemed the most promising candidate as catalytic matrix for oxygen reduction. In order to utilize these electrodes in any industrial application, they must exhibit reasonable stability for an extended time. Therefore the stability of the PANI-Nafion modified electrode containing chemically deposited Pt was investigated. Figure 6.16 shows the stability curve of a PANI-Nafion-Pt electrode. The potential of the electrode was cycled between +0.6 V and 0.0 V (vs. SCE) at 5 mV/s repeatedly in an O_2 saturated solution and the rotating disk electrode was rotated at 900

rpm throughout the experiment. In Figure 6.16, the y-coordinate is the ratio of the limiting current measured at time t and the limiting current measured at time t=0, i.e., i/i_0. The current was observed to decrease steadily with time. This degradation could be due to several factors: (i) degradation of the polymer and hence the degradation of the conductive network; (ii) poisoning of the Pt particles by the small organic contaminants from the polymer; (iii) physical loss of Pt upon continuous rotation.

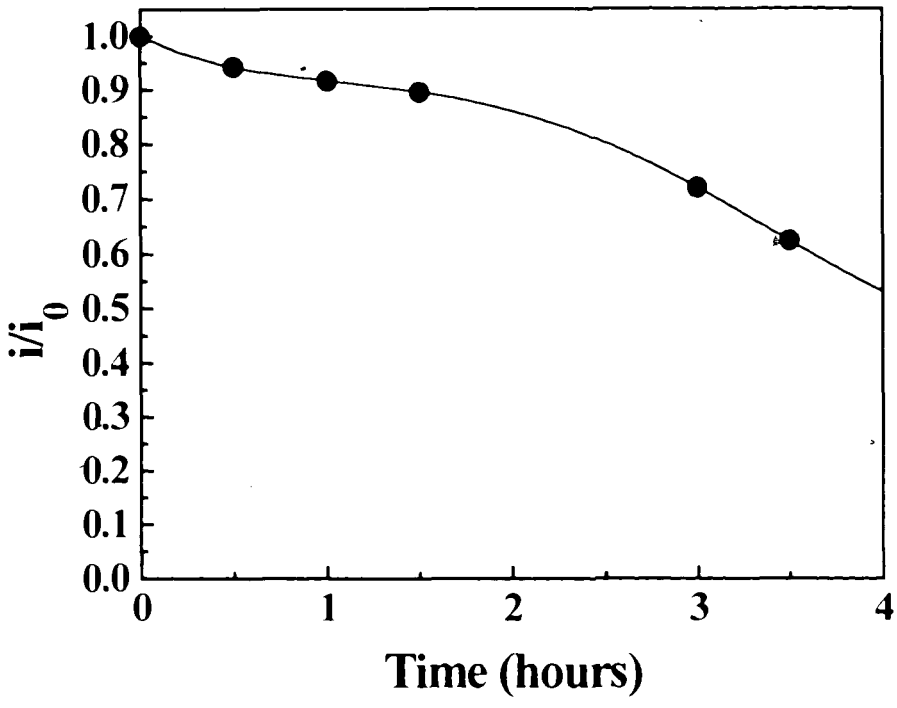

Figure 6.16 Stability plot of PANI(10%wt)-Nafion-Pt electrode with continuously cycling between +0.6V and 0.0V (SCE) at 5mV/s, rotated at 900rpm, in O_2 saturated 0.5M H_2SO_4, i_o = 1.6 mA/cm^2.

In order to examine the effect of the rotation on the physical loss of Pt, a stability test was carried out with a glassy carbon electrode with Pt deposited on it. The electrode was again cycled between +0.6V and 0.0V vs. SCE and it was rotated throughout the experiment. Figure 6.17 shows the stability plot (under similar conditions as used for the

PANI-Nafion-Pt electrode) for a glassy carbon electrode onto which Pt is electrochemically deposited.

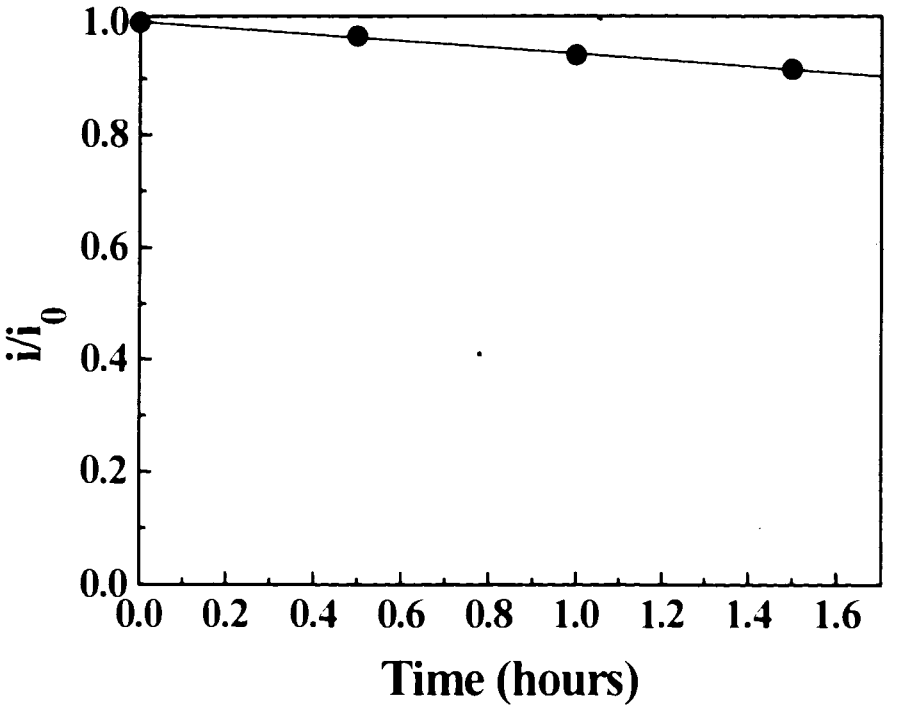

Figure 6.17 Stability curve of a GC/Pt electrode with continuously cycling between +0.6V and 0.0V (SCE) at 5mV/s, rotated at 900 rpm, in O_2 saturated 0.5M H_2SO_4, i_o = 2.7 mA/cm^2.

Similarly to the PANI-Nafion-Pt modified electrode, the current decreased steadily to 90% of the original current after 1.5 hour. Since the GC/Pt electrode does not possess any polymer on it, the physical loss of Pt particles upon rotation, or chemical poisoning is a major factor in the degradation of current.

In order to decrease the degradation of current due to physical loss, the stability of the PANI-Nafion-Pt electrode was studied again under quiescent condition. Figure 6.18 shows the stability curve of the PANI-Nafion-Pt modified glassy carbon electrode continuously cycled between +0.6 V and 0.0 V at 5 mV/s in O_2 saturated 0.5 M H_2SO_4.

The current decreased steadily to 60% of the original current before stabilizing after ~70-80 hours. Comparing the degradation rate of this electrode under rotation (Figure 6.16) and quiescent condition (Figure 6.18), it is observed that the rate of degradation in the hydrodynamic condition is much faster than in the quiescent solution due to the physical loss of Pt into the electrolyte solution. However, the degradation of polyaniline and/or the poisoning of Pt may still be an impediment in utilizing these polymer modified electrodes in industrial applications.

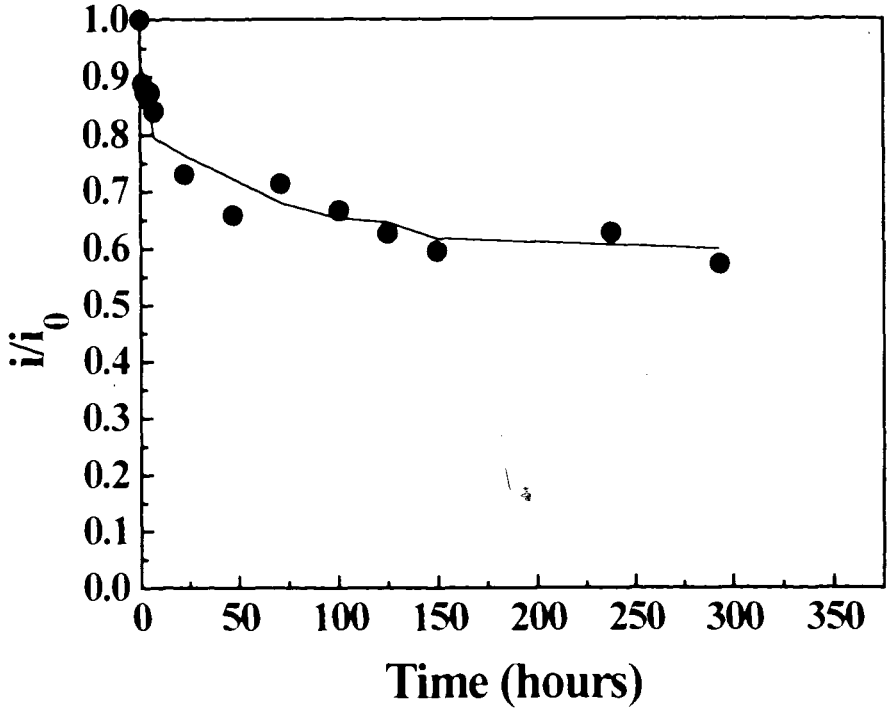

Figure 6.18 Stability plot of a PANI(10%wt)-Nafion-Pt electrode, with continuously cycling between +0.6V and 0.0 V(SCE) at 5 mV/s, in quiescent O_2 saturated 0.5 M H_2SO_4, i_o = 0.36 mA/cm^2.

6.6 Conclusions

Three different methods of incorporating Pt into polyaniline-Nafion composites were discussed. It was found that the method of Pt deposition strongly affects the spatial

distribution of Pt in the composite. Pt particles deposited by electrochemical method tend to grow within the polyaniline regions and hence may not be in direct contact with Nafion, for which O_2 permeability and proton conductivity are much higher. Therefore, although the Pt particles deposited electrochemically are found to be dispersed to a greater extent into the PANI-Nafion composite films, as compared to the pure PANI films, the electrocatalytic activity towards oxygen is poor. Pt black was also studied as a prospective catalyst, but it was found that Pt black aggregates tend to precipitate and settle onto the surface of the substrate electrode. A new method of incorporating Pt into the composite was developed in our laboratory. Pt was deposited in Nafion solution by chemical reduction of K_2PtCl_6. This suspension was then used to dope polyaniline base. The resulting PANI-Nafion-Pt mixture was found to be a promising candidate toward electrocatalytic oxygen reduction. The stability of the PANI-Nafion-Pt electrode was also studied and shows electrocatalytic activity even after 300 hours of use.

SUMMARY

In this work, polyaniline has been investigated as a host matrix for Pt in the electrochemical reduction of oxygen. The electrocatalytic activity has been evaluated and several conclusions can be made:

1) Electrochemical deposition of Pt onto PANI-CSA films results in localization of Pt particles on the top surface of the polymer. This is likely due to the compact morphology of the chemically synthesized PANI and the inability of K_2PtCl_6 to penetrate the bulk of the polymer film on the timescale of the electrochemical reaction.

2) For similar Pt loadings, the electrocatalytic activity for O_2 reduction is higher for PANI-CSA/Pt electrodes than for Pt deposited on a bare glassy carbon electrode. This indicates a higher active surface area of the catalyst in the polymer modified electrodes; however, since Pt is localized within 30-40 nm of the polymer surface, it is unlikely that this distribution of Pt would provide the largest surface area/gram of catalyst.

3) Rotating disk voltammetry shows diffusion limitation of O_2 through the PANI-CSA films. The permeability of O_2 through the PANI-CSA films was determined to be 1.18×10^{-12} mol cm^{-1} s^{-1} which is only about 1/20 of the permeability of O_2 in 0.5 M H_2SO_4.

4) Polyaniline-Nafion composites were prepared to improve the permeability of the matrix for oxygen. The permeability of PANI(10% wt)-Nafion films was determined to be 1.74×10^{-12} mol cm^{-1} s^{-1}, showing a 47% increase in permeability compared to

PANI-CSA. Moreover, it is in the same order of magnitude as the permeability through a Nafion film.

5) Pt deposited electrochemically into the PANI-Nafion films was found to disperse into the matrix to a greater extent than in PANI-CSA films; however, the electrocatalytic activity of this electrode was found to be much smaller than that of the PANI-CSA/Pt electrode. It is postulated that the low activity of the PANI-Nafion/Pt electrode is due to the nature of Pt growth in the composite matrix. Pt was assumed to deposit in the PANI regions restricting access to oxygen.

6) A chemical method of reducing K_2PtCl_6 in Nafion solution was developed by making use of the reducing power of the alcohols present in the Nafion solution.

7) The PANI-Nafion-Pt composite solution yields polymer modified electrode system with Pt homogeneously dispersed throughout the matrix.

8) The electrocatalytic activity of the PANI-Nafion-Pt electrode was found to be similar to that of the PANI-CSA/Pt electrode.

9) The difference in performance of the electrocatalytic activity between PANI-Nafion/Pt electrode and PANI-Nafion-Pt electrode suggests a strong dependence on the method of Pt deposition. The Pt particles prepared by chemical reduction span both the PANI and Nafion regions, fulfilling both electronic connectivity by PANI and accessibility of reactants by Nafion.

10) The stability of the PANI-Nafion-Pt electrode was investigated. Degradation was observed to be highest in the first 50 hours and stabilized after 100 hours. The electrode was still electroactive after 300 hours.

From the above results, it can be concluded that the PANI-Nafion composite has potential application in H_2/O_2 fuel cells as a matrix for the catalyst layer. The chemical reduction of K_2PtCl_6 provides a simple and convenient method for incorporating Pt into these matrices. This study provides fundamental information which suggests that conducting polymers might have advantages over conventional carbon supports; however, one should bear in mind that the test conditions of this study are quite different from the conditions found in fuel cells. High hydrodynamic fluxes found in operating fuel cells cannot be attained with rotating disk voltammetry; therefore one cannot fully utilize the Pt sites deep within the polymer matrix. Further studies under similar conditions used during fuel cells operation should be pursued to determine if enhanced catalytic efficiency of Pt is indeed observed under operating fuel cell conditions. It is also necessary to determine the lifetime of these electrocatalytic layers in the demanding conditions of fuel cell operation.

References

1. D.J. Berets, D.S. Smith, *Trans. Faraday Soc.*, **64**, 823 (1968)
2. H. Shirakawa, E.J. Louis, A.G. MacDiarmid, C.K. Chiang, A.J. Heeger, *J. Chem. Soc.: Chem. Commun.*, 578 (1977)
3. J.L. Bredas, G.B. Street, *Acc. Chem. Res.*, **18**, 309 (1985)
4. T.J. Skotheim, *Handbook of Conducting Polymers*, Marcel Dekker: New York (1986)
5. M.G. Kanatzidis, *C & EN*, December 3, 36 (1990)
6. A.G. MacDiarmid, A.J. Epstein, *Faraday Discuss. Chem. Soc.*, **88**, 317 (1989)
7. J.H. Burroughes, C.A. Jones, R.H. Friend, *Nature*, **335**, 137 (1988)
8. E.M. Genies, P. Hany, Ch. Santier, *J. Appl. Electrochem.*, **18**, 781 (1988)
9. D. Braun, A.J. Heeger, *Appl. Phys. Lett.*, **58**, 1982 (1991)
10. P.N. Bartlett, R.G. Whitacker, *Biosensor*, **3**, 359 (1987-8)
11. W.K. Lu, R.L. Elsenbaumer, B. Wessling, *Synth. Metals*, **71**, 2163 (1995)
12. J. O'M. Bockris, A.K.N. Reddy, *Modern Electrochemistry*, 2, 1141, Plenum Press, New York (1972)
13. G. Tourillon, F. Garnier, *J. Phys. Chem.*, **88**, 5281 (1984)
14. C.C. Chen, C.S.C. Bose, K. Rajeshwar, *J. Electroanal. Chem.*, **350**, 161 (1993)
15. J.M. Léger, C. Lamy, *Ber. Bunsenges. Phys. Chem.*, **94**, 1021 (1990)
16. K. Kost, D. Bartak, B. Kazee, T. Kuwara, *Anal. Chem.*, **60**, 2379 (1988)
17. F.T.A. Vork, E. Barendrecht, *Electrochimica Acta.*, **35**, 135 (1990)
18. S. Holdcroft, B.L. Funt, *J. Elecreoanal. Chem.*, **240**, 89 (1988)
19. M.R. Anderson, B.R. Mattes, H. Reiss, R.B. Kaner, *Science*, **252**, 1412 (1991)

20. K. Kinoshita, *Electrochemical Oxygen Technology*, The Electrochemical Society, John Wiley & Sons, Inc., Chapter 2 (1992)

21. A.J. Bard, L.R. Faulkner, *Electrochemical Methods, Fundamentals and Applications*, John Wiley & Sons, Inc., Chapter 3 (1980)

22. J.O'M. Bockris, A.K.N. Reddy, *Modern Electrochemistry*, Plenum Press, New York, Vol. 2, p.1259 (1977)

23. J.O'M. Bockris, A.K.N. Reddy, *Modern Electrochemistry*, Plenum Press, New York, Vol. 2, p.878 (1977)

24. A.J. Appleby, *Catal. Rev.*, **4**, 221 (1970)

25. K. Kinoshita, *Electrochemical Oxygen Technology, The Electrochemical Society*, John Wiley & Sons, Inc., Chapter 1 (1992)

26. G. Schivon, S. Sitran, G. Zotti, *Synth. Metals*, **32**, 209 (1989)

27. L.E. Davis, N.C. MacDonald, P.W. Palmberg, G.E. Riach and R.E. Weber, *Handbook of Auger Electron Spectroscopy: A reference book of Standard Data for Identification and Interpretation of Auger Electron Spectroscopy Data*, 2nd ed., Eden Prairie, MN: Phyiscal Electronics Division Perkin-Elmer Corp. (1976)

28. A.F. Diaz, J.A. Logan, J. *Electroanal. Chem.*, **111**, 111 (1980)

29. D.C. Trivedi, S.K. Dhawan, *Synth. Met.*, **58**, 309 (1993)

30. J. Desilvestro, W. Scheifele, *J. Mater. Chem.*, **3**, 263 (1993)

31. J. Wang, S.P. Chen, M.S. Lin, *J. Electroanal. Chem.*, **273**, 231 (1989)

32. M. Wan, *Synth. Met.*, **31**, 51 (1989)

33. Y. Ohnuki, T. Ohsaka, H. Matsuda, N. Oyama, *J. Electroanal. Chem.*, **158**, 55 (1983)

34. A. Volkov, G. Tourillon, P.C. Lacaze, J.E. Dubois, *J. Electrochem. Soc.*, **129**, 2261, (1982)

35. E.M. Genies, C. Tsintaris, *J. Electrochem. Chem.*, **195**, 109 (1985)

36. Hari Singh Nalwa, *Handbook of Organic Conductive Molecules and Polymers*, John Wiley & Sons, Inc., 2, Chapter 12 (1997)

37. L.H.C. Mattoso, A.G. MacDiarmid, A.J. Epstein, *Synth. Met.*, **68**, 1 (1994)

38. P.W. Atkins, *Physical Chemistry*, 5th Edition, Oxford University Press, London, Chapter 28, Fig. 28.7 (1990)

39. M. Angelopoulous, G.E. Asturias, S.P. Ermer, A. Ray, E.M. Scherr, A.G. MacDiarmid, M. Akhtar, Z. Kiss, A.J. Epstein, *Mol. Cryst. Liq. Cryst.*, **160**, 151 (1988)

40. C.C. Han, L.W. Schacklette, R.L. Elsenbaumer, presented at the Meeting of the Materials Research Society, Symposium on Electrical, Optical, and Magnetic Properties of Organic Solid State Materials, Boston, MA, USA, Dec. 6, page 448 (1991)

41. A. Andreatta, Y. Cao, J.C. Chiang, A.J. Heeger, P. Smith, *Synth. Met.*, **26**, 383 (1988)

42. Y. Cao, P. Smith, A.J. Heeger, *Synth. Met.*, **48**, 91 (1992)

43. A.J. Milton, A.P. Monkman, H. Phys. D: *Appl. Phys.*, **26**, 1468 (1993)

44. J. Tang, X. Jing, B. Wang, F. Wang, *Synth. Met.*, **24**, 231 (1988)

45. K. Tzou, R.V. Gregory, *Synth. Met.*, **53**, 365 (1993)

46. W.S. Huang, B.D. Humphrey, A.G. MacDiarmid, *J. Chem. Soc., Faraday, Trans.* 1, **82**, 2385 (1986)

47. T. Kobayashi, H. Yoneyama, H. Tamura, *J. Electroanal. Chem.*, **177**, 293 (1984)

48. Y.-B. Shim, M.-S. Won, S.-M. Park, *J. Electrochem. Soc.*, **137**, 538-543 (1990)

49. E.M. Genies', M. Lapkowski, J.F. Penneau, *J. Electroanal. Chem.*, **249**, 97-107 (1988)

50. E.W. Paul, A.J. Ricco, M.S. Wrighton, *J. Phys. Chem.*, **89**, 1441-1447 (1985)

51. J.W. Thackeray, M.S. Wrighton, *J. Phys. Chem.*, **90**, 6674-6679 (1986)

52. D. Ofer, R.M. Crooks, M.S. Wrighton, *J. Am. Chem. Soc.*, **112**, 7869-7879 (1990)

53. W.-H. Kao, T. Kuwana, *J. Am. Chem. Soc.*, **106**, 473-476 (1984)

54. D.A. Gough, J.K. Leypoldt, *Anal. Chem.*, **51**, 439 (1979)

55. D.A. Gough, J.K. Leypoldt, *Anal. Chem.*, **52**, 1126 (1980)

56. E.J. Taylor, E.B. Anderson, N.R.K. Vilambi, *J. Electrochem. Soc.*, **139**, L45-L46 (1992)

57. M.S. Wilson, S. Gottesfeld, *J. Electrochem. Soc.*, **139**, L28-L30 (1992)

58. C.-H. Hsu, *Synth. Met.*, **41-43**, 671-674 (1991)

59. S. Kuwabata, K. Mitsui, H. Yoneyama, *J. Electroanal. Chem.*, **281**, 97-107 (1990)

60. D. Orata, D.A. Buttry, *J. Electroanal. Chem.*, **257**, 871-882 (1988)

61. C. Barthet, M. Guglielmi, *J. Electroanal. Chem.*, **388**, 35-44 (1995)

62. *Encyclopedia of Polymer Science & Engineering*, 2nd Ed., John Wiley & Sons, Inc. Vol. 12, p.418 (1988)

63. S. Gottesfeld, I.D. Raistrick, S. Srinivasan, *J. Electrochem. Soc.*, **134**, 1455-1462 (1987)

64. Z. Ogumi, Z. Takehara, S. Yoshizawa, *J. Electrochem. Soc.*, **131**, 769 (1984)

65. Chemical Society of Japan, "Kagaku Binran", Maruzen, Tokyo (1975)

66. T.K. Gibbs, D. Pletcher, *Electrochimca Acta.*, **25**, 1105 (1980)

67. M. Watanabe, H. Igarashi, K. Yosioka, *Electrochimica Acta.*, **40**, 329-334 (1995)